TRANSIENT STABILITY IMPROVEMENT OF DOUBLY FED INDUCTION GENERATOR-BASED VARIABLE SPEED WIND ENERGY CONVERSION SYSTEM USING FLSTATCOM

(CASE STUDY ON ADAMA WIND FARM II)

A THESIS SUBMITTED

IN PARTIAL FULFILLMENT OF THE REQUIREMENTS

FOR THE DEGREE OF

MASTER OF SCIENCE

IN

POWER SYSTEM AND ENERGY ENGINEERING

BY

ELIAS EJIGU

DEPARTMENT OF ELECTRICAL AND COMPUTER ENGINEERING

HAWASSA UNIVERSITY INSTITUTE OF TECHNOLOGY

ADVISOR: - DR. BASEEM KHAN (PhD)

CO-ADVISOR:-MR. MULUALEM TESFAYE (MSc)

HAWASSA (ETHIOPIA)

November, 2023

TRANSIENT STABILITY IMPROVEMENT OF DOUBLY FED INDUCTION GENERATOR-BASED VARIABLE SPEED WIND ENERGY CONVERSION SYSTEM USING FLSTATCOM

(CASE STUDY ON ADAMA WIND FARM II)

BY

ELIAS EJIGU

A THESIS SUBMITTED TO THE
DEPARTMENT OF ELECTRICAL AND COMPUTER ENGINEERING,
INSTITUTTE OF TECHNOLOGY, SCHOOL OF
GRADUATE STUDIES

HAWASSA UNIVERSITY

HAWASSA, ETHIOPIA

IN PARTIAL FULLFILLMENT OF THE
REQUIREMENT FOR THE
DEGREE OF

MASTER OF SCIENCE IN POWER SYSTEM AND ENERGY ENGINEERING

November, 2023

HAWASSA UNIVERSITY

INSTITUTE OF TECHNOLOGY

SCHOOL OF POSTGRADUATE STUDIES

ADVISOR'S APPROVAL SHEET

This is to certify that the thesis entitled **"Transient Stability Improvement of Doubly Fed Induction Generator-Based Variable Speed Wind Energy Conversion System Using FLSTATCOM,** Case Study on Adama Wind Farm II)" submitted in partial fulfillment of the requirements for the degree of Masters of Science in Electrical Engineering with specialization in "**POWER SYSTEM AND ENERGY ENGINEERING**". The Graduate Program of the Department of Electrical and Computer Engineering, and carried out by **Elias Ejigu** ID No-GppoSyR/0005/14, under my supervision. Therefore, I recommend that the student has fulfilled the requirements and hence hereby can submit the thesis to the department.

Dr. Baseem Khan	Baseem _____	_____
Advisor	Signature	Date
Mr. Mulualem Tesfaye	_____	_____
Co-Advisor	Signature	Date

HAWASSA UNIVERSITY

INSTITUTE OF TECHNOLOGY

SCHOOL POSTGRADUATE STUDIES

EXAMINERS' APPROVAL SHEET

We, the undersigned, members of the Board of Examiners of the final Master's degree open defense, by **Elias Ejigu** have read and evaluated his thesis entitled **"Transient Stability Improvement of Doubly Fed Induction Generator-Based Variable Speed Wind Energy Conversion System Using FLSTATCOM''** and examined the candidate. This is, therefore, to certify that the thesis has been accepted in partial fulfillment of the requirement for the degree of Master of Science in Electrical Engineering with Specialization in Power System and Energy Engineering.

	Signature	Date
Dr. Solomon Mamo	_____	_____
Name of Internal Examiner		
Dr. Muluneh Lemma	_____	_____
Name of External Examiner		
Mr.Tesfahun Molla.	_____	_____
Name of the Chair Person		
Dr. Baseem Khan	_____	_____
Name of Principal Advisor		
Mr. Mulualem Tesfaye	_____	_____
Name of the Co-Advisor		
Mr.Dejene Hurissa	_____	_____
Dean of Faculty		
_____	_____	_____

DECLARATION

To the best of my knowledge and belief, this thesis contains no material previously published by any other person except where due acknowledgment has been made. This thesis contains no material that has been accepted for the award of any other degree at any university.

Elias Ejigu _____ _____

Student Signature Date

This MSc Thesis has been submitted for examination with my approval as thesis advisor.

Dr.Baseem Khan Baseem _____ _____

Advisor Signature Date

Mr. Mulualem Tesfaye _____ _____

Co-Advisor Signature Date

ACKNOWLADGEMENT

First of all, I would like to thank my almighty God for being the most beneficent and merciful, who always guides me to the right path and has helped me to complete this thesis.

I am wholeheartedly grateful to **Dr. Baseem Khan,** my advisor and chairperson of the advisory committee, for his consistent guidance, encouragement, helpful suggestions, and never-ending patience throughout the advancement of this research. I am also very grateful to **Mr. Mulualem Tesfaye,** my co-advisor, for his valuable suggestions to improve the excellence of the entire work.

I would like to express my respect and gratitude to the Hawassa University Department of ECE, especially the Power staff, for their continuous inspiration, assistance, and encouragement during the progress presentation all the way to my higher study.

I would also like to express my eternal gratitude to my family members for supporting me in all situations, directly or indirectly, and my utmost respect and appreciation to all my academic mentors who have helped me throughout my life.

Dedication to the memory of my late father

may God have mercy on his soul!!

ABSTRACT

The "doubly fed induction generator (DFIG)" is the most extensively utilized technology for wind power generation because of its adaptability to changing wind speeds and ability to capture more wind energy. However, issues like transient stability posed hurdles for the grid because wind energy has a fluctuating nature, faults, load fluctuations occur, and electronic devices are required to connect wind turbine generators to the grid. Capacitor banks are used in the research region to address the aforementioned issues and improve the variable-speed wind production system's transient stability. The investigation shows that the capacitor banks are incapable of maintaining the grid code during any kind of network fault. This demonstrates how crucial it is to use FACTS devices to increase the wind-generating system's transient stability. In this dissertation, a shunt flexible alternative current transmission system device called a static synchronous compensator (STATCOM) can offer technical solutions to enhance the overall performance of wind energy conversion systems through the creation of a suitable controller. The Thesis also presents the STATCOM control system and its effectiveness. ANFIS-controlled STATCOM is examined in this Thesis before being compared to that of STATCOM controlled by fuzzy logic. The adaptive ANFIS control approach is faster to speed control, better at responding to voltage fluctuations, and better at tracking the reactive current reference, according to simulations performed using MATLAB on grid-connected DFIG systems. Finally, the ANFIS-based STATCOM is critical in assuring the stability of power systems in the case of large disruptions and break downs.

Key word; DFIG, STATCOM, ANFIS

Table of Contents

LIST OF TABLES

LIST OF FIGURE

ABBREVIATION

DFIG	Doubly fed induction generator
WECS	Wind Energy Conversion System
Rs	Stator resistance
Ls	Stator leakage inductance
Lr	Rotor leakage inductance
Lm	Magnetizing inductance
Lls	Stator self-inductance
Llr	Rotor self-inductance
J	Inertia
Wm	Turbine angular speed
Tem	Electromagnetic Torque
V	Wind speed
Cp	Power coefficient DFIG Double fed Induction Generator
PLL	Phase Locked Loop
GSC	Grid Side Converter
RSC	Rotor Side Converter
STATCOM	Static synchronous compensator
FLC	Fuzzy Logic Controller
ANFIS	Adaptive neurofuzzy inference system
IGBT	Insulated-gate bipolar transistors
GTO	Gate turn-off thyristor

CHAPTER ONE

INTRODUCTION

1.1 Back ground of study

Wind is a renewable resource that is free to use forever, pollution-free, and environmentally friendly. Additionally, it reduces our reliance on conventional fuels like oil, gas, and coal. Although there are many fixed-speed wind generators on the market for the wind energy conversion system (WECS), the 'doubly fed induction generator (DFIG)' and permanent magnet synchronous generator (PMSG) are gaining popularity due to their capacity to capture significantly more energy when operating as variable-speed wind generator systems [1].Since DFIG uses lower-rated power electronic converters than PMSG does, it is a more appealing alternative. Besides, the DFIG offers improved speed control with fewer flickers [2]. Additionally, it has been claimed that systems using synchronous generators experience more defective events in the electronics than systems using induction generators [3]. Consequently, a particularly common technique for generating power from wind energy at the moment is the DFIG system.

Like conventional power systems, WECS should possess the property of transient stability, or the capacity to keep synchronism even in the face of a severe disturbance like a short circuit or a transmission line fault. After a malfunction in the high-voltage grid, an unstable system could cause a significant number of wind farms to be disconnected. The ability to decouple control of 'active and reactive power' in grid integrated systems, as well as variable speed operation, reduced converter cost, switching losses, and harmonics injection into the power grid, make DFIG more efficient and cost-effective than other direct drive wind energy conversion systems. 80% of the power in DFIG passes through the stator without the need for power electronics.

Due to the direct connection of the stator windings to the power system network, the power quality of integrated systems is negatively impacted by transient disturbances such as three-phase to ground fault (3LG), rapid load changes [4].

To preserve transient stability, the majority of DFIGs are outfitted with a crowbar system to safeguard the rotor circuit [5]. Additionally, a DC chopper and parallel capacitor are applied across the DC link of the DFIG system to enhance its performance when there is a malfunction. However, none of the crowbar systems, DC choppers, or DC link parallel capacitors can support

grid code maintenance for a DFIG-based WECS for all forms of power system breakdowns. Therefore, the need for auxiliary devices to enhance the DFIG wind power system's transient stability cannot be disregarded.

Flexible AC Transmission System (FACTS) devices are the auxiliary equipment that helps the WECS maintains its fault-ride-through capability. It is stated that the shunt FACTS device is utilized for dynamic VAR correction, which allows us to improve power quality and manage the grid voltage, allowing us to incorporate wind energy into a grid. The most economical way to increase voltage is by adding a FACTS device.

The static synchronous compensator (STATCOM), one of the adopted shunt compensating FACTS devices, is suggested to increase the stability of the DFIG-based wind farm-connected system. Rapid bus voltage control is STATCOM's main immediate benefit for improving transient stability. The STATCOM can be utilized, for example, to improve power transfer during low-voltage conditions, which frequently occur during failures and slow down the acceleration of nearby generators. Reduced demagnetizing effects of faults on nearby generation are another advantage. STATCOMs work similarly to synchronous compensators, with the exception that they lack mechanical inertia and may therefore react to changing system circumstances much more quickly. They lack moving parts and, unlike synchronous machines, do not contribute to short-circuit currents. Due to its symmetric lead-lag capabilities, the system can theoretically change from entire lag to full lead in a few cycles [6].

The STATCOM is already known to increase the transient stability of the wind power system by adjusting the reactive power at the ‘point of common connection. Increased transmittable power during transients is the main goal of reactive shunt compensation in transmission systems. To do this, the power transfer capability is increased or decreased as the machine angle changes. The STATCOM is "overexcited" (capacitive mode) and produces reactive power if the DC capacitor voltage, Vdc, is raised over its nominal value. The STATCOM is "under excited" (inductive mode) and absorbs ‘reactive power’ from the system if the DC capacitor bank's voltage drops below its nominal level. This is exactly comparable to changing the field voltage of the synchronous compensator [7].

The adaptive controller, ANFIS is used to control STATCOM in this thesis because of the benefits of “neural networks and fuzzy logic” are combined in ANFIS, which is especially well suited for applications containing ambiguous input. Secondly, ANFIS models are most

transparent. Thirdly, it is Adaptive learning process which can learn over time and adapt to changes in variable input-output relationships.

1.2 MOTIVATION

Doubly-fed induction generators play a vital role in grid systems. It attracted more attention due to its variable speed, reduced converter cost, fewer switching losses, higher energy efficiency, and the fact that the system can provide leading or lagging reactive power to the grid without additional devices. Additionally, under a situation where the converter current ratings are not sufficient to keep the DFIG at the required point, ancillary reactive power devices, such as static synchronous compensators (STATCOM), can be established in the vicinity of the PCC than shunt capacitors since they have less dynamic performance enhancement in variable speed. The study helps with the following attributes of the latest technology: controllability, wide-range application of STATCOM, and the ability to provide fast support at PCC either by supporting or absorbing reactive power into the system. There is a huge research gap.

1.3 PROBLEM STATEMENT

Adama II wind farm generation utilizes DFIG for its power generation and capacitor banks for their compensation systems. Due to the “direct connection of the stator windings to the grid”, 80% of power flows through the stator without power electronics. Therefore, DFIG more susceptible to transient disturbances such as three phases of ground fault. Additionally, high currents passing through the stator and rotor windings cause stability issues and induce very high DC voltages in the converter circuit. It experiences stability issues due to transmission line faults, wind turbines, generators, and loss of rotor angle problems, among other things. The installed capacitor bank hasn't made a difference in the issue. The best way to address this issue is with a solid state device called a STATCOM, which uses power electronics to regulate power flow and enhance transient stability on power grids by producing reactive power when system voltage is low and absorbing reactive power when system voltage is increased. By offering more VARs at lower voltages with very quick response times and more stability to the power system network, STATCOM offers superior voltage support and enhanced transient stability margin and to reduce maximum overshoot fewer than 50%.

1.4 OBJECTIVES OF THE STUDY

1.4.1 Main objectives of the thesis

The main objectives of the thesis are to improve the transient stability of a doubly-fed induction generator for variable-speed wind energy conversion systems using ANFIS-based STATCOM.

1.4.2 Specific objectives

- To design the mathematical modeling and system model of DFIG-based wind farms
- To model a 48-pulse GTO-based STATCOM and their control system using fuzzy logic as well as an ANFIS controller.
- To simulate with and without STATCOM connected to the PCC of the wind farm to improve the transient stability problem
- To assess the efficiency and performance of ANFIS-based STATCOM in comparison to the existing compensating method.

1.5 SCOPES OF STUDY

As it was mentioned in the introduction, many works on gain tuning for DFIG control are based on optimization techniques to reach a compromise so that the wind system can achieve good performance though not always the most desired under various operating conditions and avoid the worst-case performance under certain extreme conditions. In this thesis, It was used a different mindset to implement the FACTS device control technique. According to the suggested methodology, the DFIG system's fuzzy control gains are dynamically modified based on the dynamic, continuous sensitivity, which effectively shows the dynamic relationship between the change in control gains and the intended output. Because dynamic sensitivity is employed in the control technique, this control strategy does not need any accurate estimation. The disturbance (i.e., the wind speed measurement error) is modeled as random noise for power regulation in WECS and is not forecasted using any presumptive model.

1.6 Significance of the studies

This work can be utilized as input for other wind farms and offers significant insight into future improvements to the investigated wind farm. It also helps to recognize the operational difficulties a power grid with a large wind farm faces investigate the applicability of FACTS devices in improving dynamic performance of wind farms, Assess potential solutions for grid-connected wind farms' performance enhancement and adhere to grid connection specifications and to have efficient operation of wind turbine systems.

CHAPTER TWO

LITERATURE REVIEW

2.1 RELATED WORK

Double-fed induction generator-based variable-speed wind energy systems have emerged as the best option in the current market for wind power, according to **Abdelsattar M et al. [8].** In the DFIG-based wind energy system, the 'turbine blades are connected to the wound rotor induction generator through a gearbox'. Since the rotor windings of DFIG are "connected to the grid" via back-to-back converters and a DC capacitor bank, the stator windings of DFIG are directly "connected to the grid." By allowing the rotor power to operate at a frequency separate from the grid frequency, this design permits speed modulation. There are several advantages to the DFIG system, such as variable speed, which allows for a wide range of wind speeds to be extracted at maximum power. Active and reactive power can be controlled independently. The generator can also provide reactive power to maintain grid voltages. “Flexible alternating current transmission systems (FACTS)”devices offer significant advantages in AC transmission and regulation while responding instantaneously to improve power system stability in voltage and frequency. These things, like “Static Synchronous Compensator (STATCOM)”, “Static VAR Compensator (SVC)”, and “Static Synchronous Series Compensator (SSSC)”, Thyristor Control Series Capacitor (TCSC), and “Unified Power Flow Controller (UPFC)”, can regulate bus voltages, phase angles, and the impedance of transmission lines. STATCOM is connected to a wind farm in different PCCs to improve the overall performance of the system. Furthermore, the STATCOM can prevent the voltage protection system from tripping the wind system, thus keeping the wind system operational throughout grid failures.

Varun Kumar et al [9] suggested that wind energy conversion systems' costs have increased due to the many developments in DFIG and power electronic devices that have become competitive with other energy conversion systems. Several advantages, such as variable speed operation, reduced converter cost, low switching losses, low harmonic injection into the power grid, and the ability to disconnect ‘active and reactive’ power in a grid-integrated system, make the DFIG more efficient and cost-effective than other direct drives and energy conversion systems. In DFIG, 80% of the power flows through the stator without power electronics. Several studies have been done in the field of wind DFIG. Due to the direct connection of the stator

windings to the power system grid, the wind DFIG is more sensitive to transient disturbances such as three-phase to ground fault (LLLG), sudden load changes, and voltage sags and swells. And OWF show negative effects on the power quality of integrated systems. By using dynamic reactive power compensation, we can solve the voltage fluctuation problem. STATCOM is used for dynamic VAR compensation, by which we control the grid voltage and improve power quality, so we can integrate wind energy into a grid.

The a “doubly fed induction generator (DFIG)” has the advantages of being small in size, affordable, and frequently utilized in offshore wind farms, according to **Qin, B et al. [10]**. Flexible control of the stator windings' direct link to the power grid makes DFIG-based WGS particularly vulnerable to grid disruptions during grid voltage decreases. In order to maintain a continuous connection and provide “dynamic reactive power support during grid voltage” dips, or low voltage ride-out (LVRT) capability, many nations have established specific grid codes. DFIG-based WGS without an LVRT approach may become disconnected from the power grid during significant voltage decreases as a result of the interconnected system of wind farms, which could even compromise the stability of the grid.

Megha Vyas et al [11] Discussed on the benefit of DFIGs from generating or absorbing reactive power from the power electronic converter, which reduces the need for capacitor banks in the presence of a squirrel-cage induction generator. Control of the DFIG is performed in a rotating d-q reference frame along the d-axis aligned by the stator flux vector. The control of the stator reactive and active powers is done by changing the rotor voltage and current. Therefore, the rotor current and voltage must be dissipated in the stator's reactive and active power. Among the poor power quality problems, the problem of power surge has become the most acute problem in the advancement of wind power systems because such a surge affects the reliability of the system and causes system malfunction.

Thomas T and Asok P [12] explored regulation of DFIG WECS as ‘active and reactive power’, component and accomplished by regulating the rotor side converter (RSC) and grid side converter (GSC). To prevent stator ‘active and reactive power’ pulsations at sub-synchronous and super-synchronous DFIG speeds, the rotor currents can be used to manage the stator's active and reactive powers. To increase the transient stability of a multi-machine power system, the control of a wind farm's real and reactive power is examined. A mixed active and reactive power control method can be used for the DFIG to enhance the primary frequency support. The ‘active

power' output of the DFIG restricts its capacity for reactive power during wind speed variation. Thus, it is necessary to coordinate the active power output with the reactive power capabilities. Under varying wind speeds, dynamic demand and the reactive power limit are examined. The DFIG system's fault drive capability is increased by using a 'saturated base fault current limiter'. The updated switch type fault current limiter's new construction, which safeguards the DFIG wind turbine from both 'symmetrical and asymmetrical' grid faults, is given. To increase transient voltage stability, a DFIG-based wind farm can be used in conjunction with one superconducting fault current limiter-based passive voltage compensation and transient voltage control-based active voltage compensation.

Boubzizi, S., Abid, H., El Hajjaji, A [13] created more sophisticated WECS control mechanisms. Numerous control strategies have been developed and put into practice for wind power generation with this goal in mind, including vector control based on voltage and flux direction vectors using a d-q rotation frame to decouple active and reactive power. In fact, this approach is sensitive to changes in system parameters such as variations in resistance and inductance. 'Direct torque control (DTC)', which directly regulates the generator torque and stator flux using a specified observation table based on the estimation of stator flux and electromagnetic torque, is presented to address this issue. Similar to the 'direct torque control (DTC)' system, Direct Power Control (DPC) implements this idea. Reactive and active power decoupling, as well as direct control, are the foundations of the DPC control technique. Indeed, crucial concerns are raised by the nonlinear behavior of the mechanical and electrical components of WECS as well as the fluctuations in the electromechanical parameters. The wind turbine (WT) operates at extremely variable wind speeds, which presents a significant control issue. Different control modes are offered for the various DFIG control modes. Although the standard proportional-integral (PI) controller is frequently employed in control applications, it needs to be adjusted whenever the reference patterns change. This controller's sensitivity to outside disturbances and changes in parameters is another significant drawback.

Huang, Yet al [14], discussed briefly on the stator-voltage-oriented vector control technique is used, and PLL is used to provide a spinning d-q reference frame for converter controls with the lagged d-axis aligned with the stator voltage' (we define this reference frame as the PLL reference frame in this study). The 'grid side converter (GSC)' is used to manage the voltage of the 'DC bus capacitor' and to keep the GSC reactive current to zero. The grid-side converter

(RSC) controls the generator speed and the reactive power measured at the grid terminals. Based on the aforementioned simplifications, the inner current-control loops and DC-link dynamics are not taken into account when modeling the RSC and GSC as current sources. Systems for streamlined converter control. The reference current idr_ref that has to be injected into the rotor windings by RSC is calculated by dividing the torque command that the speed regulator generates by the scaled value of stator flux. The var-voltage regulator receives the reactive power instruction from the wind farm management system in order to obtain the reference current irq_ref that needs to be injected into the rotor windings by RSC. In order to keep the reference current igq_ref at zero, the GSC does not transfer any reactive power to the grid. The power that the GSC sends to the grid is assumed to be constantly equal to that from the rotor windings when the dynamics of the DC-link are ignored. The necessity to simulate the PLL under strong grid-strength conditions, as has been the case in the bulk of earlier research, has been shown to be unnecessary because it has been found that in a strong power system, the important eigen values do not vary considerably as the PLL parameters change. However, in weak power systems, modeling the PLL is essential since altering the PLL parameters results in.

Khani, NG [15], suggested that in order to overcome the deep voltage of the point of common coupling PCC and increase the capability of wind farms in asymmetrical fault conditions, Despite their discussion of using the static compensator STATCOM to control wind turbines in fault conditions, This feature is operated and simulated on bus-standard grids to investigate the proper operation of a wind farm on a real grid. Additionally, by controlling the reactive power, deep voltage collapse is prevented during the fault and the wind turbine STATCOM. This is the study's main strength, and their control systems are formulated in that paper.

Milkias et al [16], has exploited a detail influence of the voltage stability and the behaviors of wind plants during different wind speed conditions. The wind plants are run without the implementation of any peripheral devices in that circumstances there are variations in the system like voltage profile, active and reactive powers. These problems can be mitigated with the implementation of the STATCOM, SSSC, and UPFC near to the plants. So the FACTS devices at plants like STACOM,SSSC,UPFC, can provides evidence to the power profiles which have been improved and the voltage fluctuations have been diminished.

Kosuru, R.; Liu, S. and Shi, W. [17], performed best solutions for wind energy conversion systems (WECSs). The two main reasons for using a DFIG in a WECS are its asynchronous

characteristics and the flexibility of utilizing power electronic converters, which results in cost savings due to a lower converter rating. In DFIG-based grid-connected wind systems, the stator is directly connected to the grid, whereas the rotor is connected to the grid by using a back-to-back power electronic converter. Every power network (grid) experiences a lot of disturbances, as there may be a great number of variations, such as voltage, frequency, active power, and reactive power, at the load end or at power generating stations. For any system to operate without disturbances, power system stability and voltage regulation are critical control issues that need to be considered.

Table2. 1 Comparative related Literature

No	Authors	Titles	Methods	Advantages	Disadvantages
1	Ismail Moufid et al [18].	Impact of static synchronous compensator STATCOM installation on power quality improvement.	Using a static VAR compensator (SVC) and a static synchronous compensator.	By compensating reactive energy, the voltage drop can be reduced.	Difficult to control dynamic compensation with classical controller.
2	Yasoda Kailasa Gounder et al[19]	Enhancement of transient stability of the distribution system with SCIG and DFIG-based wind farms using STATCOM.	Several FACT devices, like STATCOM, SVC, and other algorithms	Easily inject and absorb the reactive power to maintain the voltage profile.	Complexity of several switches in FACTS devices.
3	Ayyarao et al [20]	Modified vector-controlled DFIG wind energy system based on barrier function adaptive sliding mode control.	Conventional vector control sliding-mode control.	The control parameter is updated at every instant based on the positive semi-definite barrier function.	Limitation to control both active and reactive power transfer.
4	Mr. Ketan G Damor et al [21]	Improving Power System Transient Stability by using Facts Devices**.**	All first- and second-generation FACTS devices.	Applicable to fix any kind of stability problem. i.e., steady state, transient.	Less efficient and costive.

2.2RESEARCH GAP

The majority of authors in the literature review have employed several techniques to increase the stability of power systems, including DC chopping, Crowbar protection, parallel capacitors and FACTS with classical controller to protect the grid or wind farm from faults. However, none of them can contribute to the grid code's upkeep. And also the aforementioned review's control technique did not take into account how much reactive power would need to be injected or absorbed by the system. Therefore, utilizing STATCOM devices with adaptive controller, enhance the transient stability of the DFIG wind power system can be disregarded. Instability in the power systems, such as a lack of wind speed, causes generator outages, which result in transient's on the grid.

This writing concentrated on the efficient and effective FACTS devices known as STATCOM, and it briefly explored control techniques (ANFIS). Here Capacitor Bank reduce high transient of Stator Voltage from 3160V to 1710V during faulty condition. However it is more than doubles of Stator Voltage of WT. therefore by utilizing ANFIS based STATCOM technology it is expected to improve more than half of existing overshoot time (fewer than 50% overshoot).

2.3 DESCRIPTION OF CASE STUDY AREA (ADAMA WIND FARM II)

The case study here is Adama-II Wind Farm, located in the southeastern part of the country, 95 km from Addis Ababa and 7 km from Adama town. The farm's elevation ranges from 1741 to 2173 m, and its central location is at the latitude of N 008° 34' 18" and longitude of E 039° 12' 10'. The figure2.1 shows the location map of the wind farm.

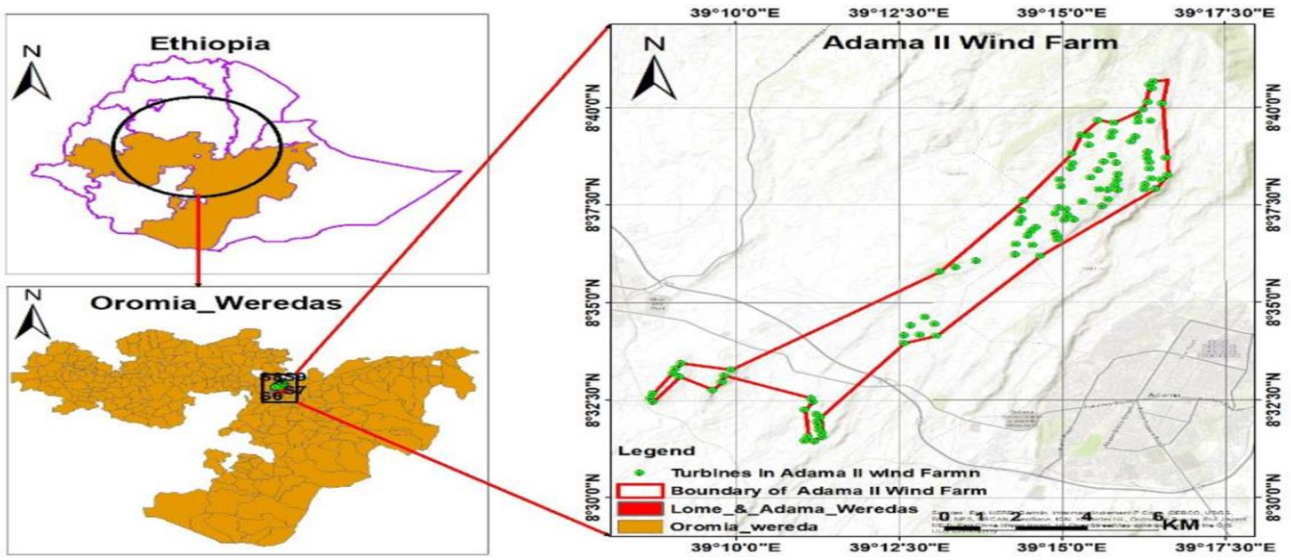

Figure2. 1Location of adama wind farm

Figure2. 2: Location of Adama II Wind Farm

2.4 Layout diagram of ADAMA II Wind farm

The Adama II wind farm has 102 turbines. Each turbine is attached to unit transformers that step up the generator voltage (690 V) to a medium voltage level of 33 kV, and all are grouped into eight clusters (cluster A to cluster H). Except for one of the clusters that has eleven turbines, the remaining seven clusters have thirteen turbines each, grouped together, and a 33 kV overhead

line connects each cluster to the main substation. The high-voltage terminal side is connected to the Koka substation with a single 230 kV overhead transmission line. The layout of the Adama II wind farm is shown in the Figure 2.3. A cluster is a group of wind turbines that are located at a site to generate electricity.

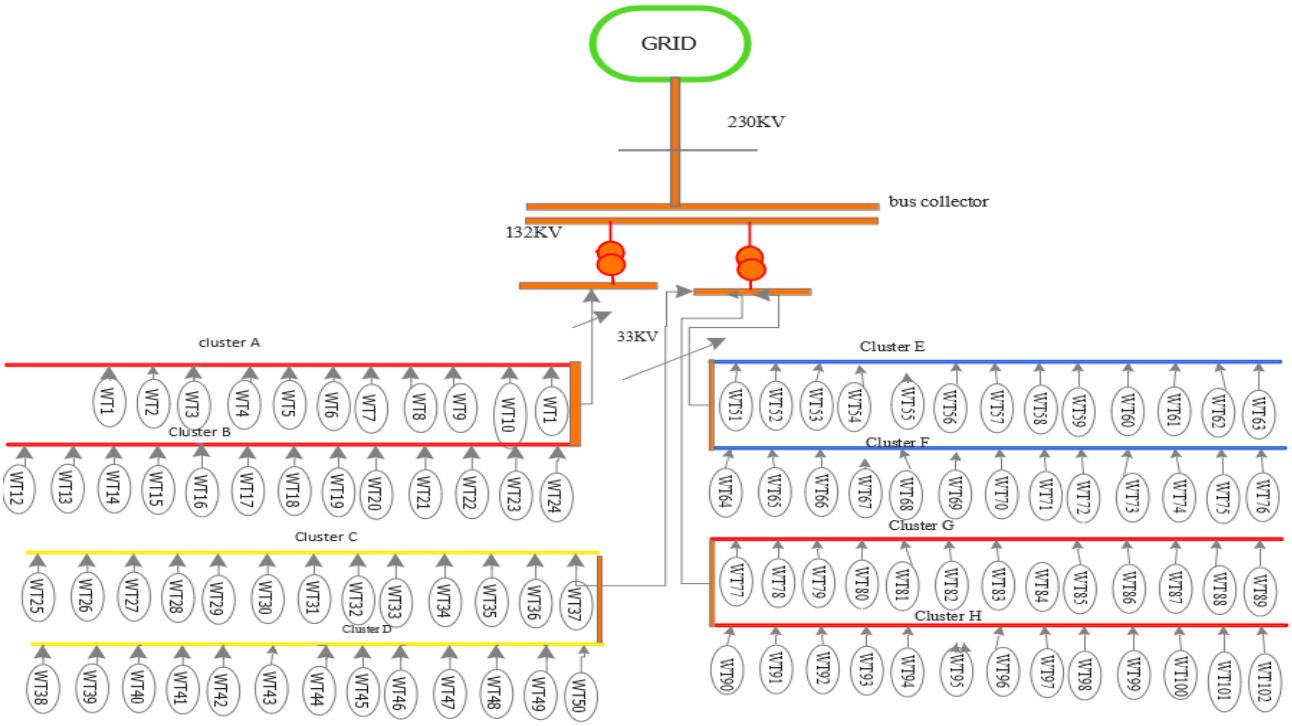

Figure2. 3Layout diagram of whole cluster

2.5 Some International Standards on Transient Stability

There are several standards and guidelines that provide recommendations for establishing acceptance criteria for transient stability indices.

The International Electro-technical Commission (IEC) has published several guidelines and standards related to wind turbine power quality. These guidelines specify the requirements for the electrical performance of wind turbines and provide recommendations for testing, Validating and measurement of their power quality.

The IEC 61400-13 standard provides guidelines for the design, installation, and operation of wind turbines to ensure that they meet the power quality requirements of the grid. It specifies the requirements for the electrical components of wind turbines, such as the generator and power electronics, to ensure that they are capable of meeting the power quality requirements of the grid.

Some IEC standards code IEC 61000 2-1:1990, IEEE 1159:1995, IEC816:1984 briefly describes the transient stability issues [22].

Here are some commonly referenced standards and guidelines in the power system industry:

IEEE Standard 421.5-2019: IEEE Guide for Transient Stability Assessment of Electric Power Systems (formerly known as IEEE Standard 1410): This standard provides guidance on transient stability assessment and includes recommendations for acceptance criteria.

CIGRE Technical Brochure 74: Transient Stability Assessment Techniques: This technical brochure by the International Council on Large Electric Systems (CIGRE, "Conseil International des Grands Réseaux Électriques" in French) provides guidance on transient stability assessment techniques. It covers various aspects of transient stability analysis, including stability indices and their use in assessing system stability. It also discusses acceptance criteria based on different indices and provides examples of their application.

NERC Reliability Standards: The North American Electric Reliability Corporation (NERC) develops and enforces reliability standards for the bulk power system in North America. While NERC standards may not directly provide acceptance criteria for transient stability indices, they establish requirements for maintaining system stability and reliability. Compliance with these standards indirectly influences the acceptance criteria used in the industry. This all standards and guidelines provide recommendations for establishing acceptance criteria for transient stability indices based on The International Electro-technical Commission (IEC).

2.6 WHY STATCOM FOR COMPENSATIONS

Capacitors are usually connected to fixed-speed wind turbines to increase the system voltage while sinking the reactor power. Mechanically switched fixed shunt capacitors can increase the voltage stability limit of the system, but they are not very sensitive to voltage changes. The dynamic response of capacitors is not good. STATCOM is the best option for dynamic reactive power compensation as it can generate more reactive power than other FACTS devices like the Static Var Compensator [23]at a lower than normal voltage range in terms of active compensation. The capability is very similar to STATCOM, but its basic operating principle is different. A STATCOM acts as a parallel synchronous voltage source, and an SVC acts as a parallel controlled reactive acceptor. This difference explains the superior functional characteristics, better performance, and greater application flexibility of STATCOM compared to those achievable with SVC. A STATCOM can control its output current independently of the

AC system voltage through the maximum rated capacitance or inductance range, while the SVC's maximum achievable compensation current decreases linearly with the AC voltage. In addition, the STATCOM typically exhibits a fast response because the firing of the thyristor does not cause a delay [24]. The performance and total load of wind turbines fluctuate continuously throughout the day. Reactive energy compensation is required to maintain normal voltage levels on the power grid. Connecting a STATCOM can minimize reactive power imbalances that can seriously affect the power grid. A STATCOM can help meet the low-voltage drive requirement as it can operate at full capacity even at low voltage. Additionally, the STATCOM can be connected to any voltage level in the power grid using a coupling transformer with a suitable turn's ratio. A STATCOM can easily be connected to an already-installed wind generator that has a voltage regulation problem.

Table2. 2 Comparison of Existing and proposed Compensation Method

No	Capacitor	STATCOM
1	takes up large space	takes up little space
2	Bulky	It substitutes small converters for the bulky passive banks and circuit components
3	It take time to inject/absorb	a very quick response time
4	Difficult to compensate in variable speed	Able to compensate in variable speed
5	Lag (capacitive)	Can lag/lead(capacitive-inductive)

CHAPTER THREE

METHODOLOGY

Due to their high efficiency and enhanced grid integration potential, DFIG-based WECS are a well-liked option for producing wind energy. DFIG-based WECS can help fulfill the rising demand for renewable energy by capturing more wind energy by adjusting the rotor-side power electronics and running at varying speeds. [25].

3.1 Components of DFIG-based WECS

DFIG-based WECS basically consists of a generator, wind turbine with drive train system, RSC, GSC, DC coupling capacitor, pitch controller, and coupling transformer, as shown in the Figure 3.1. Conventional double-fed induction generators (DFIGs) are basically three-phase wound rotor induction machines where alternating current is injected into both the stator and rotor windings. The basic configuration of a DFIG-based wind turbine system is that the stator of the machine is directly connected to the grid through a transformer, and the wound rotor is also connected to the grid using AC/DC power DC-AC converters. Two three-phase pulse width modulated (PWM) voltage source converters. The rotor side converter (RSC) and the grid side converter (GSC) are connected to a common DC link. In this research, the vector control method was used to control the RSC and GSC controllers of the DFIG, which is described in detail in [26]. The main reasons for the acceptance of DFIG in wind energy applications are that it provides better performance for variable-speed wind turbine systems. In addition, relatively small power converters are required to control the generator. As shown in Figure 3.1, the power converter using the DFIG is typically 25% to 30% of the system power rating. This converter reduces the power dissipation of the electronic converter compared to the system that has to transfer all the power. System costs are also reduced by using partially rated power converters.

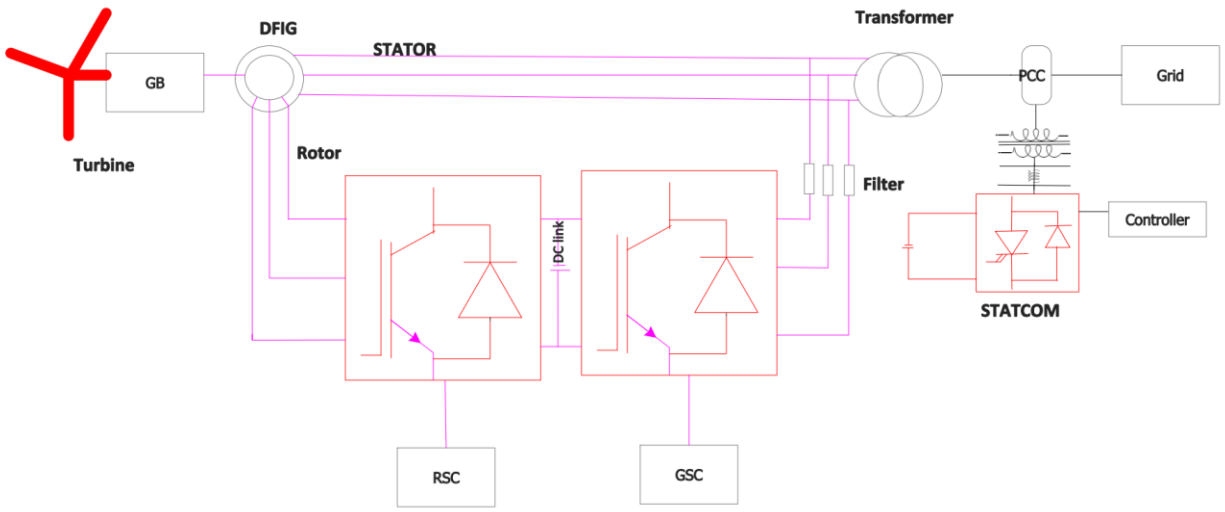

Figure3.1: Overall Circuit model of DFIG

3.2 DFIG Model

DFIG consists of stator windings and rotor windings with slip rings. The stator consists of three-phase insulated windings, which provide the desired pole arrangement, and is connected to the grid through a three-phase transformer. Similar to the stator, the rotor is made up of three-phase insulated windings. The rotor windings are connected to an external stationary circuit through a set of slip rings and brushes. These components allow the controlled rotor current to either be injected into or absorbed by the rotor windings. The dynamics of the DFIG are represented by a fourth-order state-space model using the synchronously rotating reference frame (q-d-frame).

3.2.1 Clarke transformation Model

Consider a symmetrical three-phase induction machine with stationary a-phase, b-phase, and c-phase axes placed at a 120◦ angle to each other, as shown in Figure 3.2. The main aim of a Clarke transformation is to transform the three-phase stationary frame variables into two-phase stationary frame variables α and β, and vice versa. Any three-phase voltage or current χ in a-b-c components can be converted into α-β components via Clarke transformation and can be represented in the matrix as;

$$\begin{matrix} V\alpha \\ V\beta \\ Vo \end{matrix} = \frac{2}{3}\begin{bmatrix} 1 & -\frac{1}{2} & -\frac{1}{2} \\ 0 & \frac{\sqrt{3}}{2} & \frac{-\sqrt{3}}{2} \\ \frac{1}{2} & \frac{1}{2} & \frac{1}{2} \end{bmatrix} \begin{matrix} Va \\ Vb \\ Vc \end{matrix} \quad \text{.....3.1}$$

V0 is the zero-sequence component, which equals to zero for symmetrical three phase variable

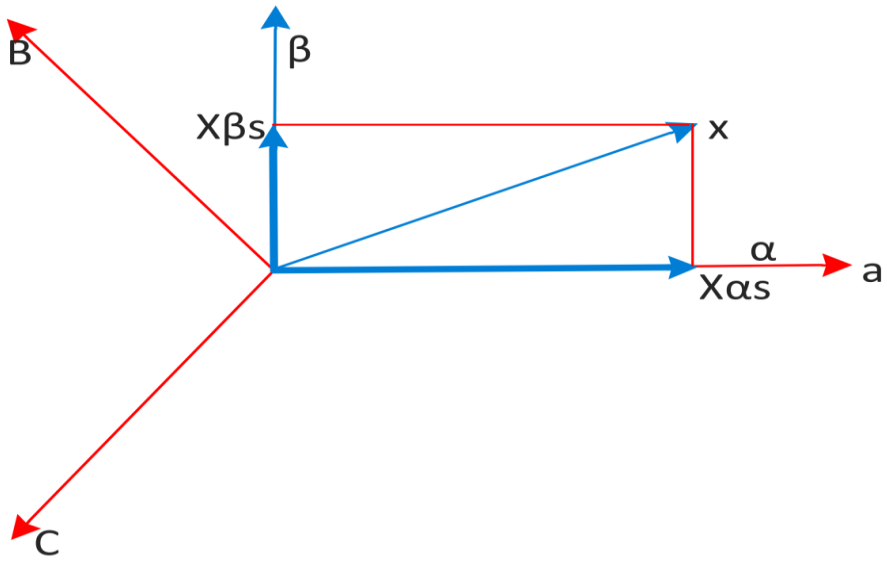

Figure3.2: a-b-c to α - β axes transformation of stationary frame

3.2.2 D-q axis transformation (park model)

The direct quadrature zero conversion is a mathematical conversion that facilitates the analysis of three-phase circuits where three AC quantities are converted to two DC quantities. Various mathematical calculations are performed on the imaginary DC quantities, and the AC quantities are recovered by an inverse transformation of the DC quantities. It is very similar to the Clarke transform and solves the problem of AC parameters changing with time [27]. Used to simplify the analysis of three-phase circuits where three AC quantities are converted to two DC quantities. Due to a smooth air gap in the induction machine, the self-inductances of both the stator and rotor coils are constant, but the mutual inductances vary with rotor motion with respect to that of the stator. Therefore, the real-time analysis of the induction machine becomes very complex due to the different mutual inductances because the voltage is nonlinear. Therefore, changing the variables for the "stator and rotor" parameters is used to eliminate the effect of varying mutual inductances. This conversion results in an imaginary magnetically decoupled two-phase machine. The orthogonally arranged symmetrical windings are called d and q windings and can be considered stationary or rotating in relation to the stator. In the steady-state frame, the ds and qs axes are fixed to the stator, with either the ds or qs axis being coincident with the phase axis of the stator. In the rotating frame, the rotating d-q axes can either be fixed to

the rotor or move at synchronous speed. Here we have three phases with 120 angle differences each. This can also be seen in the figure3.3. Our purpose is to transform the three phases into a stationary (d-q) axis and then into a rotating frame.

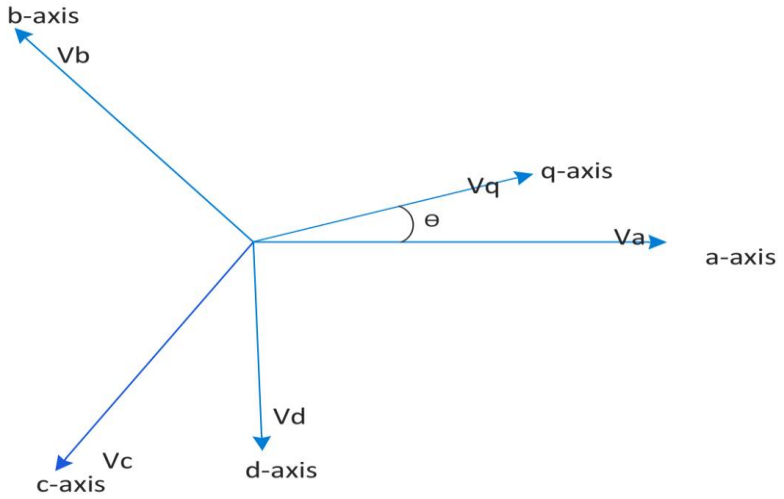

Figure3. 3Transformation of 3 phase's a-b-c to ds-qs axes

3.2.3 Transformation from Stationary to Rotating Axes

A Park transformation transfer variable from a two-phase stator stationary reference frame to a two-phase rotating reference frame through the rotation transformation matrix Tp(θ), as shown in Figure 3.4.

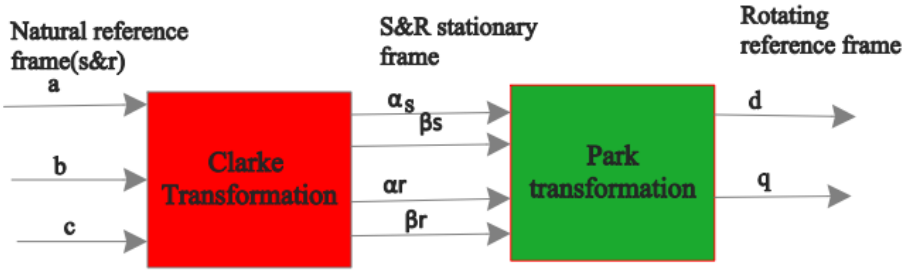

Figure3. 4Transformation of reference frames

$$\begin{matrix} id \\ iq \end{matrix} = \begin{vmatrix} \cos\theta & \sin\theta \\ -\sin\theta & \cos\theta \end{vmatrix} \begin{matrix} i\alpha \\ i\beta \end{matrix} \quad \text{.....3.2}$$

Where Tp(θ) is the park transformation matrix

$$Tp = \begin{matrix} cos\theta & sin\theta \\ -sin\theta & cos\theta \end{matrix} \quad \text{.....3.3}$$

Where θ is the angle between d-axis and α-axis

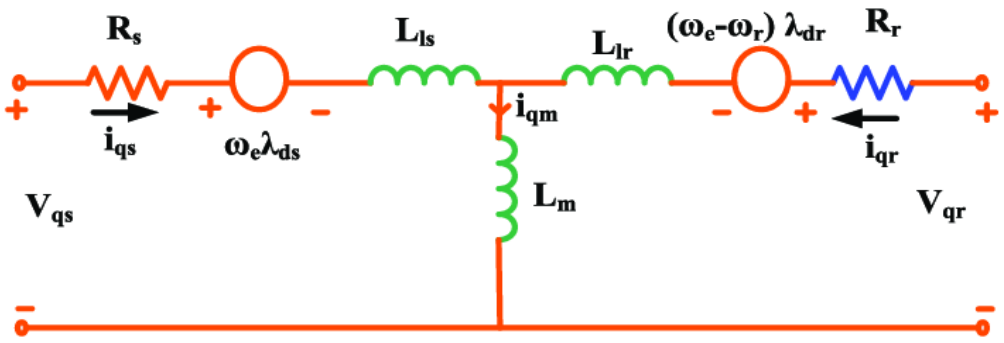

Figure3. 5 q-axis equivalent circuit of DFIG in synchronous (d-q) frame

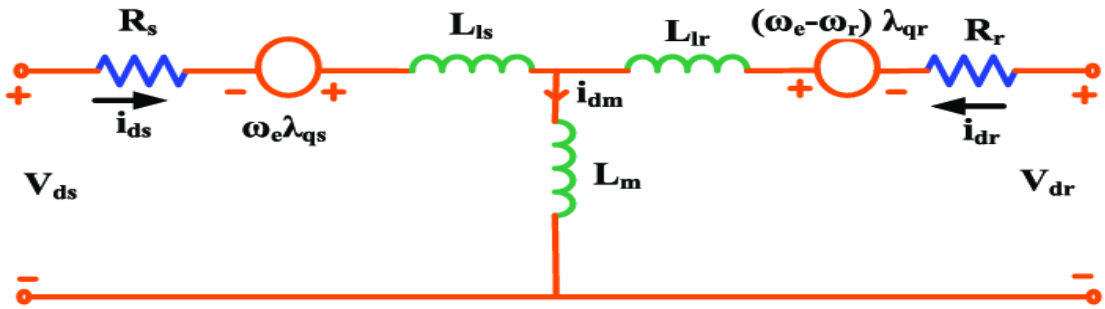

Figure3. 6 d-axis equivalent circuit of DFIG in synchronous (d-q) frame

i. Stator Voltage

$$Vds = Rs.ids - \omega s\boldsymbol{\phi qs} + \frac{d\phi ds}{dt} \quad \text{.....3.4}$$

$$Vqs = Rs.iqs + \omega s\phi ds + \frac{d\phi qs}{dt} \quad \text{.....3.5}$$

ii. Rotor Voltage

$$Vdr = Rr.idr - S\omega s\phi qr + \frac{d\phi dr}{dt} \quad \text{.....3.6}$$

$$Vqr = Rr.iqr + S\omega s\phi dr + \frac{d\phi qr}{dt} \quad \text{.....3.7}$$

Where ϕ Flux linkage

$$\phi ds = Ls.ids + Lm\,idr \quad \text{.....3.8}$$

$$\boldsymbol{\phi qs} = Ls.iqs + Lm\,iqr \quad \text{.....3.9}$$

$$\phi dr = Lr.idr + Lm.ids \quad \text{.....3.10}$$

$$\phi qr = Lr.iqr + Lm.iqs \quad \text{.....3.11}$$

Where

- ✓ Rs, Rr, Ls, and Lr are respectively the resistances and inductances of the stator and rotor windings,

- ✓ $L_s = L_m + L_{ls}$
- ✓ $L_r = L_m + L_{lr}$
- ✓ L_{ls} and L_{lr} are the stator and rotor leakage inductance respectively and L_m is the magnetizing inductance
- ✓ Vds, Vqs, Vdr, Vqr, ids, idr, iqs, iqr, ϕds, ϕdr, ϕqs, ϕqr, are direct and quadrate components of the space phasors of the stator and rotor voltages, currents, and flux, respectively**[16].**

All the equations above are induction motor equations. When the induction motor operates as a generator, the current direction will be the opposite. Assuming negligible power losses in stator and rotor resistances, the active and reactive power outputs from the stator and rotor sides are given as:

The active and reactive powers at the stator are defined as

$$Ps = \frac{3}{2}(Vds\ ids + Vqs.iqs) \quad \text{.....3.12}$$

$$Qs = \frac{3}{2}(Vqs\ ids - Vds.iqs) \quad \text{.....3.13}$$

The active and reactive powers at the rotor are defined as

$$Pr = \frac{3}{2}(Vdr\ idr + Vqr.iqr) \quad \text{.....3.14}$$

$$Qr = \frac{3}{2}(Vqr\ idr - Vdr.iqr) \quad \text{.....3.15}$$

The total active and reactive power generated by DFIG is:

$$Pt = Ps + Pr.. \quad \text{.....3.16}$$

$$Qt = Qs + Qr \quad \text{.....3.17}$$

If P_{Total} and/or Q_{Total} are positive, DFIG is supplying power to the power grid, else it is drawing power from the grid.

The electromagnetic torque is created by the interaction of the air gap flux and the magneto motive force (mmf) of the rotor. At synchronous speed, the rotor cannot see the moving magnetic field. As a result, there is no question of the induced emf as well as the rotor current, so the torque becomes zero. But at any speed other than synchronous speed, the machine experiences torque. This is true in the case of motors, while it is not true in the case of wind turbine generators.

The electromechanical torque is provided by the prime mover, which in DFIG-based WECS is a wind turbine.

The rotor speed dynamics of the DFIG is given as:

$$\frac{d}{dt}\omega r = \frac{p}{2J}(Tm - Te - Cf\omega r) \quad \text{.....3.18}$$

Where p is the number of poles of the machine, Cf is friction coefficient, J is inertia of the rotor, Tm is the mechanical torque generated by wind turbine, and Te is the electromagnetic torque generated by the machine which can be written in terms of flux linkages and currents as follows:

$$Te = \frac{P}{2}(\lambda qs\ ids - \lambda ds\ iqs) \quad \text{.....3.19}$$

Where positive or negative values of Te mean DFIG works as a generator (motor),

A 1.5 MW, 690 V, 50 Hz, 1500 rpm DFIG wind energy system and other parameters are given in Appendix I. In the manufacturer's "ABB wind turbine converters manual, the rated stator current is given as 1110A. It has a negative sign during generating mode. Thus, Rated Mechanical Torque (TM) can be calculated as follows:

$$Tm = \frac{3p[Vs^2 - (2Rs * is - Vs)^2]}{4Rs\omega s} \quad \text{.....3.20}$$

Where, P is number of pole pairs

$$Tm = \frac{3.2.[690^2 - (2 \times 0.006243 \times 1110 - 690)^2]}{4 \times 0.006243 \times 2\pi(50)} = 8.3\text{KNM}$$

Using the equivalent circuit of Figure 3.1**,** the voltage across the magnetizing branch is

$$Vm = Vs - Is(Rs + j\omega sLls) \quad \text{.....3.21}$$

$$Vm = 690\angle 0° - 1110\angle 180°(0.006243 + j100\pi \times 0.00019882)$$

$$Vm = 472.7\angle 8.4°$$

The magnetizing current is calculated by

$$Im = \frac{Vm}{j\omega s.Lm} \quad \text{.....3.22}$$

$$Im = \frac{472.7\angle 8.4°}{j100\pi \times 0.00376} = 378.6\angle 278.4°$$

Now rotor current is calculated as below

$$Is = Im + Ir \quad \text{.....3.23}$$

$$Ir = Is - Im \quad \text{.....3.24}$$

$$Ir = 1110\angle 180° - 378.6\angle 278.4° = 1232\angle 162.4°$$

In order to transform the DFIG model, in natural co-ordinates, into its equivalent space phasor form, the 120º operator is introduced:

$$a = e^{j120} \ \ and \ \ a^2 = e^{j240}$$

Thus, the current stator space phasor can be expressed as follows:

$$Is = ise^{j240}$$

$$Is = ids + jiqs \text{.....3.25}$$

$$Is = 1110\angle 180° = 0 - \text{j}1110$$

$$RE(Is) = RE\left[\frac{2}{3}(ias + aibs + a^2ics)\right] = ids = 0$$

$$IM(Is) = IM\left[\frac{2}{3}(ias + aibs + a^2ics)\right] = iqs = 1110$$

In similar way, rotor current can be expressed as follow;

$$Ir = idr + jiqr \text{.....3.26}$$

$$ir = \left[\frac{2}{3}(iar + aibr + a^2icr)\right]$$

$$RE(ir) = RE\left[\frac{2}{3}(iar + aibr + a^2icr)\right] = idr$$

$$IM(ir) = IM\left[\frac{2}{3}(iar + aibr + a^2icr)\right] = iqr$$

$$Ir = 1232\angle 162.4° = -1173.8 + \text{j}373.3$$

$$Idr = -1173.8 \text{ and iqr} = 373.3$$

Now rotor voltage will become

$$Vr = sVm - Ir(Rr + js\omega s.Llr) \text{.....3.27}$$

$$Vr = -0.2 * 472.7\angle 8.4^0 - 1232\angle 162.7^0(0.011074 + j(-0.2) * 314 * 0.00019882)$$

$$Vr = 91.2\angle 200.9^0 = -85.2 - j32.6$$

The active and reactive powers at the stator are defined as

$$Ps = \frac{3}{2}[Vds\ ids] = \frac{3}{2}(690 * 0)$$

$$Qs = -\frac{3}{2}\ Vds.iqs = -\frac{3}{2}(\ 690 * 1110) = 1.15MVAR$$

The active and reactive powers at the rotor are defined as

$$Pr = Vdr * idr + Vqr * iqr$$

$$Qr = \frac{3}{2}[Vqr\ idr - Vdr.iqr] = 32.6 \times 1{,}173.8 + j85.2 \times 373.2$$

$$Qr = \frac{3}{2}(38{,}265.9 + j31{,}796.64) = 74.63KVAR$$

$$Qt = Qs + Qr$$

$$Qt = 1.15 + 0.07463 = 1.2246MVAR$$

3.3 DFIG performance during fault

For a synchronously rotating reference frame, the equations of an induction machine can be described as follows [28], where all the parameters and variables are considered from the stator side.

$$\tilde{V}s = Rs * Is + \frac{d(ls\ is + lm\ ir)}{dt} + j\psi s * \omega s \quad \text{.....3.28}$$

$$\tilde{V}r = Rr * Ir + \frac{d(lr.ir + lm.is)}{dt} + j(\omega s - \omega r)\psi r \quad \text{.....3.29}$$

Where

$$Ls = Lm + Lsl \quad \text{.....3.30}$$

$$Lr = Lm + Lrl \quad \text{.....3.31}$$

V, i, ψ, R, and L indicate the voltage, current, flux linkage, resistance, and inductance, respectively. And the subscripts s, r, m, and l symbolize the stator, rotor, mutual, and leakage quantities, respectively.

The equivalent circuit of the induction machine in order to analyze the transient stability is shown in Figure3.7.

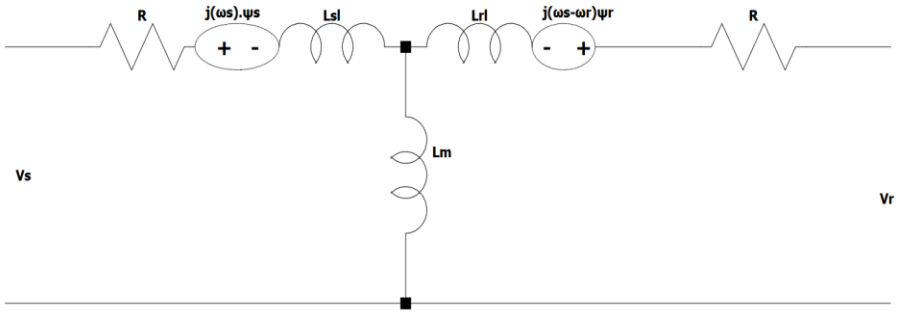

Figure3. 7 Equivalent circuit of induction machine for transient stability

The stator and rotor current can be written as follows

$$is' = \frac{1}{Ls-\frac{Lm^2}{Lr}}\psi s - \frac{Lm}{Lr}\frac{1}{Ls-\frac{Lm^2}{Lr}}\psi r \quad \text{.....3.32}$$

$$ir' = -\frac{Lm}{Lr}\frac{1}{Lr-\frac{Lm^2}{Ls}}\psi s + \frac{1}{Lr-\frac{Lm^2}{Ls}}\psi r \quad \text{.....3.33}$$

The transient stator and rotor inductances are introduced, which are represented by, Ls', and Lr'.

$$L's = Lsl + \frac{Lm.Lrl}{Lm+Lrl} \quad \text{.....3.34}$$

$$L'r = Lrl + \frac{Lm.Lsl}{Lm+Lsl} \quad \text{.....3.35}$$

The stator and rotor coupling factors are Ks and Kr, respectively, which can be represented by

$$Ks = \frac{Lm}{Ls} \quad \text{.....3.36}$$

$$Kr = \frac{Lm}{Lr} \quad \text{.....3.37}$$

Leakage factor is represented by l, which is as follows

$$l = 1 - \frac{Lm^2}{Ls.Lr} \quad \text{.....3.38}$$

Now, both the stator and rotor currents can be simplified by the following two equations

$$is = \frac{\psi s}{Ls'} - Kr\frac{\psi r}{Ls} \quad \text{.....3.39}$$

$$ir = -Ks\frac{\psi s}{Lr'} + \frac{\psi r}{Lr'} \quad \text{.....3.40}$$

3.4 Drive Train Model

Doubly-Fed Induction Generator is a type of electrical generator commonly used in wind turbines. In a wind turbine, the DFIG is connected to the wind turbine rotor, which is rotated by the force of the wind. The DFIG then converts the rotor's mechanical energy into electrical energy that can be transmitted to the power grid. adama II wind farm generated by the variable speed but rated speed is 12m/s, 6.2 tip-speed ratio, air density of 1.225 kg/m3, at diameter of 75m blades, ,and other parameters are given in Appendix I. Thus, rotational speed of rotor, tip-speed and gear ratio is needed to match the rotor speed to the generator speed can be calculated as follows:

$$\lambda = \frac{\Omega R}{V} \quad \text{.....3.41}$$

The rotational speed (rpm) of the rotating part of the wind turbine at a tip-speed ratio of 6.2 is calculated as

$$\Omega = \frac{\lambda * V}{R} = \frac{6.2 * 12m/s}{37.5m} = 1.984 rad/sec$$

$$Nrotor = \frac{\Omega(rad/sec)(60sec/min)}{2\pi\ rad/rev} = 19\ rpm$$

Now the tip speed is calculated as;

$Utip = \Omega R$. This is equivalent to (1.984rad/sec*37.5m)=74.4m/s.

The gearbox is used to increase the speed of the rotor so that it can turn the generator at the required speed. The gearbox also helps to match the rotational speed of the rotor to the generator. If the generator turns at super synchronous speed, the amount of gear ratio needed to match the rotor speed to the generator speed is calculated as

$GR = \frac{Ngenerator}{Nrotor} = \frac{1800rpm}{19rpm} = 94.7$ ……3.42

The DFIG drive train model is designed to maximize the efficiency of the wind turbine and to ensure that the power generated by the turbine is of the appropriate quality for transmission to the power grid. The control system of the DFIG drive train model plays an important role in regulating the power output of the wind turbine based on wind conditions and in maintaining the stability and reliability of the power grid.

3.5 Wind Turbine and Pitch Controller

The power contained in the form of kinetic energy in the wind crossing at a speed and surface area is denoted by

$P = \frac{1}{2}\rho A v^3$……3.43

The wind turbine can recover only a part of that power:

$P = \frac{1}{2}\rho A v^3 Cp$……3.44

Cp is known as 'Power co-efficient' and it is a function of Tip-Speed Ratio and pitch angle, where tip-speed ratio, $\lambda = \frac{\Omega R}{V}$

The torque generated by the rotor has been defined by the following expression:

$T = \frac{P}{\omega} = \frac{1}{2\omega}\rho A v^3 Cp = \frac{1}{2}\pi R^3 v^2 Ct$……..……3.45

Where, Ct is the co-efficient of torque. Cp and Ct are related as

$Cp(\lambda) = \lambda\, Ct(\lambda)$……3.46

Both Cp and Ct are functions of pitch angle and tip-speed ratio. Their relationship is shown in Figure 4.8. Figure4.8a shows wind power can be expressed in terms of turbine torque i.e. aerodynamic torqueis obtained from the power received and the speed of rotation of the turbine. Figure 4.8b shows power curve during pitch angle is zero which indicates the maximum power is captured at this point on curve

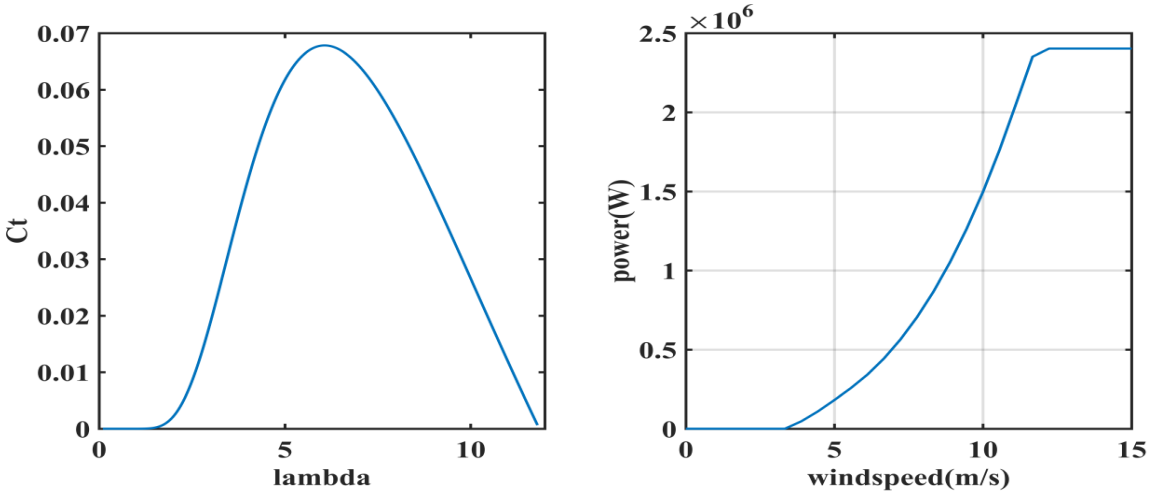

a) Ct Vs λ and power curve

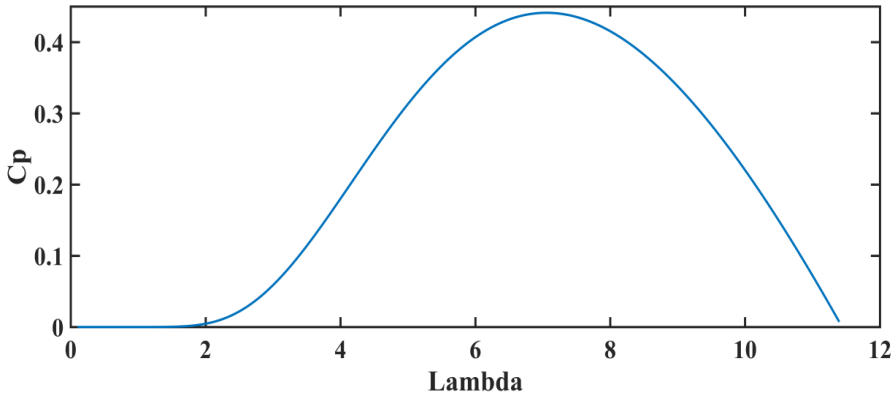

b) Cp Vs λ curve

Figure3. 8; a) Ct Vs λ curve with respective power curve ,b) Cp Vs λ curve

For wind turbine, pitch control system is important for power limitation purpose at high wind speed condition i.e. greater than rated wind speed.

- For P*out*< P*rated*, the blade pitch is kept fixed. This is generally done to limit the pitch mechanism
- At P*out* ≥ P *cut-out*, the blade is pitched to a position that minimized the rotor aerodynamic torque.
- Mechanical or electrical/reactive breaking is sometimes used to further prevent rotor rotation above P *cut-out*, Pitch control technique

Here P*out* denotes mechanical output power; P *cut-out* denotes power output at cut-out wind speed and P*rated* denotes rated output power of generator

3.6 Load flow analysis

Load flow analysis is a power system analysis technique used to calculate the steady-state voltage and current flow in a power system under various operating conditions. Load flow analysis is also known as power flow analysis or load flow calculation. It is a fundamental tool for power system planning, design, and operation.

The three methods used for load flow analysis are, Gauss seidel Methods, Newton-Raphson method and Fast Decoupled method. The Newton-Raphson method is the most efficient load-flow algorithm. Because of no approximations in Newton-Raphson algorithm and it's based on the formal application of a well-known algorithm for the solution of simultaneous non-linear equations. As shown in APPENDIX-II the weak bus is determined by this method.

The load flow analysis provides information about the voltage level, power flow, and losses in the system. The key outputs of the load flow analysis are primarily used to ensure the voltage levels at all the buses in the system within acceptable limits. Secondly, it helps to identify power flow bottlenecks and ensure that the power flow in the system is within equipment limits, and lastly it help to identify areas of high losses and to optimize the system maximum efficiency.

3.7 Transmission Line Parameter of Wind farms

Adama II wind turbine Consider the following data:-

$$Vb = 230KV$$

$$Sb = 100MVA$$

Where; Vb and Sb are base voltage and base power, respectively. The formula that is used for length of transmission can be as follows:

$L = \frac{\sqrt{XB}}{2\pi f} \times v$ ……3.47

Where L is length of transmission line in kilometers from cluster B to Grid which is 6.18 KM, X is reactance of cluster B=0.048pu, B is susceptibility per unit, f is system frequency, and v is speed of light in kilometers per second, but speed of light in meters per second is when it changes to km/s which is 3*10^5Km/s.

The transmission line parameter calculation is as follows: The transmission line parameter consists of resistance, capacitance, and inductance, and some formulas can be used for calculation:

$$Ractual = Rbase * Rpu$$

$$Xactual = Xbase * Xpu$$

$$Bactual = Bbase * Bpu$$

$$Cactual = Bactual/2\pi f$$

$$Lactual = Xactual/2\pi f$$

$$Rbase = Xbase = \frac{Vbase^2}{Sbase}$$

$$Bbase = \frac{Sbase}{V^2base}$$

Transmission line parameter, sequence of transmission line parameter for Selected cluster (B) can be as follows: - Positive and zero sequence Resistance can be:-

$$B = \frac{(L2\pi f)^2}{X.Vb^2} = \frac{(6.18 * 2 * 3.14 * 50)^2}{0.048(3 * 10^5)^2} = 8.72e - 4\mho$$

Base resistance is calculate as

$$Rbase = \frac{Vbase^2}{Sbase} = \frac{(230e3)^2}{100e6} = 529$$

$$Ractual = Rbase * Rpu = 529 * 0.126 = 66.65\Omega$$

Base susceptibility is calculate as

$$Bbase = \frac{1}{Rbase} = \frac{1}{529} = 1.89e - 3\mho$$

$$Bactual = Bbase * Bpu = 1.89e - 3\mho * 8.72e - 4 = 1.648e - 6\mho$$

Positive and zero sequence resistance calculate as

$$R1\left(\frac{\Omega}{KM}\right) = \frac{Ractual}{line\ length} = \frac{66.65}{6.18} = 10.78\frac{\Omega}{KM}$$

$$\mathrm{R0}\left(\frac{\Omega}{\mathrm{KM}}\right) = 3 * \mathrm{R} = 3 * 10.78 = 32.35\frac{\Omega}{\mathrm{KM}}$$

Positive and zero sequence capacitance can be:-

$$\mathrm{Cactual} = \frac{\mathrm{Bactual}}{\text{line length}} = \frac{(1.68 * 10^{-6})}{2 * 3.14 * 50} = 5.248 * 10^{-9}\mathrm{F/KM}$$

$$\mathrm{C1}\left(\frac{\mathrm{F}}{\mathrm{KM}}\right) = \frac{\mathrm{Cactual}}{\text{line length}} = \frac{5.248 * 10^{-9}}{6.18} = 8.49 * 10^{-10}\mathrm{F/KM}$$

$$\mathrm{C0}\left(\frac{\Omega}{\mathrm{KM}}\right) = 3 * \mathrm{C1} = 3 * 8.49 * 10^{-10} = 2.54\mathrm{nF/KM}$$

Positive and zero sequence inductance can be:-

$$\mathrm{Xactual} = \mathrm{Xbase} * \mathrm{Xpu} = 529 * 0.06 = 31.74\mathrm{H}$$

$$\mathrm{Lactual} = \frac{\mathrm{Xactual}}{2\pi f} = \frac{31.74\mathrm{H}}{100\pi} = 0.101083\mathrm{H/KM}$$

$$\mathrm{L1}\left(\frac{\mathrm{H}}{\mathrm{KM}}\right) = \frac{\mathrm{Lactual}}{\text{line length}} = \frac{0.1145}{6.18} = 0.01646\mathrm{H/KM}$$

$$\mathrm{L0}\left(\frac{\Omega}{\mathrm{KM}}\right) = 3 * \mathrm{L1} = 3 * 0.0185 = 0.049389\mathrm{H/KM}$$

3.8 Control of DFIG-based WECS

The DFIG-based WECS control system consists of two parts: the electrical control of DFIG and the mechanical control of the wind turbine speed and blade pitch, as modeled in Figure3.1.A Control of the DFIG are through control of the variable frequency drive, which includes control of the RSC as shown in figure3.9 and control of the GSC as shown in figure3.11. The aim of the RSC is to enable the DFIG wind turbine to control active and reactive power in a decoupled manner. This allows for a high degree of flexibility that allows the turbine to extract maximum energy from the wind while supporting the grid with reactive power. The goal of the GSC is to keep the intermediate circuit voltage constant regardless of the magnitude and direction of the rotor power.

3.8.1 Modeling Rotor Side Converter (RSC) Controller

The rotor-side converter (RSC) shown in Fig. 3.9 is used to control both the active power and the reactive power of the stator connection of the DFIG [26]. The RSC is a power electronic universal bridge converter that converts the DC voltage of the intermediate circuit into a voltage

and connects it to the rotor of the machine. Because the rotor in DFIG is powered by an inverter, the rotor currents are typically controlled using a rotating frame aligned with the stator flux [27]. The RSC controller uses the terminal active power and reactive power as inputs and controls the output active and reactive power. It is assumed that the Parks transform transforms the three-phase quantities into the equivalent d and q components and vice versa. A classic controller is used to generate appropriate reference signals for the three-phase PWM signal generator block.

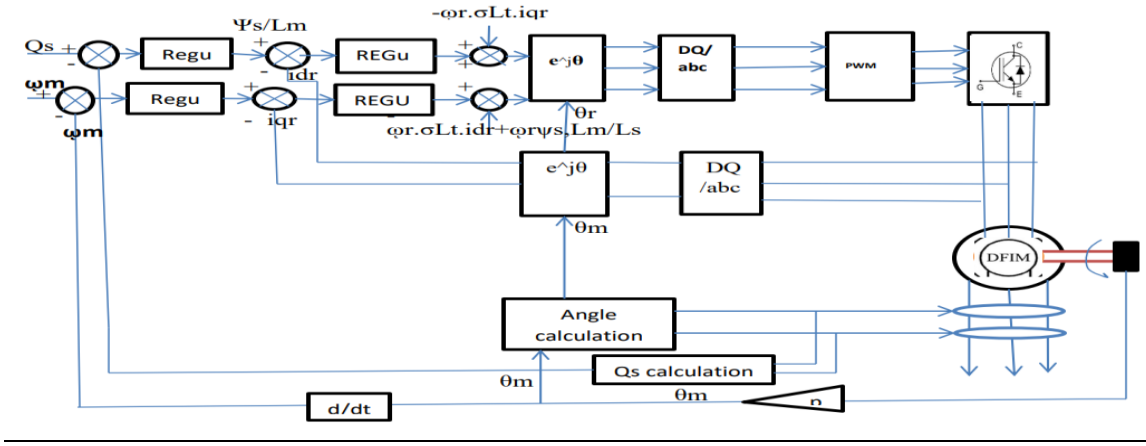

Figure3. 9 Rotor side control

3.8.2 DC Link Voltage Control

The intermediate circuit voltage, which is subject to transient conditions due to the change in power produced by the generator, must be controlled in order to deliver optimum power to the grid via the converter. Increasing the power generated will result in an overvoltage, while decreasing it will result in an under-voltage. From the point of view of DC voltage regulation, power changes lead to voltage fluctuations, which should be compensated for by charging or discharging processes. Therefore, the active power flow through the rotor must cross the intermediate circuit and then be transferred to the grid. Controlling only the DC bus variable to a constant value ensures this active power flow through the converters, along with the guarantee that both line and rotor side converters have the DC voltage required for proper operation. Thus, DC voltage regulation is achieved by controlling the power exchanged from the converter to the grid by changing the reference value for the AC control loop, as performed in this work. In this case, the DC voltage level is reduced or increased by feeding more or less power into the grid than is generated by the wind turbine. The simplified block diagram of the DC link with converters on both sides is shown in the figure 3.10.

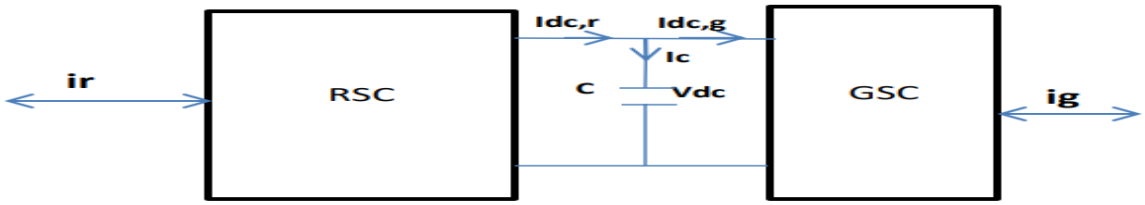

Figure3. 10 DC link with both side converters

$$Ic = Idc,r - Idc,g \quad \text{.....3.48}$$

$$Vbus = \frac{1}{Cbus}\int Ic.dt \quad \text{.....3.49}$$

In order to determine appropriate parameters for the DFIG under study, according to the methods, the initial parameters specified by the designer are used: base values are determined and used: the rms value of the grid voltage (Vgrid) or the grid angular frequency(s) for the designed system; Nominal power (PN) for the system and the converter, expressed in watts; Boundary conditions specified by the designer for changes in the intermediate circuit voltage level (VDC) and the switching frequency (fsw);

Base value calculation

$$\text{Zbase} = \frac{\text{Vn}^2}{\text{Pn}} = \frac{(690V)^2}{1.5M} = 0.3174\ ohm$$

$$\text{Lb} = \frac{\text{Zb}}{\omega\text{N}} = \frac{0.3174}{2 * Pi * f} = 0.001H = 1mH$$

$$\text{Cb} = \frac{1}{\text{Zb}.\,\omega\text{N}} = \frac{1}{0.3174 * 100 * pi} = 0.010029F$$

3.8.3 Grid side converter (GSC) Controller

The grid-side converter (GSC) control shown in Fig. 3.11 uses the DC link voltage Vdc and the rotor line reactive power as inputs to regulate the DC link voltage and produces an independent reactive power that is injected into the grid [28]. In order to control the reactive power of the DFIG, the injection and consumption of reactive power must be controlled by either the rotor or the stator circuit. In fact, the GSC in the rotor circuit always regulates the reactive power to zero [29]. For this reason, iqs_ref is considered zero. The GSC ensures energy balance on both sides of the intermediate circuit by maintaining the fixed intermediate circuit voltage. In the DFIG model, a 40 µF capacitor is used to minimize ripple on the 1150 volt DC voltage.

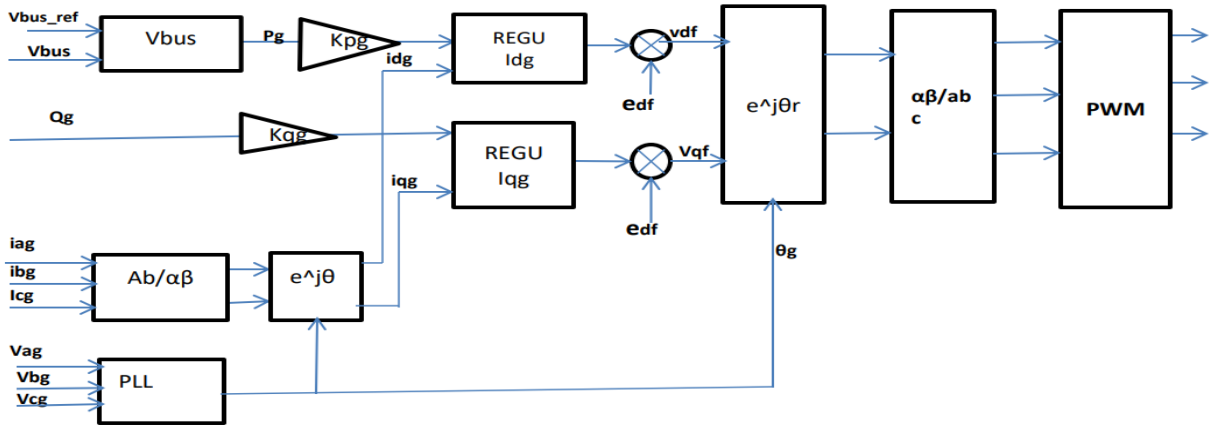

Figure3.11 Grid side Converter

3.9 Transient stability problem

"Doubly Fed Induction Generator" is a type of wind turbine generator that uses a partially rated power converter to control the rotor-side power electronics. Temporary stability issues in DFIGs can occur due to a variety of factors, such as sudden changes in wind speed, grid faults, or lightning strikes. During a transient stability event, the DFIG can experience a sudden change in the balance between mechanical power input and electrical power output. This can cause a loss of synchronism between the "rotor and stator", resulting in a drop in output voltage and frequency. If the DFIG cannot recover from the event quickly enough, it can go offline or even cause a system-wide power outage. [30]

Here are some potential causes of transient stability problems in DFIGs:

1. Changes in wind speed: DFIGs rely on the wind to generate electrical power, so sudden changes in wind speed can lead to a sudden change in the mechanical power input. If the DFIG is unable to adjust its output quickly enough, it may experience a transient stability problem.

2. Grid faults: Grid faults, such as 3LG, can cause sudden changes in the electrical power output of the DFIG. If the DFIG is unable to ride through the fault, it may trip offline or cause a system blackout.

3. Lightning strikes: Lightning strikes can cause voltage transients in the power system, leading to sudden changes in the electrical power output of the DFIG. If the DFIG is unable to ride through the transient and adjust its output quickly enough, it may trip offline or cause a system-wide blackout.

3.9.1 Assessment of transient stability system

Transient stability refers to a power system's capacity to resume a stable operating point following the occurrence of a disturbance that modifies its topology. The following two aspects have received the most attention when assessing the transient stability of power systems that incorporate DFIG turbines:

Qualitative assessment

A qualitative evaluation is conducted by looking at the post-fault state of several generating parameters. These are the parameters:

Rotor angle: The generators are prone to losing synchronism when the rotor angle drifts out of phase, resulting in momentarily unstable conditions.

Rotor speed/active power: The system is considered transiently unstable when the rotor speed/active power continuously increases without bound or experiences rapid undamped oscillations after the fault.

Terminal voltage: quicker recovery of the generator terminal voltage following the fault provides solid assurance that the system is stable.

Reactive power: The system may experience transitory instability if the fault is followed by a high reactive power demand on the grid. This might be caused by a network voltage breakdown brought on by a decrease in reactive power reserves.

Quantitative assessment

Quantitative assessment is carried out by the following transient state measurement units:

Transient rotor angle stability index (TRASI): The TRASI is a comparative measure of rotor angle separation following a transient fault and is defined as follows:

$$\text{TRASI} = \frac{360° - \delta^{post}max}{360°} \times 100 \quad \text{.....3.50}$$

Where $\delta^{post}max$ is the maximum post-fault (typically measured from the first swing of post-fault trajectory), with respect to a reference machine. The TRASI varies from 0 to 1. With the TRASI value closer to 1, the system is considered to be more stable.

Transient stability index (TSI): The TSI (η) is defined as follows

$$\text{TSI}(\eta) = \frac{360° - \delta max}{360° + \delta max} \times 100 \quad \text{.....3.51}$$

Where is the maximum angle of separation between two machines followed by a fault? The TSI varies from -100 to +100. With η value > 0, the system is considered to be stable. These qualitative and quantitative methods for transient stability assessment can be applied to evaluate the transient response of the DFIG wind turbine.

To address transient stability issues in DFIGs, various control strategies can be implemented to improve the DFIG's response to sudden changes in power input or output. The Adama Wind Farm II uses a capacitor bank to solve this problem. However, this is only useful at constant speed since DFIG has variable speed. A STATCOM device is suggested to fix the problem.

The double-fed induction generator is delivering 1.0 p.u.

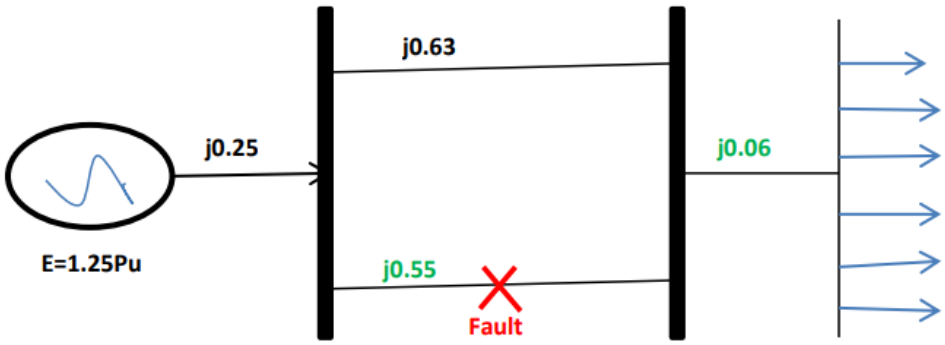

Figure3. 12: infinite bus

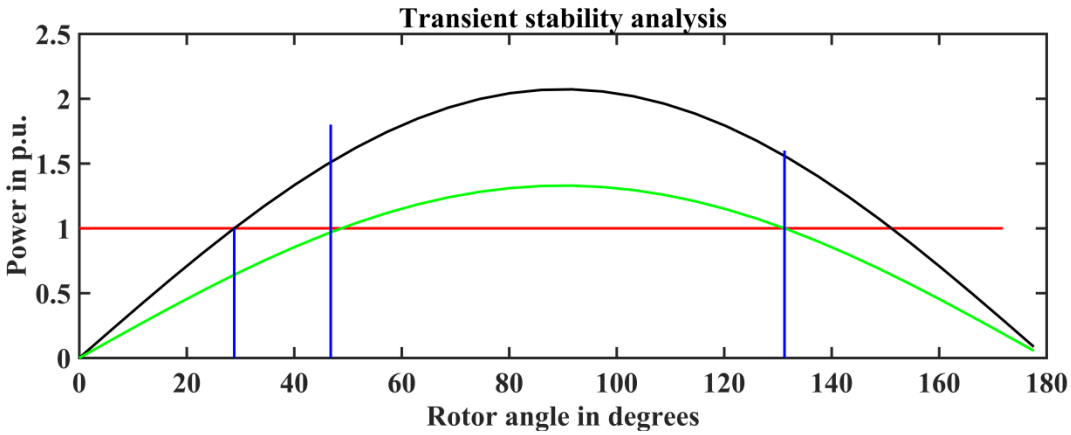

Figure3. 13 Transient stability conditions

Critical clearing angle is the maximum change in the load angle curve before clearing the fault without loss of synchronism. In other words, when the fault occurs in the system the load angle curve begin to increase, and the system becomes unstable. The angle at which the fault becomes clear and the system becomes stable is called critical clearing angle. It calculated as below

$$cos\delta cc = \frac{\frac{\pi}{180} pi(\delta max - \delta 0) - Pmaxb * cos\delta 0 + Pmaxc * cos\delta max}{Pmaxc - Pmaxb} \quad \text{.....3.52}$$

Before faults

$$X^I = 0.25 + \left(\frac{(0.55*0.63)}{0.55+0.63}\right) + 0.06 = 0.604,..$$

$$Pe^I = \left[E.\frac{V}{X^I}\right] sin\delta = \frac{1.25 * 1}{0.612} sin\delta = 2.071 sin\delta$$

$$Pe^I = Pi = 2.0424 sin\delta 0 = 1$$

$$\delta 0 = \sin^{-1}(1/2.0424) = 28.87°$$

During faults $Pe^{II} = 0$

Post faults $X^{III} = 0.25 + 0.63 + 0.06 = 0.94$

$$Pe^{III} = \left[E.\frac{V}{X^I}\right] sin\delta 0 = \frac{1.25 * 1}{0.94} sin\delta 0 = 1.329 sin\delta m$$

$$\delta \mathrm{m} = 180 - \sin^{-1}\left(\frac{\mathrm{Pi0}}{\mathrm{PIIImax}}\right) = 180 - \sin^{-1}\left(\frac{1}{1.329}\right) = 131.24°$$

$$cos\delta cc = \frac{1(131.24° - 28.87°)(\frac{\pi}{180}) - Pmaxb * cos\delta 0 + Pmaxc * cos\delta max}{Pmaxc - Pmaxb}$$

$$cos\delta cc = \frac{1(131.24° - 28.87o)\left(\frac{\pi}{180}\right) - 0 + 1.329 * \cos(131.24)}{1.329 - 0} = 0.68427$$

$$\delta cc = \cos^{-1}(0.68427) = 46.8°$$

Critical clearing time (CCT): The CCT is the maximum period of a fault during which the system maintains transient stability. The operating point, topology, and system characteristics that make up the pre-fault system conditions, the nature and location of the fault, as well as the post-fault conditions that are dependent on the protective relaying strategy used, all play a role in determining the CCT.

$$tcc = \sqrt{(\frac{\left(2 * H(\delta cc - \delta 0)\right)}{\pi f Pi})} \quad \text{.....3.53}$$

Where pi initial power angle And the Inertia constant is equal to 5 MJ/MVA and Time clearing fault is calculate as

$$tcc = \sqrt{(\frac{\left(2 * 5\mathrm{MJ/MVA}(54.1736 - 28.89)\right)}{180 * 50 * 1.0}$$

$$\underline{\mathrm{tcc} = 0.1412\mathrm{sec}}$$

3.10 An Overview and Comparisons of Various FACTS Devices

FACTS (Flexible AC Transmission Systems) devices are power electronic components used in power transmission and distribution systems to improve grid effectiveness, dependability, and controllability. These devices use power electronics to control the voltage, current, and power flow of the grid.

There are several types of FACTS devices,

Static Var Compensator (SVC): A SVC is a shunt-connected device that is used to regulate the voltage in the power grid by adjusting the reactive power in the system. It consists of a thyristor-controlled reactor and a thyristor-switched capacitor bank.

Static Synchronous Compensator (STATCOM): A STATCOM is a shunt-connected device that is used to control the voltage and reactive power in the power grid. It consists of a voltage source converter (VSC) that is connected to the grid through a transformer.

Thyristor-Controlled Series Capacitor (TCSC): A TCSC is a series-connected device that is used to control the power flow in the grid by adjusting the series capacitance of the transmission line. It consists of a thyristor-controlled reactor and a capacitor bank.

Unified Power Flow Controller (UPFC): A UPFC is a combination of a series-connected and a shunt-connected device that is used to control the voltage, current, and power flow in the power grid. It consists of a VSC, a thyristor-controlled reactor, and a thyristor-switched capacitor bank.

Interphase Power Controller (IPC): An IPC is a series-connected device that is used to control the power flow in the grid by adjusting the phase angle of the transmission line. It consists of a series transformer and a converter that is connected to the grid [31]. The technology consists of a variety of power electronic devices with the aim of controlling both power and voltage at a certain location of the electricity grids during disturbances. In general, the FACTS devices were invented to improve the existing transmission line capacity and provide a controllable power flow for a selected transmission direction [32].

The FACTS devices are basically divided into two groups. The first group includes quadrature tapped transformers, including traditional thyristor switched capacitors and chokes, and the second group includes voltage source converters based on thyristor switched gate turn-off converters (GTO) [33]. The first group introduced the Thyristor-Controlled Phase Shifter (TCPS), the Static Var Compensator (SVC) [34], and the Thyristor-Controlled Series Capacitor (TCSC). The Static Synchronous Series Compensator (SSSC) [35], the Static Synchronous

Compensator (STATCOM), the Interline Power Flow Controller (IPFC), and the Unified Power Flow Controller (UPFC) emerged from the second group. Each generation of FACTS devices has its own performance and characteristics [36]. The first group of FACTS devices uses capacitor and reactor banks and fast solid-state switches that can be connected in series or in parallel with the power grid to compensate for reactive power on the PCC. However, a real power exchange with the system is not possible with such systems.

The FACTS group's voltage source converter-based device uses self-commutated converters equipped with GTO thyristor switches. With an appropriate control scheme, this group is capable of internally generating capacitive and inductive reactance. In addition to independent reactive power control, the voltage source converter can be integrated into the energy storage system to allow decoupled control of active and reactive power exchange with the system to which it is connected [37].

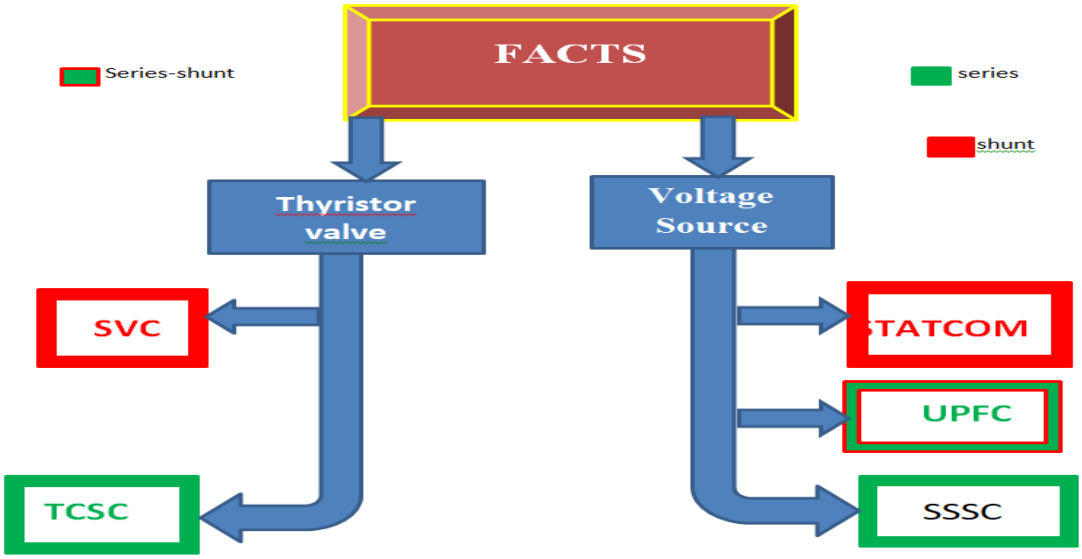

Figure3.14; Classification of FACTS

Table3. 1 Comparison of Various FACTS Devices

FACTS	Performance during Fault's	Generation of harmonics	Region of operation
TCSC	Medium	Medium	Capacitive
SVC	Low response	High	Mostly capacitive

STATCOM	Higher response	Low	Both capacitive and inductive
UPFC	Higher than other FACTS	Medium	Inductive and capacitive regions

FACTS devices at a suitable place, wherever the reactive power upkeep is wanted the most, are an effective way to raise the voltage stability margin.

Table3. 2 : Comparison of Facts in terms of Cost can be as follows in [38].

No	FACTS Controllers	**C**ost(USD)
1	Capacitor	25/kVar
2	SVC	40/kVar
3	TCSC	40/ kVar controlled rations
4	STATCOM	50/kVar
5	UPFC series portions	50/kVar through the power
6	UPFC shunt portions	50/kVar control

3.11 Proposed FACTS device to improve transient stability

In this study, static synchronization compensators are used to improve transient stability. A STATCOM is a converter-based, parallel-connected switching device that controls voltages and electric power flows by “injecting or absorbing reactive power”. A STATCOM is a parallel static synchronous generator that can control the quantity of reactive power either capacitively or inductively, according to the IEEE specification for FACTS devices. Rapid response, great precision, compact size, and optimal dynamic properties under a variety of operating conditions are only a few advantages of STATCOM. The device has a coupling transformer, a DC capacitor, and a voltage converter that primarily uses GTO to produce a controlled AC voltage at its output. It is modeled as a "voltage-controlled" current source, meaning that the coupling transformer's primary and secondary voltages determine its value. The STATCOM contact terminals are used to directly measure a primary voltage, and an indirect calculation is used to determine a secondary value. The STATCOM's primary duties include creating a sinusoidal waveform in the PCC and managing the flow of reactive current [39].

To reduce power quality difficulties, STATCOM performs incredibly well and is user-friendly. It Support reactive power from STATCOM for wind turbines and grid. For quick dynamic

responses, the adaptive controller is implemented in STATCOM. Reduce high order harmonics [40]. A STATCOM is a reactive-power compensation device that can generate, absorb, or both and whose output can be adjusted to control particular aspects of an electric power system.

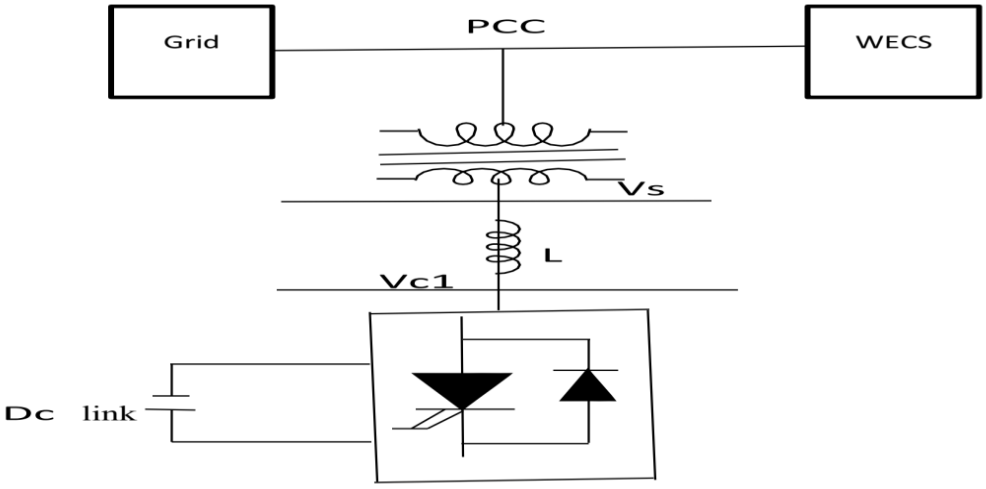

Figure3. 15 Modeling of STATCOM

3.11.1 THE 48-PULSE VOLTAGE SOURCE GTO CONVERTTER

In a STATCOM, the DC voltage is considered to be constantly available through the capacitor, and the necessary voltage source output is produced by inverting the DC voltage. The initially charged capacitor is completely discharged because of component losses in the inverter if the actual power supplied to the inverter from the grid is kept at zero. This is because practical STATCOMs are not lossless. In order to draw enough current from the network's AC line to make up for any losses caused by reactive current flow, a technique for adjusting the phase angle of the VSC output voltage must be used. By changing the capacitor voltage and subsequently the output, this method may adjust the reactive power produced or absorbed by the STATCOM.

The phase angle of the inverter output voltage with respect to the AC side source voltage is adjusted in this method, which is also referred to as a synchronous link-based control method [43]. The suggested 48-pulse STATCOM design's circuit schematic is shown in the accompanying image. Four 12-pulse GTO converters that are 7.5 out of phase and connected in parallel in the DC section with a DC capacitor (40 µF) are used to implement the 48-pulse model. The secondary windings of four zigzag-phase shifting transformers linked at (Y) or (Δ) receive the outputs from each pole of the four VSCs.

Table3. 3 Phase shift angles for 48-pulse STATCOM including VSCs

Transformer connection	VSC switching angle (°)	Transformer phase shift angle (°)
Y–Z	+7.5	-7.5
Δ–Z	−22.5	-7.5
Y–Z	−7.5	+7.5
Δ–Z	−37.5	+7.5

For electromagnetic summing, the linear segment of the primary winding of the transformers is wired in series with four 12-pulse GTO converters. As a result, the voltage waveform at the intersection has 48 steps and a 7.5-degree shift angle. Using various pulses in each half-sequence of the output voltage during multi-pulse operation reduces the harmonic content. Four diode-clamped, three-level, 12-pulse VSCs are used in the 48-pulse STATCOM. The secondary windings of four phase-shifting transformers with phase shifts of -7.5, -7.5, +7.5, and +7.5 are applied with the four sets of three-phase voltages acquired at the output of the four three-phase VSCs. Reduce the low-level harmonics' rejection. By connecting the primary windings in series, the primary components of the voltage that is taken from the 33 kV sides of the transformers are added in phase. Each VSC's output voltage is based on the pulses that the STATCOM controller supplies.

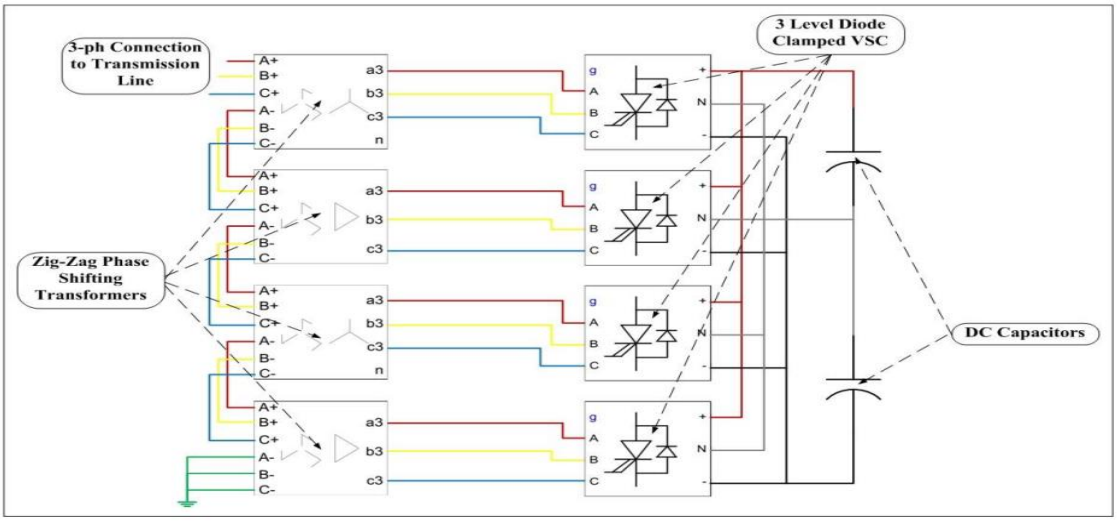

Figure3.16: 48-pulse switched STATCOM

Reactive power flow is controlled by the interaction between the voltage at the STATCOM AC-side terminals and the AC system voltage. Reactive power is injected into the system from the STATCOM and acts as a capacitor when the voltage at the STATCOM terminals is greater than

the system voltage. The STATCOM works like an inductor, and reactive power flow is reversed when the voltage across it is lower than the AC voltage. Both voltages are equivalent, and there is no current exchange between the STATCOM and the system during normal operation. The STATCOM voltage and STATCOM current characteristics are depicted in the figure below.

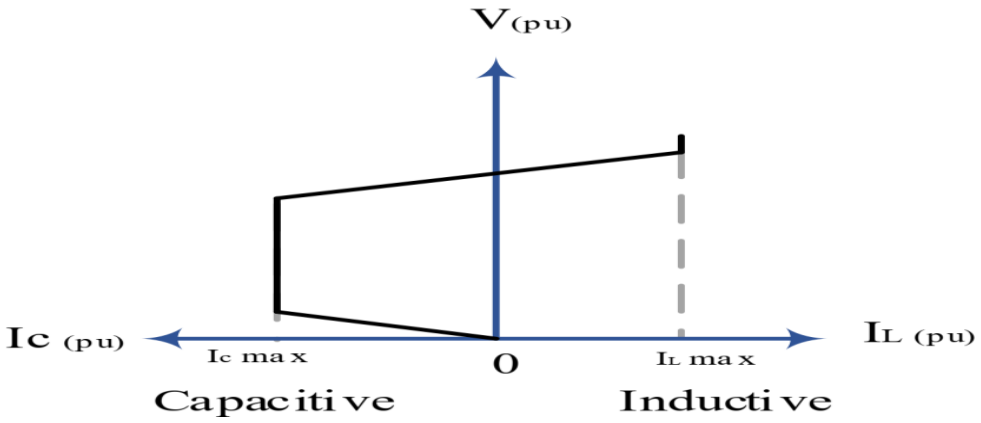

Figure3. 17: V-I characteristics STATCOM

In general, they are solid-state switching converters with output terminals that can generate or sink independently regulated active and reactive power when fed from an energy source at the input terminals. In more detail, the STATCOM under consideration here is a "voltage source converter" that generates a series of three-phase AC output voltages from a given DC voltage input, each of which is in phase with and connected to the corresponding AC system voltage via leaky reactance. An energy storage capacitor provides the DC voltage. The STATCOM enhanced different aspects of power system performance. i.e transmission and distribution systems' dynamic voltage control; it regulates real power in line as necessary, along with voltage flicker control and transient stability; Power oscillation damping in power transmission systems. STATCOM considerably tighter voltage compensation control at the receiver end of the AC transmission line, and improved line stability under changing loads. It is designed to work as a source of reactive power, and it is connected to a transmission line using a power electronics voltage source converter. In order to control the magnitude of the voltage at its terminals, the STATCOM controls the amount of "reactive power injected into or absorbed from the power supply" [38].

3.11.2 Mathematical Model of the STATCOM

A STATCOM is a parallel unit that regulates the system voltage by generating reactive power when the system voltage decreases or by sinking reactive power when the system voltage increases. The secondary side of the transformer is connected to a voltage source converter (VSC) that ensures adequate reactive power control [41]. A STATCOM is a converter-based, parallel-connected switching device used to control voltages and electric power flows by injecting or absorbing reactive power. A STATCOM is a parallel static synchronous generator that can modulate the amount of reactive power capacitive or inductively, according to the IEEE definition for FACTS devices. Numerous benefits of STATCOM include its quick response time, high degree of accuracy, small size, and adaptability to changing operating conditions. The device has a coupling transformer, a DC capacitor, and a voltage converter that uses solid-state switches, usually Gate turn off thyristor (GTO), to produce a controlled AC voltage at its output. It is described as a voltage-controlled current source whose value is determined by the coupling transformer's primary and secondary voltages. The STATCOM's terminals are used to directly measure the primary voltage, and an indirect calculation is used to get the secondary voltage. The STATCOM's primary duties include creating a sinusoidal waveform in the PCC and managing the flow of reactive current [42].

i. Selection of the Nominal DC Bus Voltage

One of the crucial criteria is the choice of the V_{DC} reference voltage on the DC side of the capacitor. While the lower capacitor voltage will determine the STATCOM's ability to force its current to follow the intended reference wave shape, the peak capacitor voltage is the maximum voltage that can be maintained by the switches. The capacitor voltage could operate improperly if it drops below the reference voltage since STATCOM won't be able to control its current as intended. The DC link voltage of VSC typically needs to be twice as high as the peak phase voltage. By taking into account the ac output voltage, the design criteria for the selection of the reference DC bus voltage can be met. Consequently, the DC link voltage is 690V because the ac line voltage is 690V.

$$Vdc \geq \frac{2*\sqrt{2}*Vs}{m*\sqrt{3}} = \frac{2*\sqrt{2}}{\sqrt{3}} * 690 \geq 1126.7V \quad \text{.....3.54}$$

$$Vdcmin = 1126.7\,V$$

Where Vs is the AC three-phase line voltage, m modulation index, i.e. assuming the modulation index is 1.

Considering the nominal AC voltage variation constant, filter voltage drops, and dead band in PWM output:

$$Vdc \leq \frac{1.05*1.05*1.1*\frac{2*\sqrt{2}*Vs}{m*\sqrt{3}}}{d} = Vdcmax = \text{ 1,366.5 V} \quad \text{.....3.55}$$

Where 1.05 is dead band factor due to PWM switch, 1.05 is nominal ac voltage variation factor and 1.1 is filter voltage drop factor and d is duty cycle which is 1. Therefore, input DC bus voltage can be calculated $1{,}126.765V \leq VDC \leq 1{,}366.48V$ and in this thesis 1,150V DC is used to get the equivalent three phase ac voltage of 690V from VSC of STATCOM.

ii. Selection of DC Bus Capacitor

The DC side capacitor has two main functions: (i) it maintains a steady-state DC voltage with minimal ripple; and (ii) it acts as a source of actual power during transients by storing the energy difference between the load and the source. In the steady state, the source's real power output should be equal to the load's real power demand plus a tiny amount to account for STATCOM loss. As a result, a reference voltage for the DC capacitor can be maintained. The genuine power balance between the mains and the load will be upset nonetheless when the load state changes. The DC capacitor is intended to make up for this actual power differential. The DC capacitor voltage is shifted away from the real power that the capacitor charges or discharges offsets the real power that the load uses. The real power supplied by the source should again be equal to that used by the load if the DC capacitor voltage is recovered and reaches the reference voltage. By controlling the average voltage of the DC capacitor, it is possible to acquire the peak value or the reference source current in this way. A DC capacitor value that is lower than the reference voltage indicates that the source's actual power output is insufficient to meet the demands of the load. Therefore, it is necessary to raise the source current, or the actual power drawn from the source. While attempting to reduce the reference source current, there is a DC capacitor voltage that is higher than the reference voltage. Under transient conditions, a modest value of the DC capacitor may cause a significant steady-state ripple and a significant fluctuation in the DC bus voltage. A greater value of capacitor, however, will raise the system's overall cost and size while reducing DC bus voltage swings and ripple.

$$Vdc = 2 * \sqrt{2} * V1 \quad \text{.....3.56}$$

$$Vc1 = \frac{Vdc}{2 * \sqrt{2}} = \frac{1150V}{2 * \sqrt{2}} = 406.6V$$

For three phase

$$Vc1 = \sqrt{3} * 406.6\,V = 704.2V$$

For Vs. =690V and L=11mH

$$Ic1 = \frac{Vc1 - Vs}{\omega fL} = \frac{Vc1}{\omega fL}(1 - \frac{Vs}{Vc1}) = \frac{704.2 - 690}{2 * pi * 50 * 11mH} = 4.11\text{A}$$

$$Ic1 = \frac{704.2}{2 * pi * 50 * 11mH}\left(1 - \frac{690}{704.2}\right) = 4.11A$$

Therefore

$$Qc1 = Ql1 = 3 * Vs * Ic1 = 3 * 690 * 4.11A = 8.5KVAR$$

$$Qc1 = \frac{Vrms^2}{Xc}$$

$$Xc = \frac{Vrms^2}{Qc1} = \frac{\sqrt{2} * 690^2}{8.5e3} = 79.2\,\Omega$$

$$C = \frac{1}{Xc * \omega * f} = \frac{1}{79.2 * 2pi * 50} = 40.2\mu F$$

A coupling inductor connects the voltage source converter, which is the fundamental component of a STATCOM, to the grid. The connecting inductance can be a transformer or a reactor if the gadget is made to connect directly to the bus bars' voltage level. A STATCOM can be described as an AC voltage source where the output voltage's amplitude, phase angle, and frequency can all be adjusted.

The complex power transferred from PCC bus g to STATCOM bus becomes

$$\begin{cases} Sstat = Vg.Istat^* \\ Sstat = \frac{Vg(Vg-Vc)}{Xc} \\ Sstat = jB.[Vg^2 - Vg.Vc]\angle(\theta - \Upsilon) \\ jB.[Vg^2 - Vg.Vc]\left(\cos(\theta - \Upsilon) + jsin(\theta - \Upsilon)\right) \\ Sstat = B.[VgVc - Vg^2]\sin(\theta - \Upsilon) + B.[Vg^2 - Vg\,Vc]\cos(\theta - \Upsilon) \end{cases} \quad \text{.....3.57}$$

Active and reactive powers becomes

$Pstat = B.[Vg.Vc - Vg^2]\sin(\theta - \Upsilon)$.....3.58

$Qstat = B.[Vg^2 - Vg.Vc]\cos(\theta - \Upsilon)$ 3.59

Bus of PCC and STATCOM are in phase and so θ =γ. Now we have

$$Pstat = B.[Vg.Vc - Vg^2]\sin(0) = 0$$

$$Qstat = B.[Vg^2 - Vg.Vc]\cos(0) = B[Vg^2 - Vg.Vc]$$

$$Qstat = \frac{V^2}{Xc} = \frac{33KV^2 - 33KV.690V}{79.2} = 13.5MVAR$$

Where the current through the STATCOM becomes

$$Istat = B[Vg - Vc] \quad \text{.....3.60}$$

The equation above indicates that the STATCOM can be represented by a current source with the control signal as the voltage on the AC side of the VSC. By regulating Vc, the current can flow from the VSC towards the grid (Qst injection) or can flow towards the VSC from the grid (Qst consumption). This STATCOM current can be limited to the maximum capacitive current and the maximum inductive current.

3.11.3 Optimal Location of the STATCOMS

Optimizing the location of STATCOMs often involves conducting power system studies, such as load flow analysis. It helps to identify weaknesses system, voltage problems, and areas where STATCOMs can be most beneficial. In conventional distribution networks, the permissible variation of voltage level is ±5% of the nominal voltage. Proposed FACTS devices maintain the desired voltage has a beneficial solution. As we know, capacitors can provide voltage support only during steady-state conditions, whereas STATCOM provides steady-state voltage support and improves transient voltage stability as well. As it recommended to place in weakest bus, It has been taken at bus 3 which is same as PCC and size of 5.98 MVAR (0.9647pu)) as shown in Table 3.5. The proposed placement of buses is the correct location of the STATCOM, which is placed at PCC. In this study, the STATCOM is placed at the PCC because of the following two reasons: The location of the reactive power support should be as close as possible to the point where the support is needed, since the voltage and the resulting power loss (I2R loss) in the transmission line will change due to the reactive power flow, and In the system examined, the effect of the voltage change is strongest at this node.

Table3. 4 Placement and size of STATCOM

STATCOM bus	Voltage shunt	Angle (degree)	Q Shunt(pu)
3	0.8682	10.0288	0.9647

3.11.4 STATCOM CONTROLLER

3.11.4.1 Fuzzy logic based STATCOM

Modern energy systems are large, complex, geographically distributed, and highly nonlinear. In addition, the operating conditions and topology of the power grid change over time, and interruptions are unpredictable. With conventional controllers based on a linear system model, it is exceedingly challenging to properly address issues with power system stability because of these uncertainties. Therefore, in recent years, the fuzzy logic control approach has emerged as a field of artificial intelligence that complements the traditional approach. A fuzzy logic controller is an intelligent controller, and this is its biggest additional benefit. Human knowledge can be easily linked to governing laws. In addition, the fuzzy logic controller is a nonlinear controller and is insensitive to changes in system topology, parameters, and operating conditions. These properties make it very attractive for applications in power systems [45].

One of the key figures in computational intelligence is the fuzzy system. It is different from conventional math. It deals with uncertainties brought on by randomness, approximation, and vagueness. It is about soft or quasi-truth or partial falsity. It has several applications. Compared to traditional logic systems, it is far more universal. Word arithmetic and other innovative natural language processing technologies are supported by fuzzy logic. Making precise claims about a system's performance becomes harder and eventually more challenging as its complexity rises. When it comes to identifying the issue, the fuzzy technique is the only viable option [46].

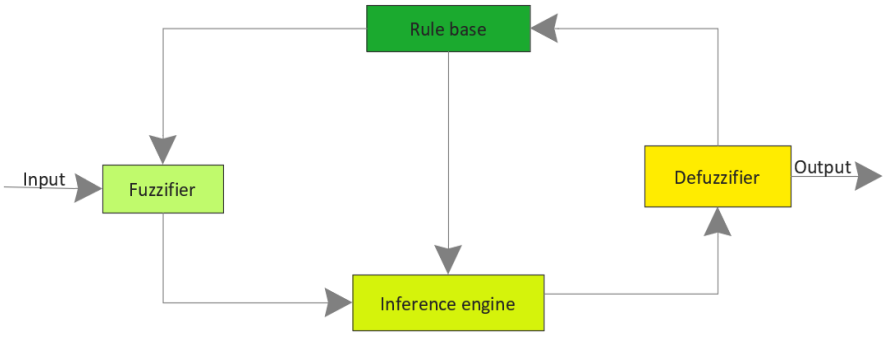

Figure3. 18: Fuzzy Logic Architecture

Fuzzification

Fuzzy logic is used to convert the crisp value (a numerical variable) into the fuzzy value (a linguistic variable). It is based on a knowledge-based membership function to explain the input

variable into the fuzzy variable. It does not use numerical variables. The error between the output signal and reference signal is consigned as negative small (NS), negative big (NB), negative medium (NM), zero, positive small (PS), positive big (PB), and positive medium (PM). The "triangular membership function" is utilized for fuzzification.

Fuzzy Interference

The fuzzy interpolation process is mapped from the supplied input to the output through fuzzy logic. Fuzzy sets (so rule) and fuzzy logic provide a mapping of nonlinear output. The mapping range and domain will be fuzzy sets or points in multidimensional spaces. Fuzzy interpolation systems are successfully implemented in various fields such as automatic control, data classification, decision analysis, expert systems, computer vision, etc. A fuzzy inference system is also known as a fuzzy rule-based system, fuzzy associate memory, fuzzy expert system, fuzzy logic controller, fuzzy model, or fuzzy system due to its variety of functions.

Defuzzification

It is used to convert the fuzzy value (linguistic value) into the crisp value (numerical value) from a mathematical calculation. It uses various defuzzification methods that have the minimum error and easily fit in the system. For the best result, the output membership function is compared with different process cycles from the most significant point.

Mapping Expert Knowledge to Fuzzy Rules

There are two inputs to the FLC. One is the control error e(k), which is the difference between the desired (reference) value and the measured value x (t), and the other is the rate of change in the control error Δe(k). These two inputs, defined in equation below, are first fuzzified and converted to fuzzy membership values that are used in the rule base in order to execute the related rules so that an output can be generated.

$$e(k) = \mathrm{x}*(\mathrm{t}) - \mathrm{x}(\mathrm{t}) \quad \text{.....3.61}$$

$$\Delta\mathrm{e}(\mathrm{k}) = \mathrm{e}(\mathrm{k}) - \mathrm{e}(\mathrm{k}-1) \quad \text{.....3.62}$$

Where;

- ✓ $\mathrm{x}*(\mathrm{t})$ The desired (reference) value
- ✓ $\mathrm{x}(\mathrm{t})$ Measured value
- ✓ $\mathrm{x}(\mathrm{t})$ Represents for speed, Voltage and reactive current

The fuzzy rule base, which may also be called as the fuzzy decision table, is the engine mapping the two crisp inputs, e (k) and Δe (k) to the fuzzy output space defined on the universe of $\Delta(k)$.

In order to intuitively generate the set of rules for the FIS, the system response is analyzed thoroughly first. The time response of the control error (k) for a step input can be represented by the generalized step response error of a second-order system. This error signal may have a damped or an oscillatory response with a decaying exponential component. The latter one is considered for constructing the rule table since it includes overshoot effects, leading the rule base to represent more generalized cases.

Table3. 5 below shows 49 rules

$e(k)$	Δe(k)						
	NB	NM	NS	ZE	PS	PM	PB
PB	KV	IS	IM	IB	IB	IB	IB
PM	DS	KV	IS	IM	IB	IB	IB
PS	DM	DS	KV	IS	IM	IB	IB
ZE	DB	DM	DS	KV	IS	IM	IB
NS	DB	DB	DM	DS	KV	IS	IM
NM	DB	DB	DB	DM	DS	KV	IS
NB	DB	DB	DB	DB	DM	DS	KV

From the general conventional control, the error is given by $e(k) = \mathrm{x} * (\mathrm{t}) - \mathrm{x}(\mathrm{t})$and assuming a constant set point one can arrive at $\frac{de(k)}{dt} = -\frac{dx(t)}{dt}$

Where e (k) = error signal

$\mathrm{x} * (\mathrm{t})$ = desired output signal

x(t)= actual output signal

- $e(k)$= negative, which means “the DFIG output power”, is greater than the reference power, so the DFIG needs to decrease its output.

- e(k)= positive, Means “the DFIG output power” is less than the reference power, so the DFIG needs to increase output power until it reaches the desired value or until error is zero.
- $\frac{dx(t)}{dt}$ = negative, means power is decreasing this implies $\frac{de(k)}{dt}$= positive. Therefore, a positive change in the error rate indicates the power is decreasing.
- $\frac{dx(t)}{dt}$= positive, means output power is increasing this means $\frac{de(k)}{dt}$= negative. Therefore, a negative change in the error rate indicates the power is increasing.

3.11.4.2 Adaptive Neuro-Fuzzy Inference System (ANFIS) controller

ANFIS is a sort of adaptive control that uses a combination of fuzzy logic and neural networks to learn the dynamics of the system and provide control signals. Reactive power output can be modified by STATCOM using ANFIS based on current and voltage measurements taken in real-time. The benefits of fuzzy logic and neural networks are combined in this particular sort of artificial neural network. The input layer, fuzzy layer, normalization layer, rule layer, and output layer are the five layers that make up the ANFIS architecture as shown in figure 3.18. The input layer receives the input variables, which are subsequently sent to the fuzzy layer, where fuzzy sets are defined and evaluated and membership functions are applied. The input values are scaled in the normalization layer to a common range, and the fuzzy sets are combined in the rules layer to produce rules. The output layer produces the output by applying a weighted sum of the rules.

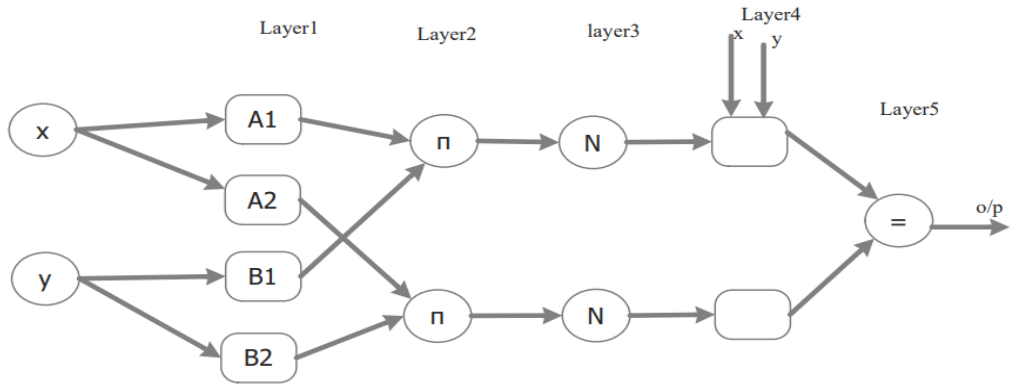

Figure3.19; Internal Structure of ANFIS

ANFIS uses a hybrid learning algorithm that combines gradient descent and least squares methods to adjust the parameters of the membership functions and rule weights. This allows ANFIS to learn from data and adapt to changes in input-output relationships. ANFIS has been

successfully applied to a variety of problems, including prediction, classification, and control [47].

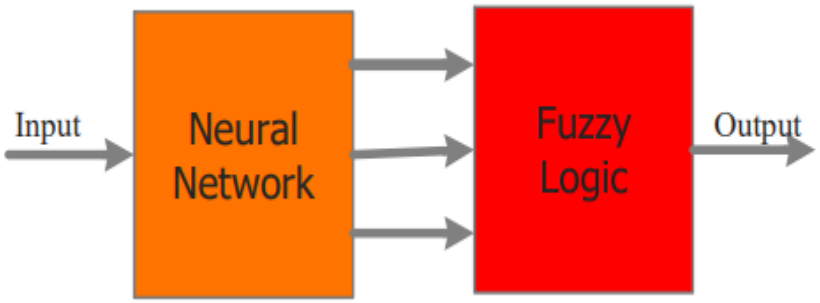

Figure3. 20; Structure of ANFIS

Advantages of ANFIS

The adaptive controller, ANFIS is used to control STATCOM in this thesis because of the following several advantages over other machine learning techniques in certain applications:

1. Approach based on fuzzy logic: The benefits of "neural networks and fuzzy logic" are combined in ANFIS, which is especially well suited for applications containing shaky or ambiguous input. The use of fuzzy logic enables ANFIS to handle complex, non-linear input-output relationships that are difficult to model using traditional statistical or machine learning techniques.
2. Transparency: ANFIS models are transparent and interpretable behind the output which easily understood and explained.
3. Adaptive learning: ANFIS can learn over time and adapt to changes in input-output relationships. This makes it suitable for applications where the underlying relationships between the input and output variables may change or evolve over time.
4. Hybrid Learning Algorithm: The model is optimized by ANFIS using a "hybrid learning algorithm" that combines gradient descent and least squares techniques. This allows ANFIS to learn from both the input data and the expert knowledge encoded in the membership functions.
5. Efficient calculation: ANFIS models are computationally efficient and can be trained with relatively small amounts of data. This makes them suitable for applications that require real-time or near-real-time processing.

Objective function

Grid-connected DFIG system is mainly to minimize transient instability, to minimize the system losses associated with reactive power flow and to model cost effective STATCOM as described below.

Voltage Regulation: One of the primary objectives of a STATCOM is to regulate and maintain the voltage within the desired limits. The objective function can be formulated to minimize the voltage deviations from the target voltage set point at specific buses or throughout the system.

Reactive Power Compensation: STATCOMs are used for reactive power compensation in power systems. The objective function can aim to minimize the reactive power flow or optimize the reactive power exchange between the STATCOM and the system. This objective helps improve the power factor and reduce system losses.

Transient Stability Improvement: Another objective is to improve the transient stability of the power system. The objective function can be formulated to minimize deviations in voltage and frequency during transient events, such as faults or disturbances, by providing fast reactive power support.

Loss Minimization: The objective function can also consider minimizing the system losses associated with reactive power flow. By optimizing the reactive power output of the STATCOM, aim to reduce losses and improve overall system efficiency.

CHAPTER FOUR

RESULTS AND ANALYSIS

In this study, a WECS powered by a 13*1.5MW 690 V DFIG is modeled and tested for temporary (transient) stability. The appendix-I contain a list of all the parameters taken into account for the DFIG model. The effectiveness of the suggested approach is evaluated in light of transients on the converter and grid sides during fault conditions.

The MATLAB Simulink software was used to design and execute all simulations for the grid-connected DFIG WECS. In spite of this, a study was conducted on a system of variable wind speed generators. In the investigation, the transient stability is taken to be at 10 m/s. Time constraints mean that the wind speed in the transient stability research is insignificant.

4.1 MATLAB DESIGN OF CONTROLLER

4.1.1 Design of FLC and Choice of Membership Functions in MATLAB

The FLC-based STATCOM is modeled in MATLAB Simulink using the Simscape Power Systems special package. The fuzzy controller is developed using MATLAB's Fuzzy Logic Designer toolbox, which may be used to build and test fuzzy inference systems to characterize complex system behavior. The FLCs developed for STATCOM (for wind speed, voltage, and reactive current control) are based on the Sugeno fuzzy inference system type, which uses the max-min aggregation approach and is based on the centroid defuzzification methodology. The "internal architecture of the controller" is depicted in Figure 4.1.

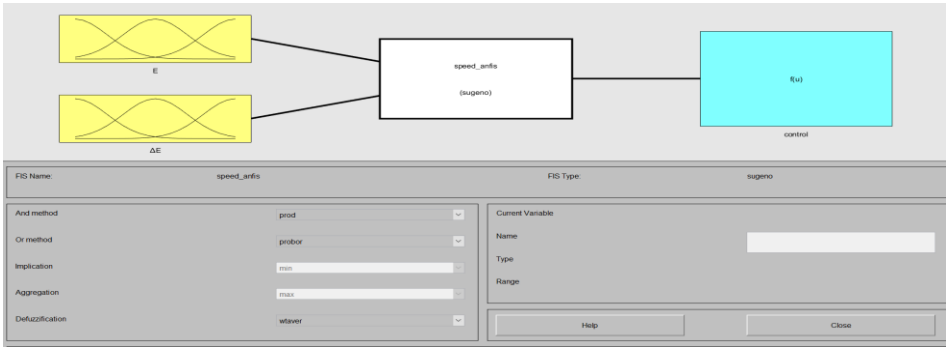

Figure4.1; Sugeno FIS

The performance of FLC-based systems depends to a large extent on knowledge of the system to be controlled. A thorough analysis and experimentation with STATCOM are performed to

determine the optimal choice of membership functions in terms of range and the way they are partitioned so that the fuzzy inference algorithm can provide the best results. With the FLC wind speed controller, the first input to the FLC is the error signal (e) between the desired wind speed and the actual speed. For perfect tracking, the universe of this signal is chosen to be in a very narrow range [-3, 4]. A mixture of "triangular" membership functions is used to partition the fault universe into seven fuzzy sets, as shown in Table 3.5.The different fuzzy sets are labeled with the following linguistic variables: negative large (NB), negative medium (NM), negative small (NS), zero (Z), and positive small (PS), positive medium (PM), and positive large (PB).

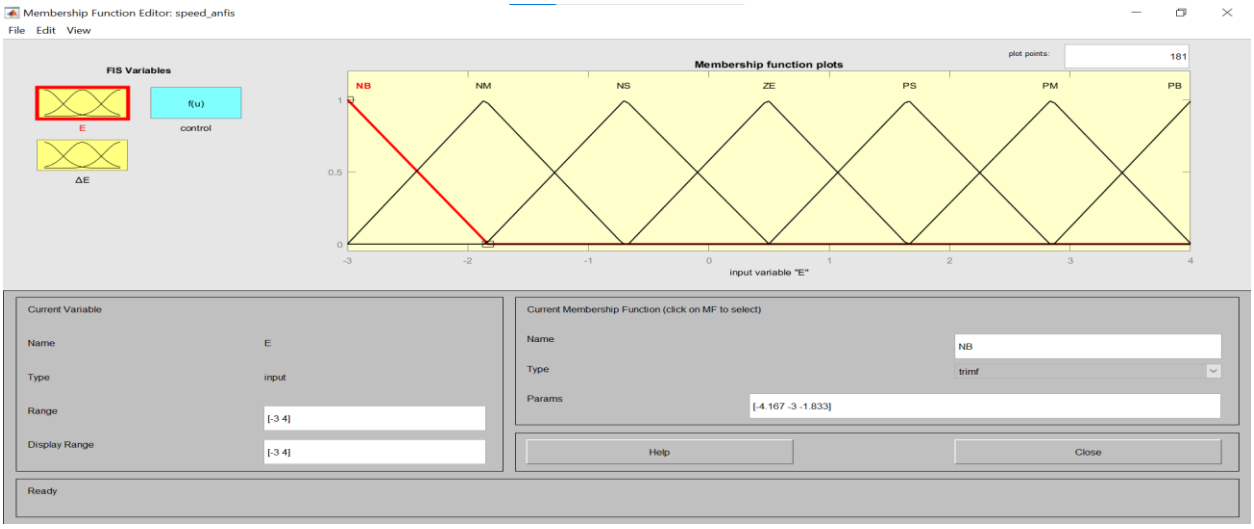

Figure4. 2 Error of membership function

The second input to the speed controller FLC is the error rate of change (ec). After analyzing the model simulation, it is decided that the universe of this signal should be in the range of [-5.52, 2.14]. Similar to the error input, a mixture of triangular membership functions is used to partition the error rate change universe into 7 fuzzy sets labeled with 7 linguistic variables (NB, NM, NS, Z, PS, PM, and PB). The error rate of change membership functions is shown in the figure showing the bounds of each fuzzy set.

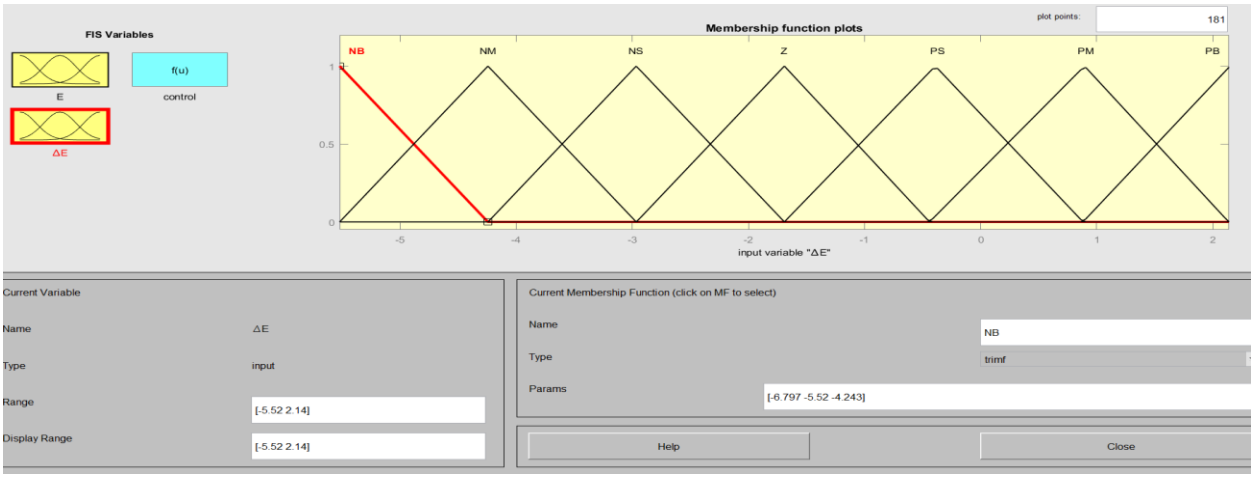

Figure4. 3 rate of change of Error membership functions

As for the output variable (Δα), the universe range is selected so increments or decrements in α are neither so small as to slow down the response nor too large, causing unnecessary overshooting oscillations in α. The universe range is selected to be [0, 27], and a mix of triangular membership functions is used to split the effective change in the universe into 7 fuzzy sets labeled with 7 linguistic variables (NB, NM, NS, Z, PS, PM, and PB). Δα membership functions.

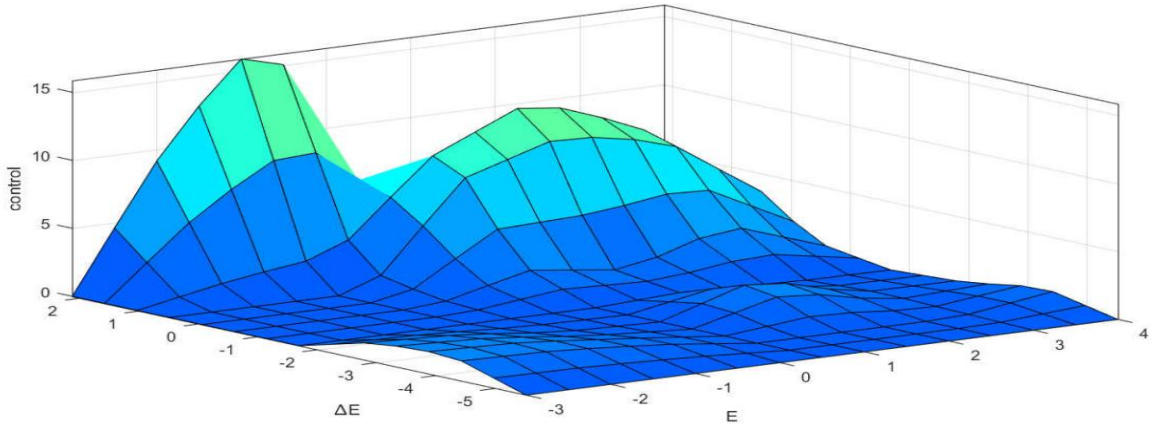

Figure4. 4Control signal surfaces of FLC

4.1.2 MATLAB Model of ANFIS

The input and output properties of wind are used in the adaptive neuro-fuzzy interference system design in MATLAB. This indicates that a DFIG wind turbine just needs wind speed as an input. ANFIS controllers use training data to improve input and output characteristics so that they reach

synchronous and close to synchronous speeds so that DFIGs can produce power. Training data is the disturbance of input/output characteristics, which means the input is not reaching synchronous speed or is not nearly reaching synchronous speed for wind turbines.

Training data on MATLAB

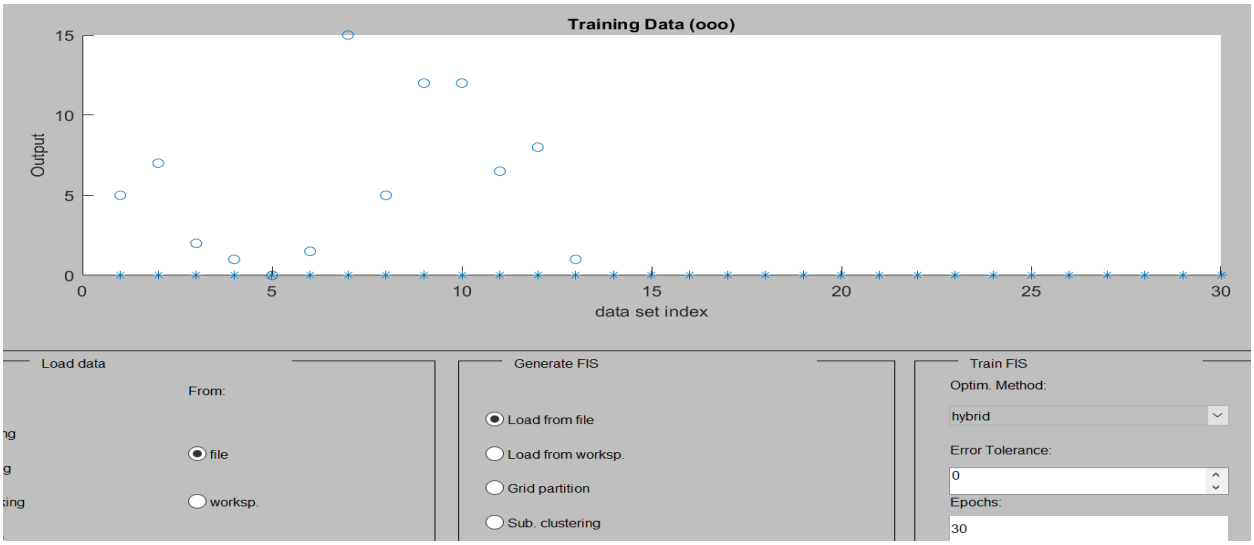

Figure4. 5 Training data of ANFIS

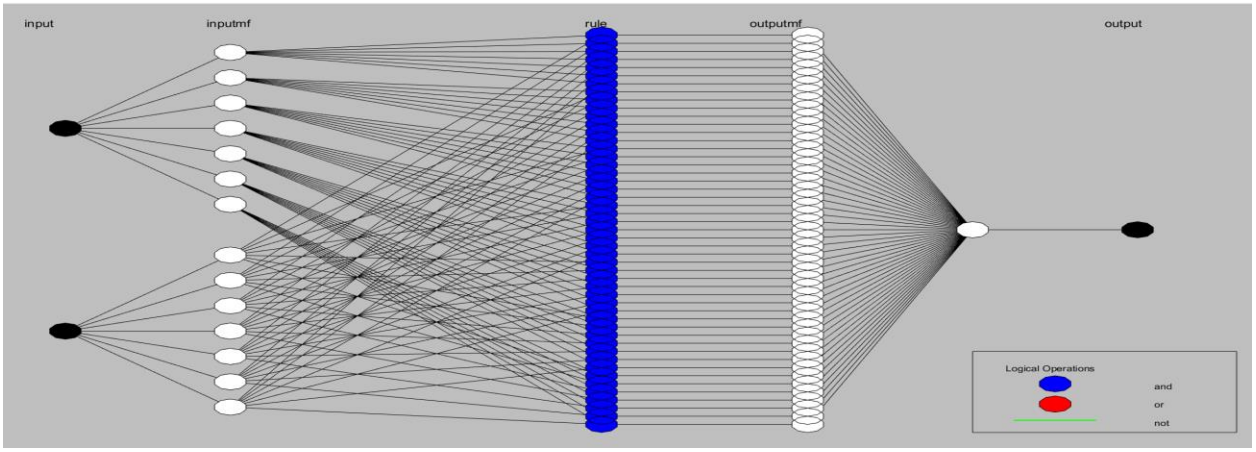

Figure4. 6ANFIS structure on MATLAB

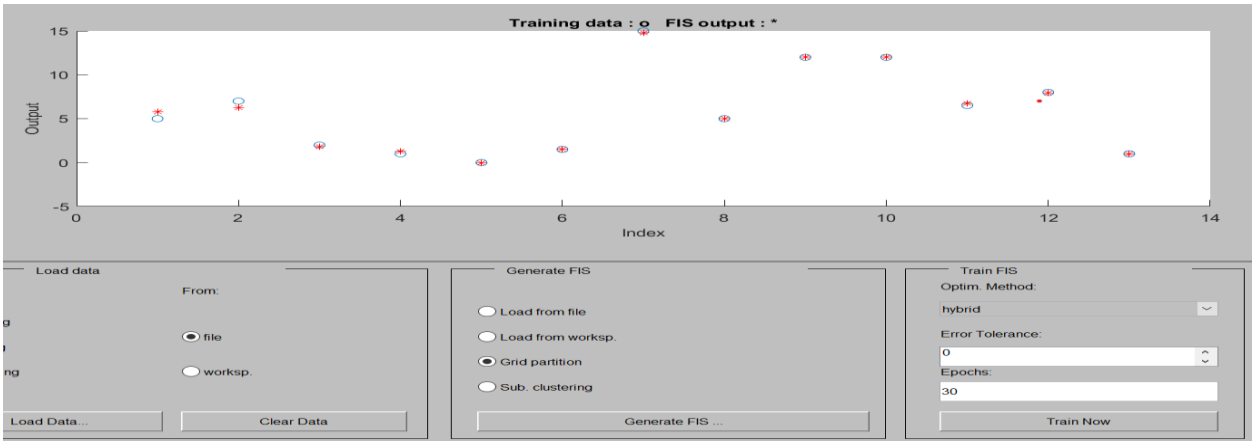

Figure4.7 Training data Vs. ANFIS output

4.1.3 Comparison of classical and adaptive controller

Adaptive controllers usually require an initial training period to estimate the system dynamics and adapt their control parameters. This training time may be a disadvantage in situations where the system dynamics change frequently or where real-time response is critical. Classic controllers do not require training time since their control parameters are predetermined.

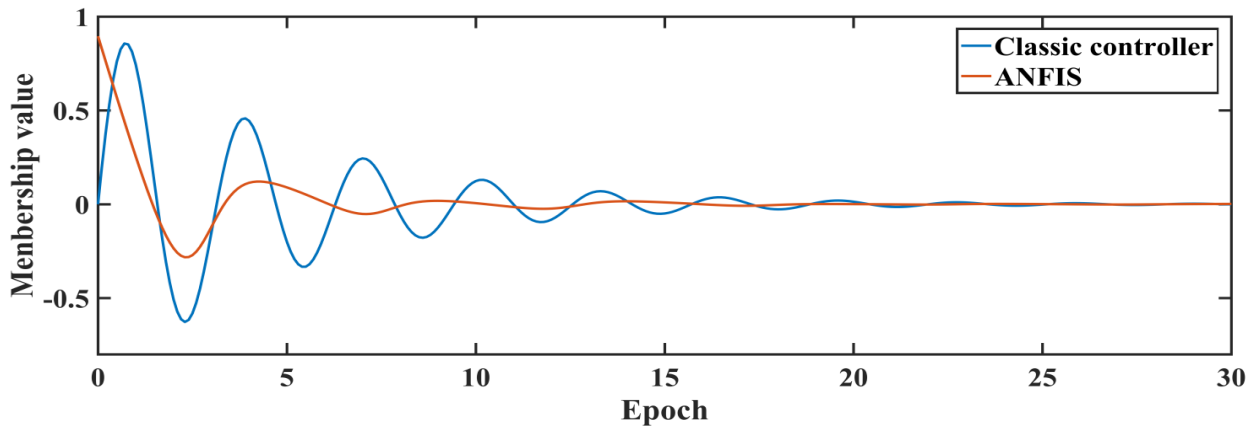

Figure4.8 comparison of controller

4.1.4 MATLAB Model of ANFIS in SIMULINK

As it was proposed before, ANFIS Controller is selected due to adaptively control Dynamic system. Here figure 4.9 shows how modeled adaptive neuro fuzzy inference system is incorporated in MATLAB Simulink to control 48-pulse GTO based STATCOM. Figure 4.9a, shows control of Speed in the turbine. Up to it gets rated value of speed it remains at zero pitch angles. When it increased more than rated speed value the angle of pitch adjusted to minimize power to rated value.

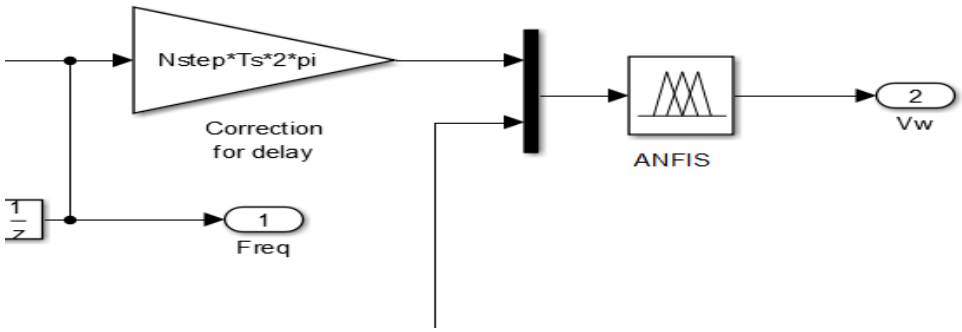

a. **Speed control using ANFIS**

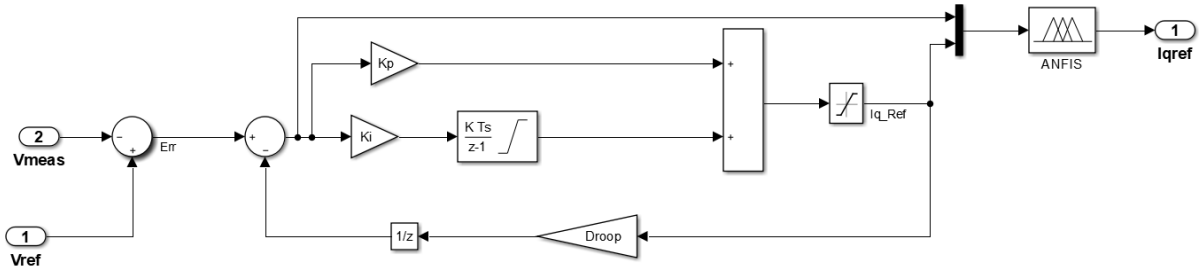

b. ANFIS controlled Voltage

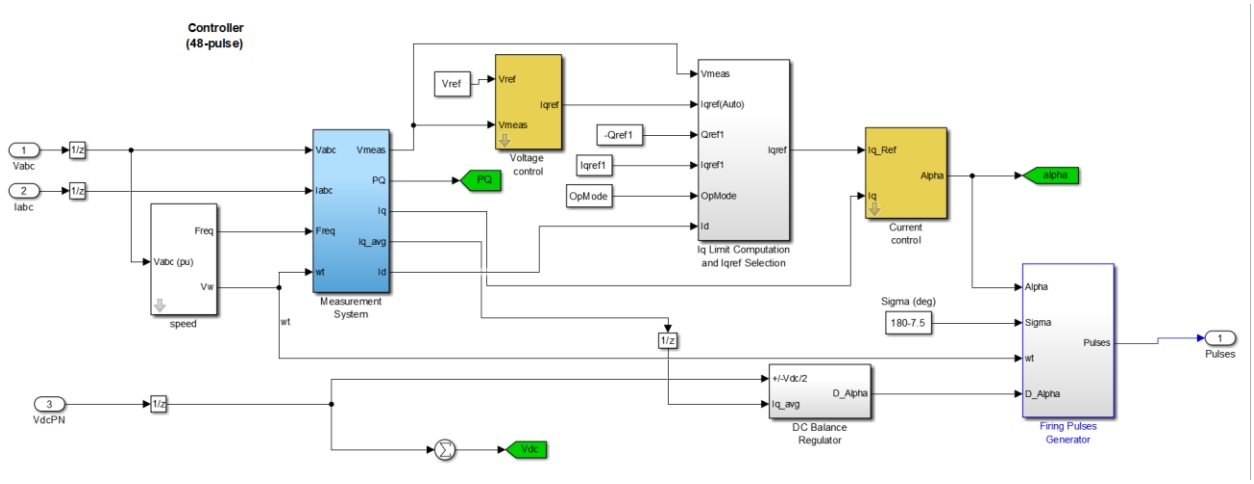

c. over all control circuit of STATCOM

Figure4. 9 a, Speed control b, ANFIS controlled Voltage c, over all control circuit of STATCOM

4.2 OVER ALL MATLAB MODEL OF DFIG BASED WECS

A doubly-fed induction generator that is connected to the grid is seen in this Simulink graphic. Wind turbine protection techniques are required for protection against three-phase failures. With the 19.5 MW wind turbines (13 of which are 1.5 MW each), step-up transformers, and a pi-transmission coverage of 6.18 km from cluster B wind farm connected to a 33 kV line that is generated from Koka at a distance of 10 km to Adama substation. When winds are stronger than the generator's nominal speed (12 m/s), the pitch angle is adjusted to keep the output power at a low level. Because of the power generation, the DFIG speed should be slightly above the essential synchronous speed. The speed varies and the pitch angle control output signal. After the active force is extended to its rated value, the angle controller tries to increase the blade angle to protect the wind turbine from any external damage.

The overall Simulink model of DFIG based WECS is shown in the following Figure 4.10

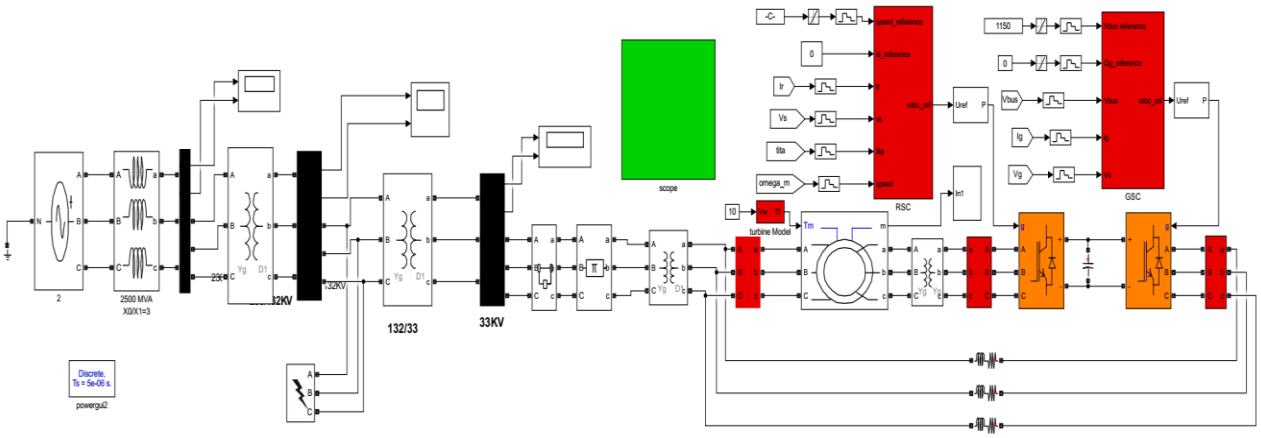

Figure4.10: over all circuit diagram of grid connected DFIG

4.3 EXISTING SYSTEM SIMULATION ANALYSIS (SHUNT CAPACITOR BANK)

Adama Wind Farm employed DFIG and a capacitor bank to adjust for reactive power generation. A capacitor bank is a group of capacitors connected to a power system that store and release electrical energy in response to variations in voltage and current. By adjusting the size and configuration of the capacitor bank, it also controls the flow of reactive power in the system in the Limited Variable Speed Wind Turbine. DFIG uses variable speed with partial power electronics conversion, and it has the ability to rotor power controllers remain active during faults. At this time, it needs fast compensation to remain stable. But capacitors cannot fully

upkeep compensation because of their capacitive characteristics, which have a lower response. The reactive power is required to create the magnetic field that drives the generator. However, the amount of reactive power generated by DFIGs varies with wind speed and load conditions, which can lead to transient instability and power quality problems. When the DFIG generates more reactive power than required, the capacitor bank can absorb the excess reactive power and store it as electrical energy in the capacitors. When the DFIG needs more reactive power than it generates, the capacitor bank can release the stored energy, giving the system the reactive power it needs. The great concept is the capacitor time response of compensation, and the controlling strategy is so weak.

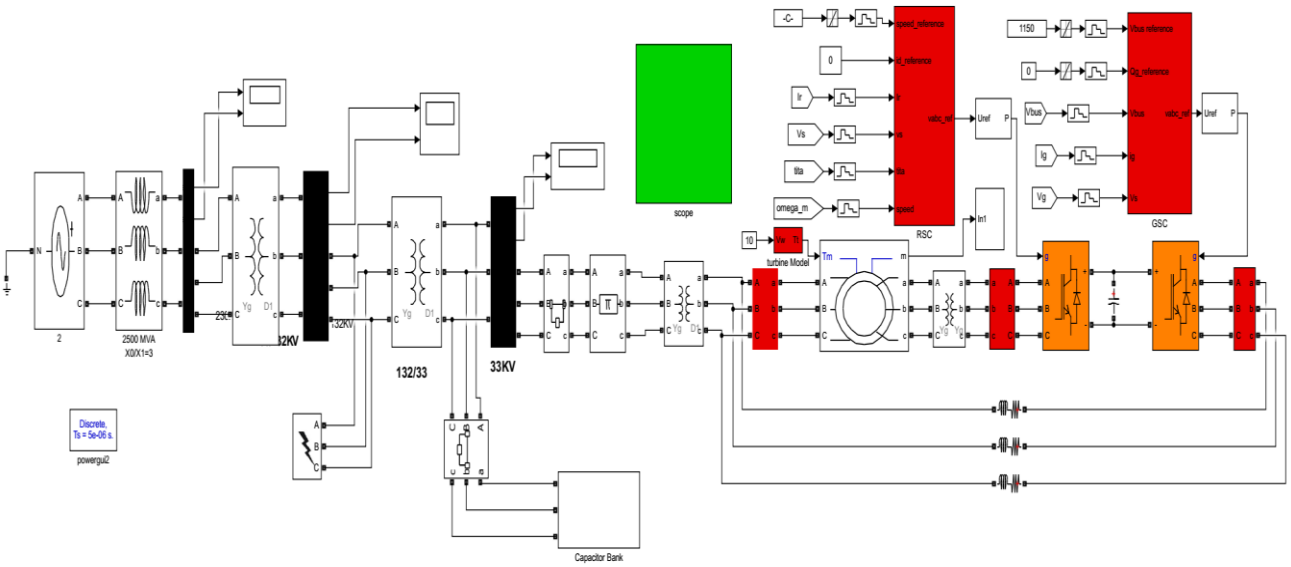

Figure4. 11: existing capacitor compensation system

4.2.1 Transient stability Analysis during 3LG faults of Existing systems

Simulation results shown in Figure 4.12, indicates the stator voltage of the DFIG terminal which clearly shows the capacitor-controlled devices has less to improve voltage transient during a 3LG fault reaches 1710Vin stator voltage terminal. It has high overshoot which is more than doubles from desired values, this makes system instability and high transient.

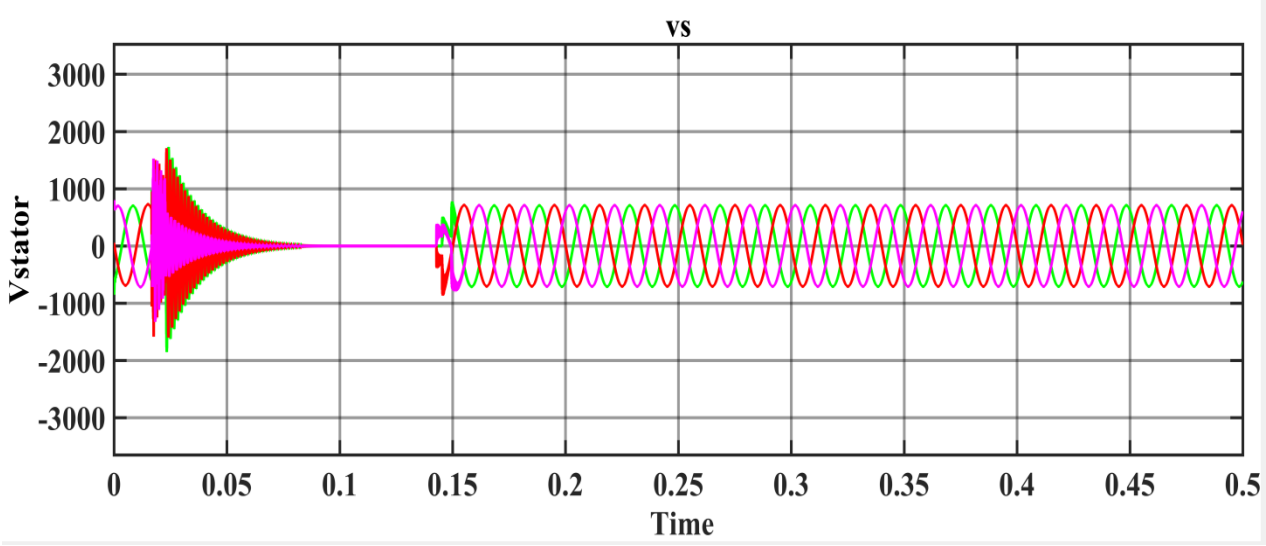

Figure4. 12: stator voltage

The simulation shown in figure4.13 was conducted to evaluate the performance of the capacitor bank in 3LG faults. As shown clearly in figure4.13 the direct axis current of rotor terminal of DFIG has transient at time of 0.02s and it reaches higher undershoot.

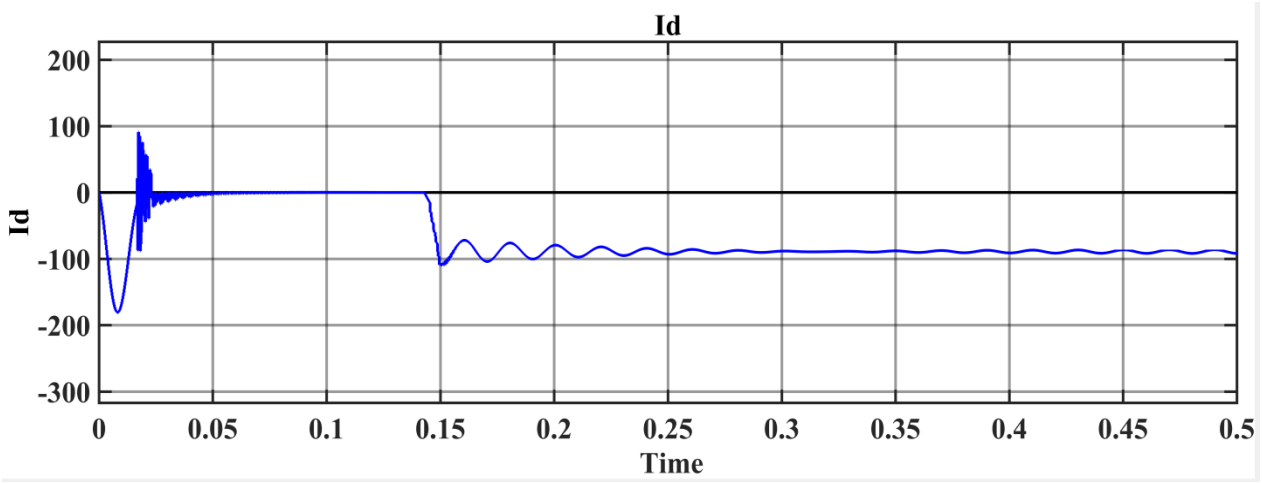

Figure4. 13: Id with the capacitor controlled during 3LG fault

As depicted in Figure 4.14. Shunt-capacitor-controlled devices manage to reduce the fault current. The fault current increases when there is no controller present. But a parallel capacitor reduces the error current.

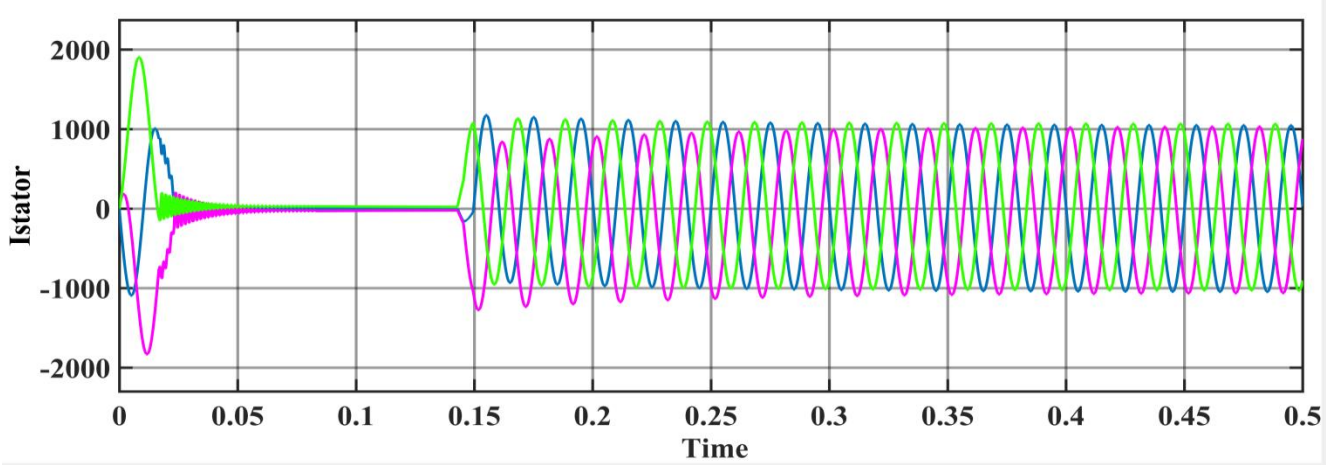

Figure4. 14: Current at DFIG terminal

Figure4.15 shows that grid side converter direct axis voltages which fluctuate during fault and improved by small values compared with no compensation system.

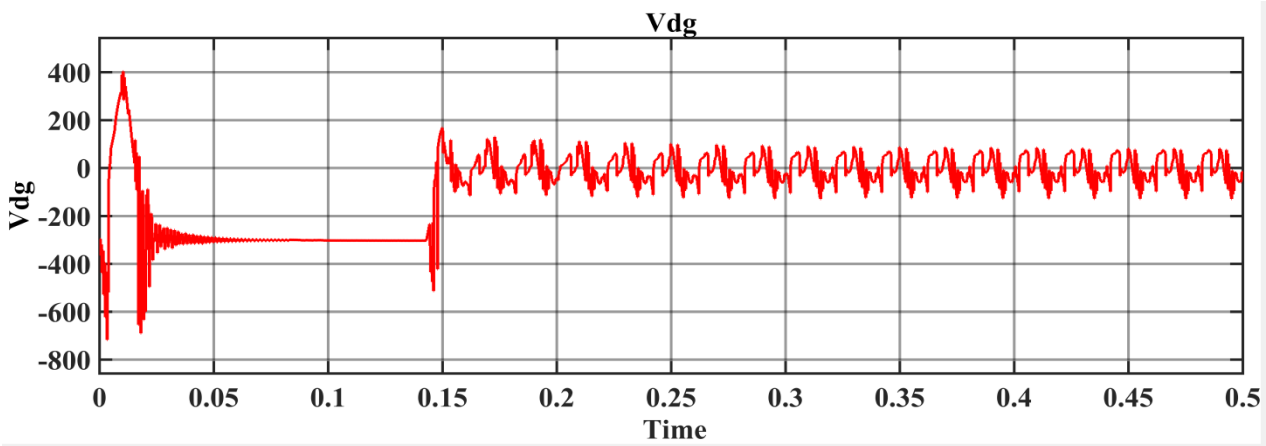

Figure4.15 direct axis Voltage of grid

4.4 SIMULATION RESULTS OF TRANSIENT STABILITY WITH STATCOM

The simulation's output includes a variety of simulated scenarios, including fault conditions (pre-, during, and post-fault conditions) in various locations, switching operations, unexpected increases in load, and system enhancement using STATCOM at the "PCC between the grid and the wind turbine". However, due to this situation, pre- and post-fault conditions might not have much of an impact; it mostly focused on fault conditions. In these simulation findings, it was categorized at the 230 KV side, the 132 KV side, and the side of the wind turbine (stator, rotor, and grid). It took into account real and reactive power as well as the current and voltage (d-q) at

a wind turbine and the locations of faults is on the grid sides. The wind turbine system can be optimized for power output and grid stability by integrating the STATCOM into the ANFIS-based control system, improving system performance and efficiency.

According to the following situation, ANFIS-controlled STATCOM injects and absorbs:

- If the bus terminal voltage Vbus and the STATCOM's output voltage Vstatcom are in phase,
- If Vstatcom is greater than Vbus, the STATCOM will supply reactive power to the system. And Vstatcom absorbs reactive power from the power system if it is less than Vbus.
- No power will be exchanged, and STATCOM will operate in floating mode if VSTATCOM and Vbus are equal.

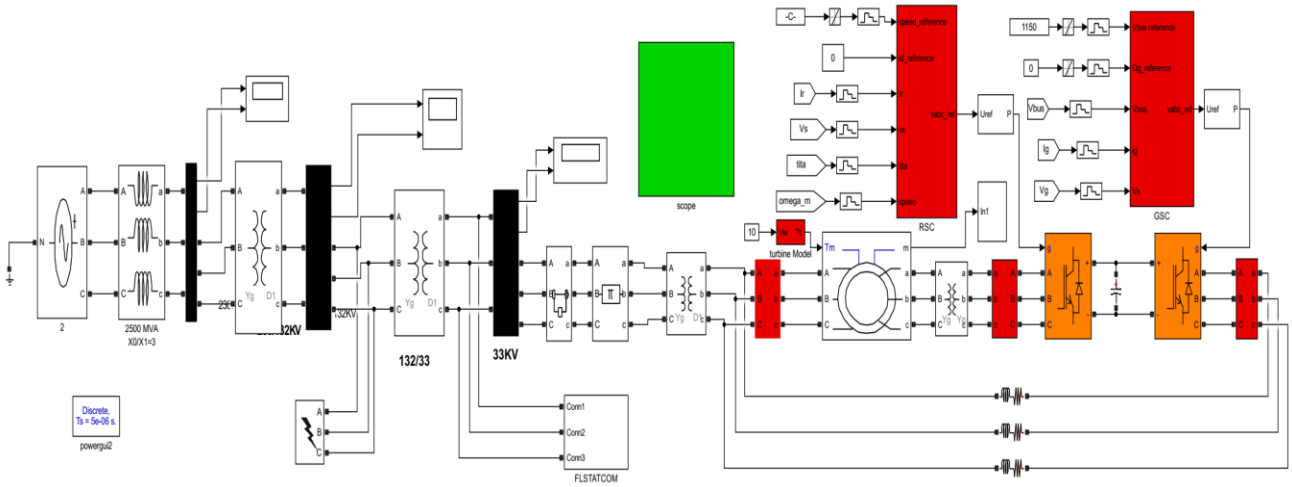

Figure4. 16: over all block diagram of proposed system

4.3.1 Transient stability analysis of DFIG during 3LG faults with ANFIS controlled STATCOM

The voltage across the grid is affected during the three-phase short circuit event in the base case of no STATCOM, as shown in Figure 4.17. When the STATCOM is connected to the system, the current overshooting is reduced through fault duration.

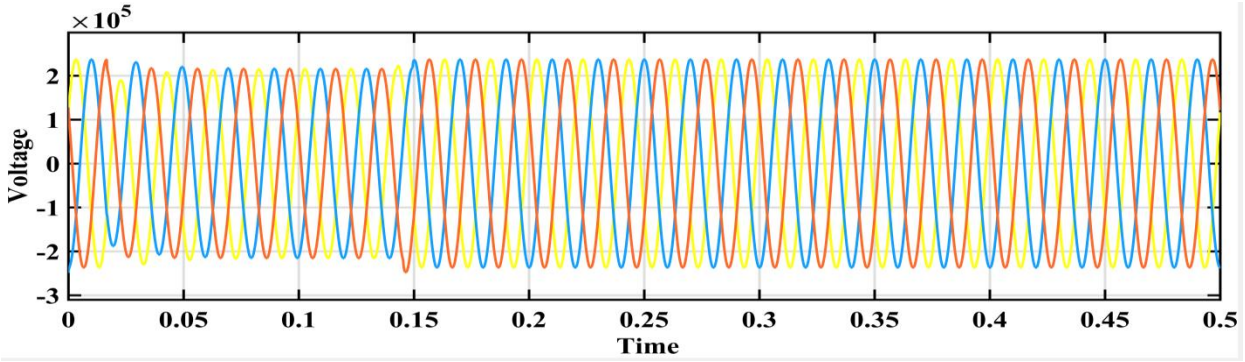

Figure4. 17:230 KV side Voltage

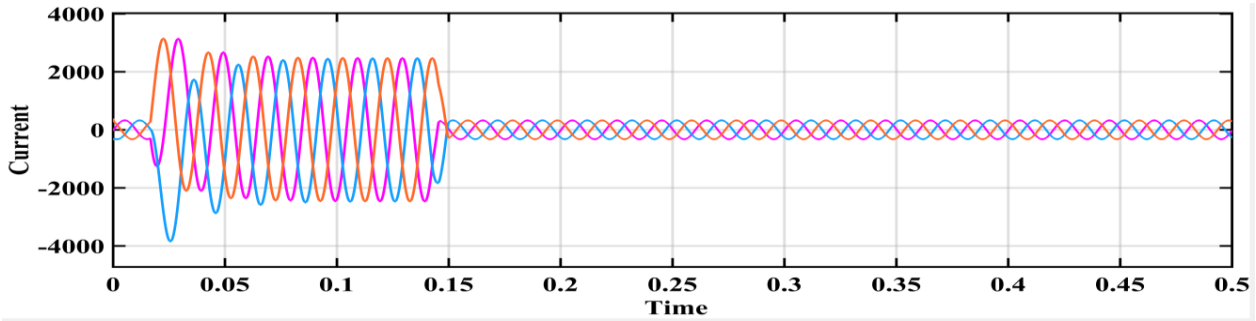

Figure4. 18:230 KV side Current

The graph in Figure4.19 demonstrates how the voltage at the 132 KV side is lowered to almost nil and then returns to normal functioning at 132 KV once the fault has been resolved. The voltage was more disrupted during the fault time.

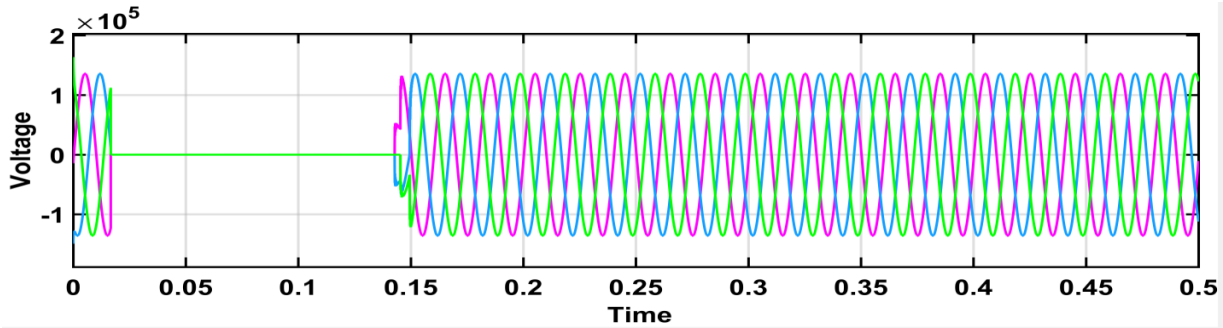

Figure4. 19: 132 KV side voltages

Figure 4.20 depicts the 132 KV side current increasing from 0.013 to 0.1412 seconds during the fault and returning to normal after the fault has been cleared the voltage is settled after a time t=0.15sec.

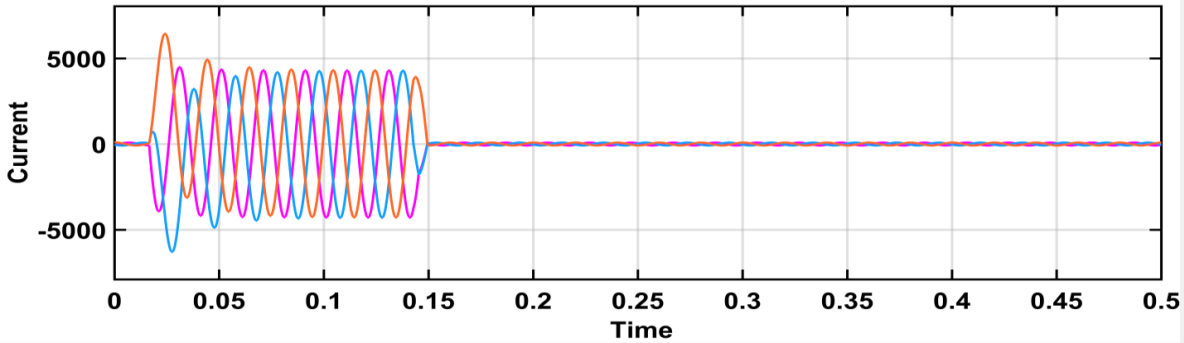

Figure4.20 132 side Current

Figure 4.21 shows the GSC terminal current, which declines during fault time and also increases after the fault is cleared.

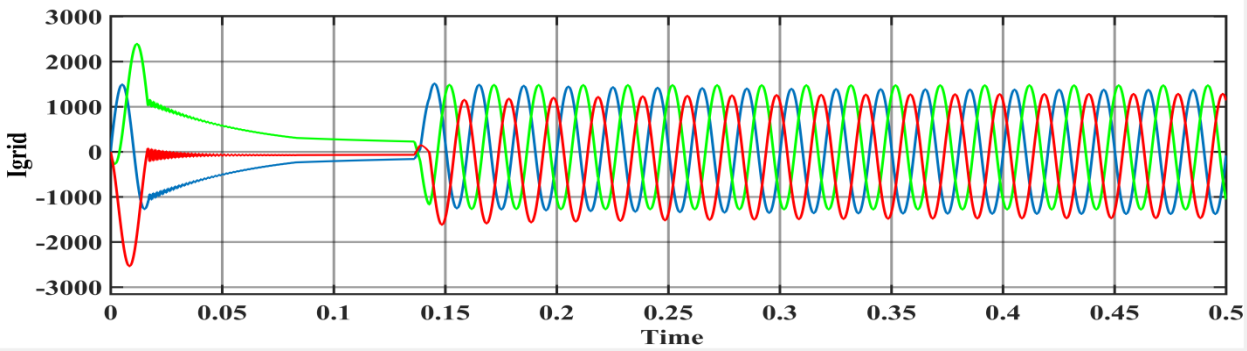

Figure4.21: GSC terminal grid current

The simulation result shown in figure 4.22 indicates that the voltage at the wind turbine side is increased to 1020V during 3LG fault at time ranges of 0.013 to 0.1412 sec. This means the voltage is near rated value during the fault condition and after 0.1412seconds (fault removed) voltage level is at desired value (690V). It has low percentage of the overshoot time and high raise time which indicates how ANFIS controlled STATCOM improved transients to normal values.

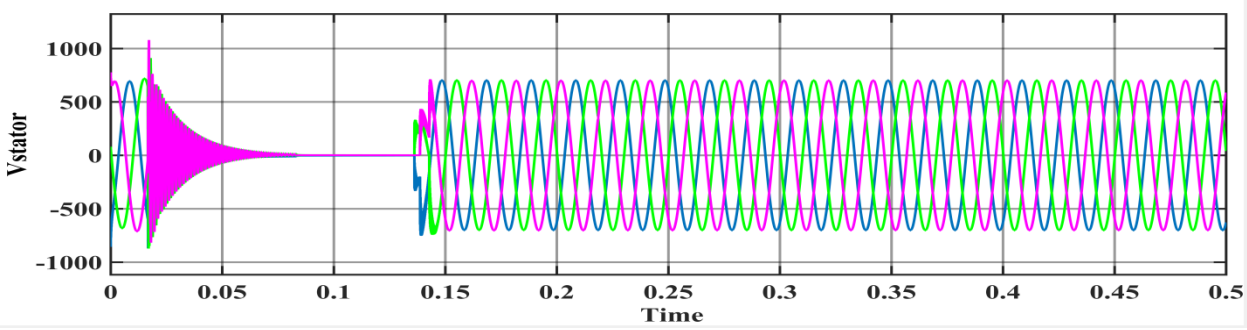

Figure4. 22; stator voltage of RSC terminal

In figure4.23 the simulation result indicates that, the stator current with the compensation of STATCOM back to stable after fault is cleared. During faulty time the current level is decreased up to time t=0.1412sec.

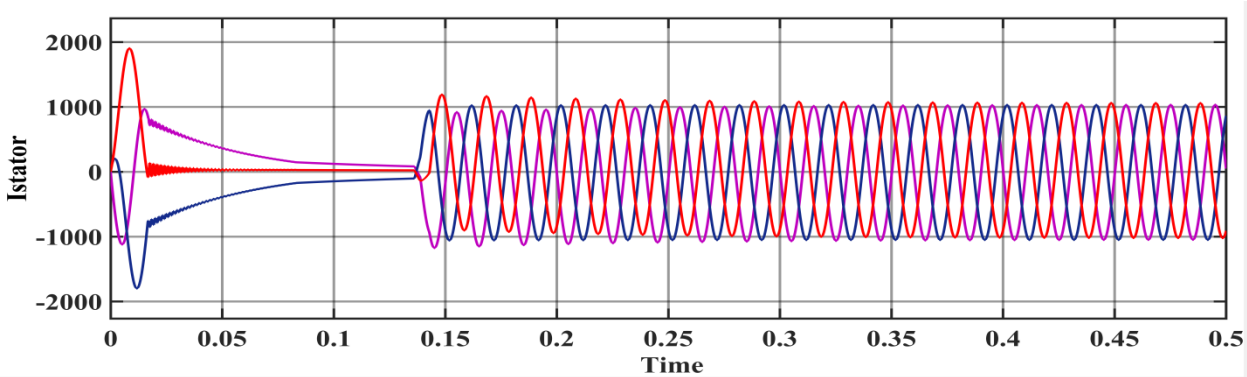

Figure4.23 stator Current of RSC terminal

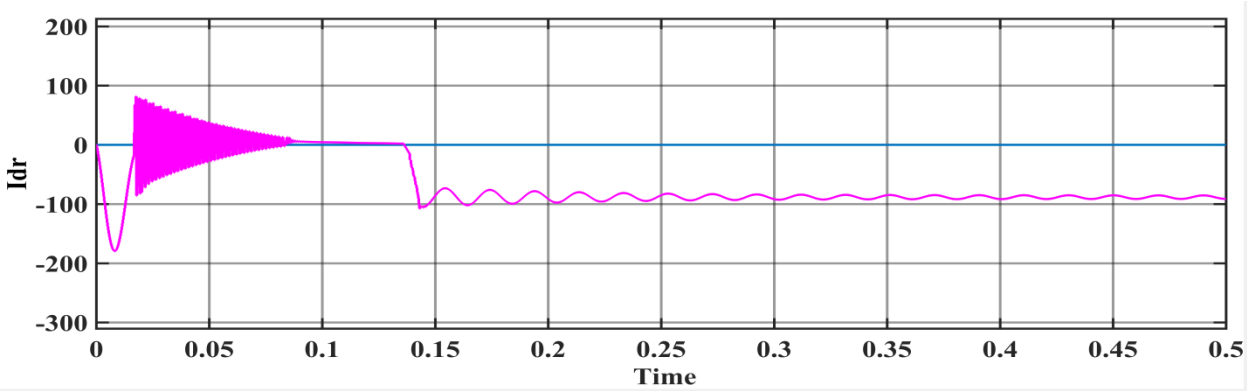

Figure4.24: RSC side direct Current

The real power loss and overload occurred during 3LG faults. Due to this case, during fault time (0.02-0.1412s), real power is around 0 MW, and after the fault is removed, real power is back to its normal condition around 11 MW.

In fact, the DFIG output active power is significantly reduced due to the short circuit fault at the grid side, and this gets improved with the connection of the STATCOM, as shown in Fig. Due to the drop in the generated power, the DFIG shaft speed is accelerated to compensate for the power imbalance, and the shaft will experience oscillations; otherwise, these oscillations are substantially reduced when the proposed STATCOM controller is connected (Fig. 4.25).

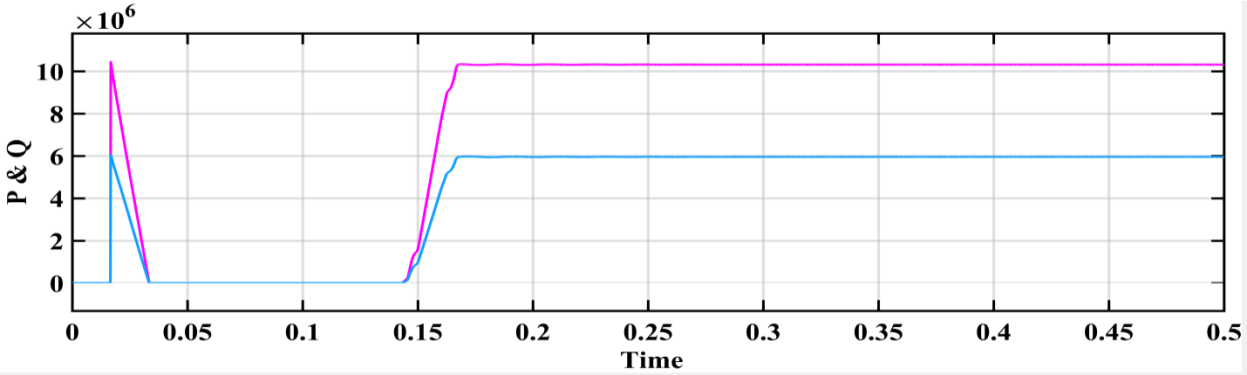

Figure4.25 active power of wind turbine

Also, reactive power generated is higher, as shown in the figure4.26. During fault time, reactive power generated by STATCOM is 5.89 MVAR.

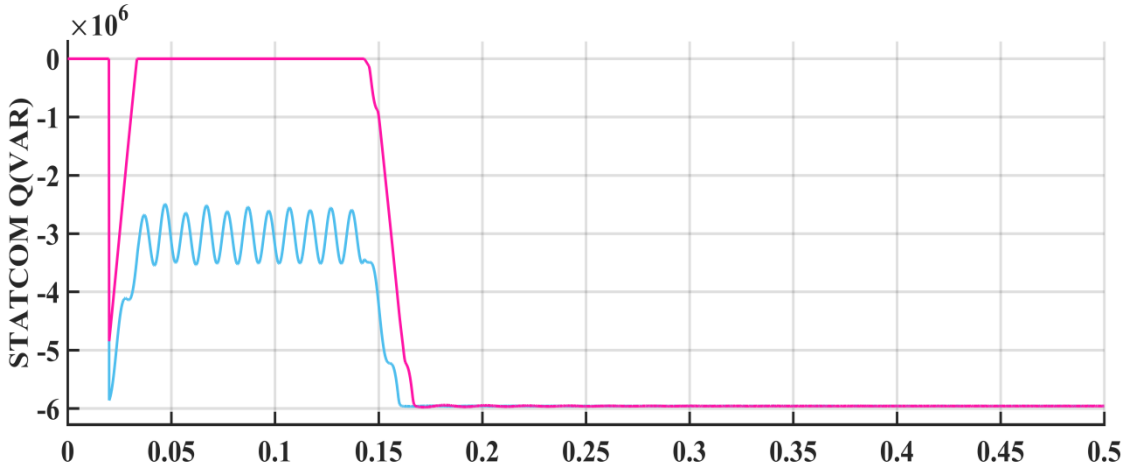

Figure4.26 reactive power Injected during faults

4.5 Comparative analysis of transient stability of DFIG Variable speed based WECS with existing and proposed scheme

A fault of a three-phase short circuit is simulated at the grid side of the system and cleared at t = 0.1412s. The simulation shows that the dynamic response of the existing and proposed scheme of the system, i.e., the connection of the STATCOM. The voltage magnitude at the fault drops to some cases. When the STATCOM is connected, the voltage drop is decreased, which is attributed to the reactive power support of the STATCOM, as clearly seen in the Figure 4.27.

The comparative simulation result shown Figure 4.27 indicates the voltage level on PCC. During faults condition and with existing compensation system the voltage level at 33 bus where 0.8835

under range after compensation returns to normal 1.038 pu (33 kV).Figure 4.27 shows that during the fault voltage on the PCC drops to zero. After fault clearing, the voltage gradually recovers 1.038 pu (33KV) with STATCOM but the DFIG equipped without STATCOM cannot recover to normal acceptable grid voltage.

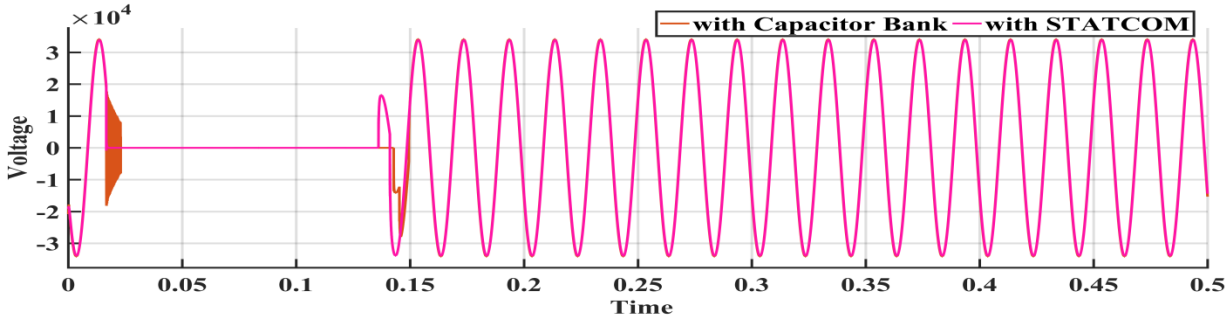

Figure4. 27: Voltage at PCC

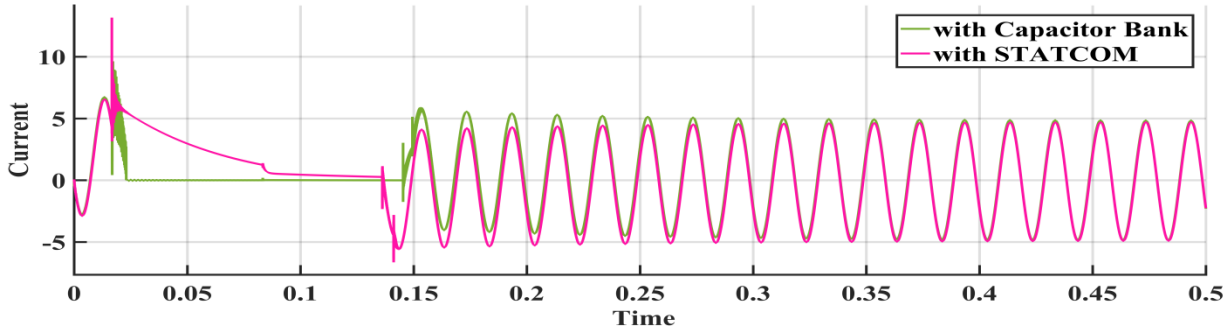

Figure4. 28: Current at PCC

During fault conditions, the current increases. This means during fault time the current is up to 1800A, and after fault removal the current decreased to normal value. The improvement of STATCOM is shown clearly in Fig. 4.29 over the capacitor bank.

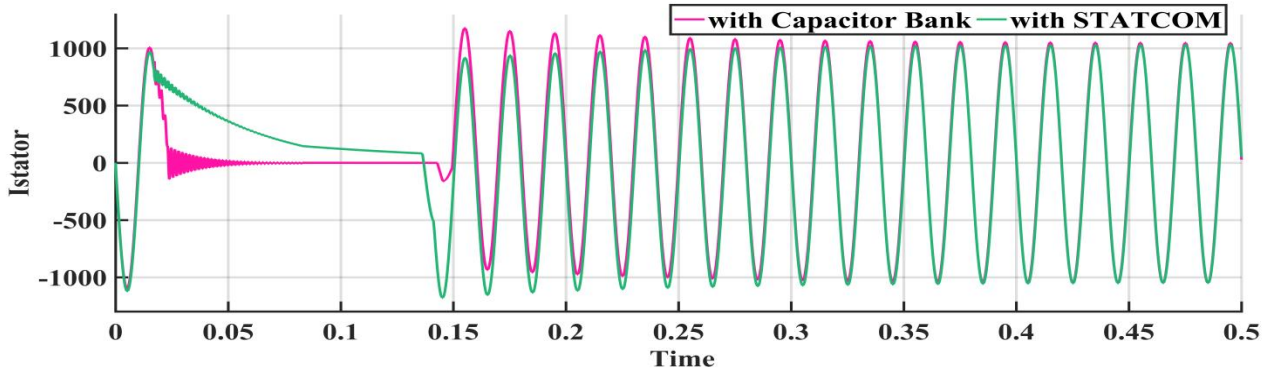

Figure4. 29 stator current comparison b/n existing and STATCOM

As shown in Figure 4.30,STATCOM based quadratre current of Rotor side converter terminal has good achivement during faults and it also decrease undershoot by 27 as shown clearly in figure. As comparatively with Capacitor Bank , quadratre current of Rotor side converter is zero and high undershoot at t=0.02sec. this shows how ANFIS controlled STATCOM is better performance than existing compensations.

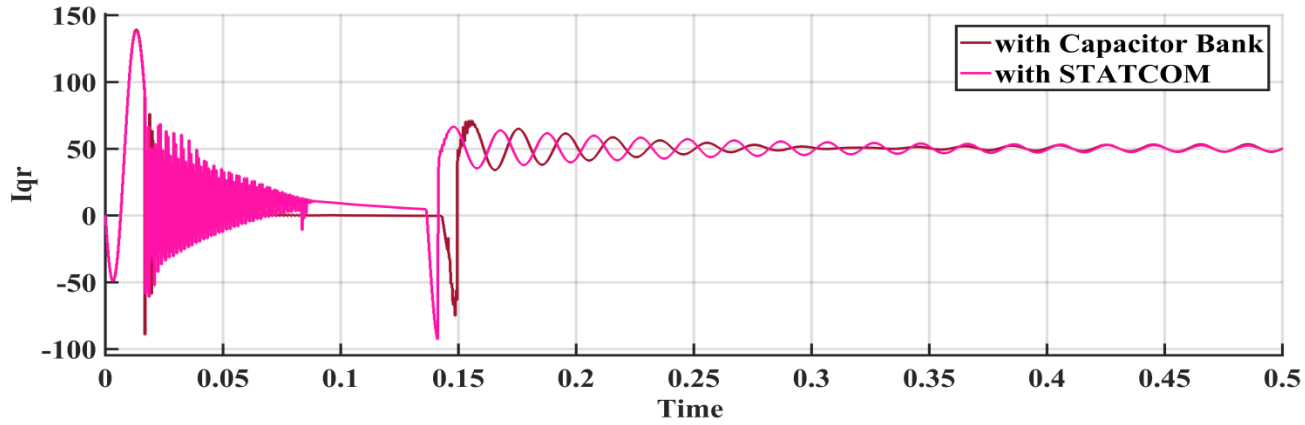

Figure4.30: quadrature Current of RSC terminals

Figure 4.31 shows the rotor current by compensating the VAR to the system. The rotor current feds to machine depends on slip speed of the generator which generates constant frequency and voltages at the stator terminal. As shown figure4.31 uncontrolled rotor currents with its frequency are varies when speed deflects its value.

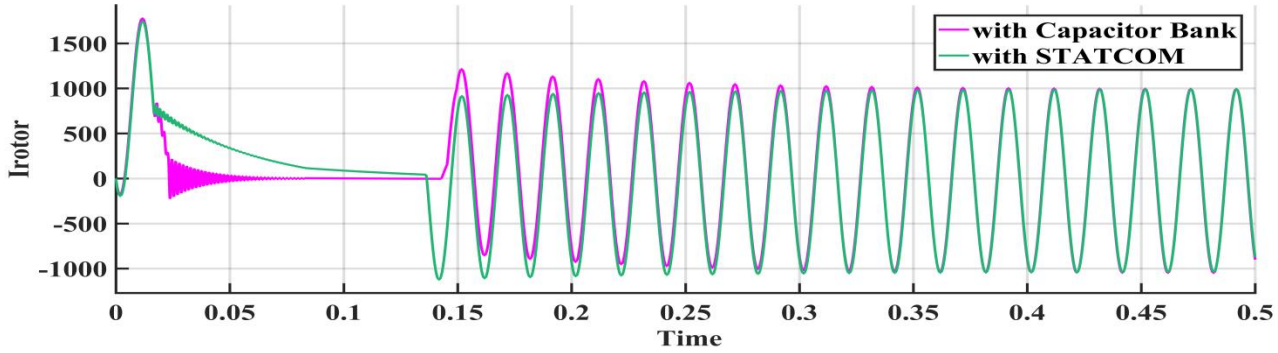

Figure4. 31 rotor Current change across RSC terminals during 3LG faults

Figure 4.32 shows stator voltage of the wind turbine with capacitor Bank and STATCOM. The overshoot transient of STATCOM is 28.6% these shows how STATCOM has high responses and fast controlled system. This makes it advantageous over capacitor bank.

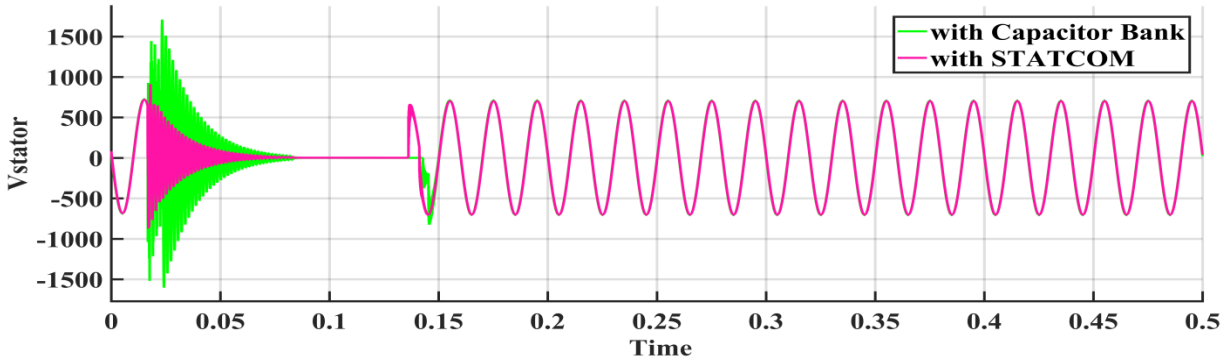

Figure4. 32: stator Voltage change across RSC terminal during 3LG faults

4.6 Comparative analysis of transient stability of DFIG Variable Speed based WECS with and without STATCOM

Transient stability of DFIG with and without STATCOM is Compared using simulation data inspector of MATLAB. It shows how STATCOM improved the grid-connected wind energy conversion systems during 3LG faults on the same x-y axis.

The simulation result shown in Figure 4.33, indicates the rotor current is high oscillator without STATCOM, but after STATCOM is connected to the system, it has decreased to normal values. In the presence of STATCOM, the reactive power support provided by the DFIG to the grid has decreased by 50 between at t=0.02sec and 0.1412sec. Consequently, the steady-state condition is reached.

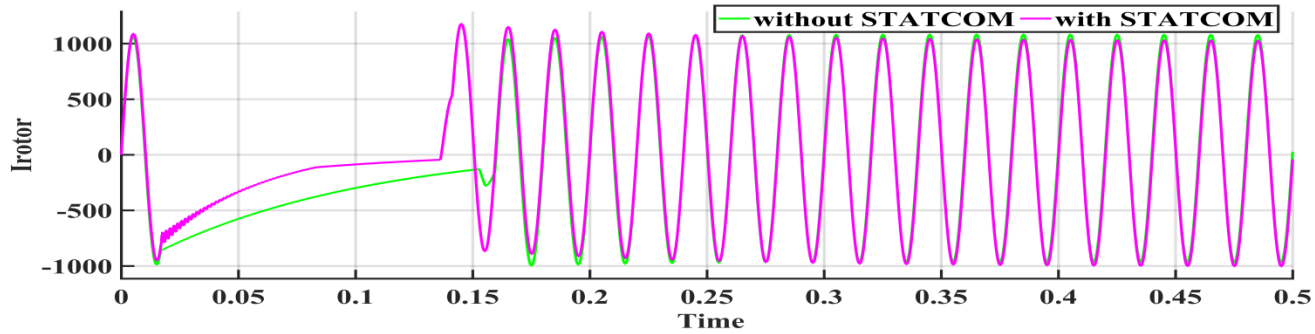

Figure4.33: Effect of 3LG fault on Ir of DFIG with and without STATCOM

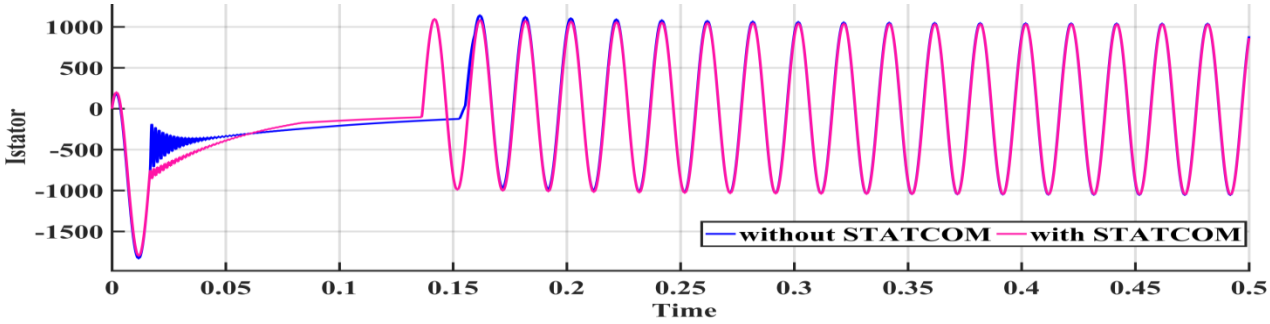

Figure4.34: Effect of 3LG fault on Istator of DFIG with and without STATCOM

The dynamic reaction of the DFIG with and without the connection of the STATCOM is shown in Figure 4.35. When the STATCOM is connected, the voltage level is 1020V, which is attributable to the STATCOM's support of reactive power. The voltage magnitude reaches 3100 when the STATCOM is not connected.

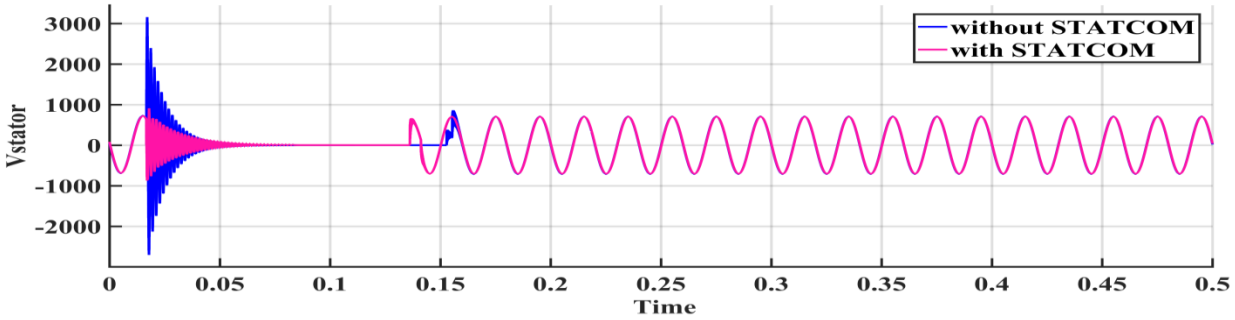

Figure4.35: Effect of 3LG fault on Vstator with and without STATCOM

Simulation shown in figure4.36 shows a comparison of quadrature current with and without STATCOM. As the figure4.36 clearly shows there is undershoot before it reaches settle point, there is an improvement after STATCOM compensated by 30.

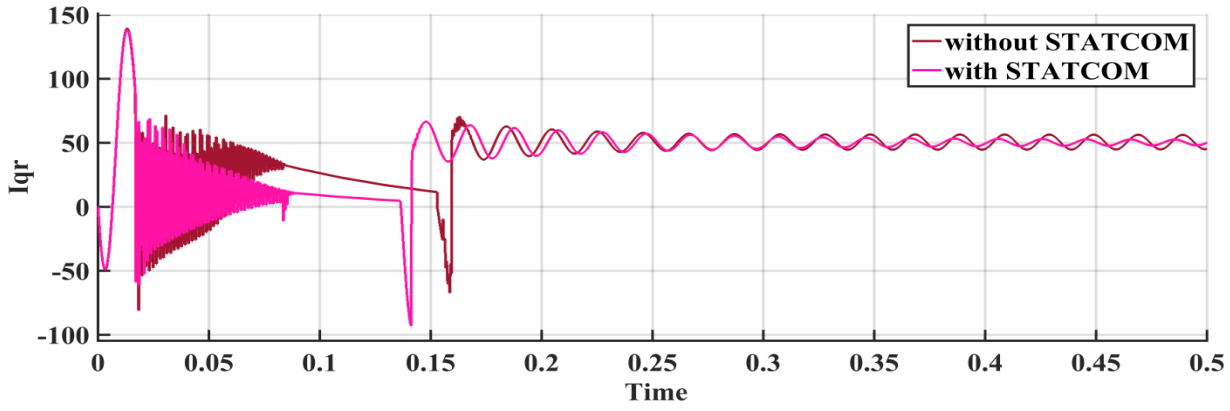

Figure4.36: Effect of 3LG fault on Iq with and without STATCOM

4.7 Testing and validating transient stability analysis

To validate transient stability, accepted criteria for the transient stability indices based on system requirements standards. These criteria define the acceptable range of values for each index. A certain index may need to be within a specified limit for the system to be considered stable as discussed in section 2.5. These indices provide quantitative measures to evaluate the system's ability to maintain stable operation. The various indices are TRASI, TSI, and CCT.

Table4. 1Validation Test of results after compensating STATCOM.

No	Indices	Value	Constraints	Validation test
1	TRASI	0.87 (87%)	$0 \leq TRASI \leq 1$	Stable
2	TSI	0.769 (76.9%)	$-100 \leq TRASI \leq 100$	Stable
3	CCA &CCT	$46.7958° \; and \; 0.1412sec$	Low CCA & CCT	Stable

ANFIS controller makes the STATCOM more effective. FLSTATCOM also guarantees much superior performance as compared to Capacitor Bank, in terms of overshoot time, rise time and settle time.

The percentage of overshoot represents the magnitude of the response exceeding the reference value during a transient event. In normal circumstances, the overshoot percentage is a positive value and ranges from 0% to 100%. From the Table4.2, the only STATCOM is in normal condition. Capacitor Bank and no compensation overshoot is more than 100%, which means that the response has exceeded the reference value by more than double. This typically indicates a highly unstable and poorly controlled system response in the capacitor bank and also suggests severe instability and diverging responses exist in the capacitor. Such high overshoot values can lead to voltage or current magnification, equipment stress, and potential system instability.

The rise time indicates how quickly the response reaches its final value after the onset of the transient. A shorter rise time implies a faster response, while a longer rise time suggests a slower response.

Table4. 2; Comparison of Capacitor and STATCOM performance during fault

Parameter	Compensation	Controller	Overshoot	Rise time	Settle time
Stator Voltage	No-Compensation	No	323%	0.33msec	0.166 sec
	Capacitor Bank	Simple switch	147%	0.309msec	0.156 sec
	STATCOM	ANFIS	28.6%	0.3msec	0.142 sec

4.8 Cost analysis

The range of costs of FACTS devices is available in the Siemens AG Database. A polynomial cost function of FACTS devices is resulting and used for the FACTS allocation study and it includes transportation cost, installation cost and operating cost.

The investment costs of STATCOM.

$$Cstatcom = (0.0004S^2 - 0.3225S + 128.75)\frac{\$}{year} \quad \text{.....4.1}$$

From the formula above we can calculate the cost of STATCOM as follows: and the reactive power produced by STATCOM is 5.89Mar in the improvement conditions.

$$Cstatcom = (0.0004(5.89)^2 - 0.3225(5.89) + 128.75)\frac{\$}{year} = 126.8\$perKVAR$$

The overall investment cost of STATCOM, if the wind turbine works schedule.

$$ICstatcom = \frac{Cstatcom * Sstatcom}{hour\ in\ year} \quad \text{.....4.2}$$

If the wind turbine works for 14 hours in one day, it works for about 5475 hours over the years. Then the overall investment cost of STATCOM is calculated as

$$ICstatcom = \$126.8/KVAR * 5.89 * 1000\ /KVAR = \$747{,}205.4$$

$$year\ of\ payback\ payment = \frac{\$747{,}205.4}{126.8} per\ operating\ time = 1.5$$

The installation of a STATCOM helps reduce reactive power consumption in a power system, resulting in cost savings. Cost of the FACTS is compared in Table 3.2.

To provide a detailed cost breakdown for each component of an 8.8MVAR capacitor bank at 33 kV, here a general breakdown of the key components typically found in a capacitor bank and their cost:

$$Total\ Investment\ Cost =$$

$$\text{Design and Engineering Cost} + \text{Material Cost} + \text{Installation Cost} +$$

$$\text{Testing and Commissioning Cost} + \text{Annual Maintenance Cost} \times \text{Lifespan} +$$

$$\text{Transprtation cost} + \text{Contingency Cost} \quad \text{.....4.3}$$

1. Design and Engineering Cost=0.05×Total Project Cost

Design and Engineering Cost=0.05×Total Project Cost**=$27026.05**

2. Material Cost: Obtain costs for capacitors, switching devices, and control and protection equipment.

For an 8.8 MVAR capacitors bank, the cost of capacitors can was calculated.

8.8*1000KVAR*25/KVAR=$220,000

The cost of the switching mechanism, including vacuum switches, can be 3*50,000=$150,000

A comprehensive control and monitoring system for an 8.8MVAR bank can be $100,000.

The cost of protection devices such as overvoltage protection, overcurrent protection, under frequency protection, and surge arresters can vary based on the manufacturer, specifications, and quantity. CH surge protector=$65, Voltmeter-Ammeter-Voltage-Protection=$442. The cost of the enclosure and mounting hardware cost for a suitable outdoor enclosure were $20,000. The cost of grounding and earthing components, including copper conductors, grounding rods, connections= $3,000.

Total material cost =$540,521

2. Installation Cost=0.10×Total Project Cost

Installation cost =0.1*$540,521=$54,052.1

3. Testing and Commissioning Cost=Cost of Testing Equipment + Cost of Commissioning Service

Cost of purchasing or renting specialized testing equipment needed to assess the performance of the capacitor bank. This may include instruments for measuring capacitance, voltage, current, and power factor, fees for engineers who oversee the commissioning process. This may involve verifying the wiring, calibrating control systems, and ensuring that the capacitor bank operates according to design specifications. Labor costs are associated with the personnel performing the tests and commissioning activities. This includes the time spent by skilled technicians and engineers. Costs associated with preparing commissioning documentation, reports, and certification, commissioning services involve professionals traveling to the site, consider travel expenses, accommodation, and per diem costs. Training costs for personnel who will be operating and maintaining the capacitor bank after commissioning, $80,000.

4. Annual Maintenance Cost=Estimated Annual Maintenance Cost

An Operating and maintenance cost was $300 per year.

5. Contingency Cost = 0.05×Total Project Cost

   0.05*=$540,521 =$27,026.05

6. Lifetime Cost=Total Project Cost Lifespan /lifespan

Assume a 20-year lifespan for the capacitor bank. Lifetime Cost =$27,026.05

7. Transportation cost $10,000

   Total of investment cost

   $ICt = \$27{,}026.05 + 540{,}521 + 54{,}052.1 + \$80{,}000 + \$3{,}000 + \$27{,}026.05 +$

   $\$27{,}026.05 + \$10{,}000 = \$768651.25$……..4.4

As it was mentioned in previous chapter, material cost of Material cost of Capacitor Bank is cheap but it has additional other components for controlling, monitoring (protection), these all components plus material cost make it expensive. $21445.75 is saved if STATCOM is utilized and also installation of the STATCOM reduced annual reactive power consumption.

Before STATCOM Installation (with Capacitor Bank):

-Annual reactive power consumption: 5475 hr*8.8 MVAR=48,180 MVARhr

-Reactive power tariff: $50 per KVAR

- Reactive power cost :($50/KVAR)* 8.8 MVAR = $440,000

After STATCOM Installation:

- Annual reactive power consumption: 5475 hr*5.89MVAR=32,247.75MVARhr

- Reactive power tariff: $50 per KVAR

-Reactive power cost :($50/KVAR)*(32,247.75* 1000 KVARhr/5475 hr) = $294,500

Cost Savings:

- Reactive power consumption reduction: (48,180 -32,247.75) MVARhr=15,932.25MVARh

- Cost savings due to reactive power reduction: (15,932.25MVARh /5475 hr.)*$50 per KVAR = $145,500

In this thesis, the installation of the STATCOM helps to reduce annual reactive power consumption by 15,932.25MVARh. With a reactive power tariff of $50per MVAR, the cost savings due to the reduction in reactive power consumption amount to $145,500 annually.

CHAPTER FIVE

CONCLUSION AND FEATURE WORK

5.1 Conclusion

In order to enhance the performance of a “DFIG-based WECS”, this thesis introduces a new STATCOM application that modifies both active and reactive powers at the point of common coupling during various disturbance occurrences. ANFIS controllers form the foundation of STATCOM's planned control system. Below is a summary of this study's main findings.

The dynamic behavior of variable-speed wind energy conversion systems is compared with the presence of the capacitor bank and STATCOM in the event of a major disturbance. Then the performance of STATCOM for system stability improvement is compared with the capacitor bank. It is clear from the simulation results (Fig 4.27–4.32) that there is a considerable improvement in the system performance with the use of STATCOM, for which the settling time in post-fault is found to be around 0.1412 sec. and the fault clearing angle is 46.8. It reduce maximum overshoot from 174% to 28.6%, these shows how ANFIS based STATCOM is advantageous over Capacitor Bank.

The dynamic behavior of the power system is compared with and without STATCOM in the system in the event of a 3LG fault. The performance of With-STATCOM in the simulation results clearly showed that there is a considerable improvement in the system performance with the use of STATCOM, as shown in the results (Fig.4.33-4.36).it reduce overshoot from 323% to 28.6%, these shows great achievement of ANFIS based STATCOM.

The three-phase short circuits on the grid side have a substantial impact on the DFIG's dynamic performance. The results of the simulation revealed that in some situations, the voltage at the point of common coupling exceeds the restrictions of some of the current codes, indicating the need to disconnect the WECS from the grid. The suggested STATCOM was demonstrated to enhance the DFIG's dynamic performance during the analyzed fault events to the extent that the connection of the wind turbine to the grid will be maintained during such faults.

The ANFIS control algorithm is difficult to implement, but the findings demonstrate that it is more adaptive and has high performance to improve the DFIG during fault events at the grid side or within the DFIG's converter station.

Although the proposed STATCOM proved successful in enhancing the DFIG's overall performance, widespread adoption of the STATCOM is anticipated soon due to the quick advancement of power electronics.

5.2 Recommendation

Without reservation, I strongly recommend that Ethiopian electric power (EEP) utilize STATCOM for grid protection, to increase transmission line reliability and efficiency, and to reduce the socio-economic problem.

5.3 Feature Scope

This project was concerned with the wind energy conversion system's transient stability. Future study will concentrate on applying more efficient control strategies like model reference adaptive control with dynamic compensation techniques, such as UPFC, while keeping economic aspects and evaluating their usefulness in enhancing the wind farm's dynamic performance.

REFERENCE

[1] H. S. Ruiz, X. Zhang, and T. A. Coombs, “Resistive-Type Superconducting FaultCurrent Limiters: Concepts, Materials, and Numerical Modeling,” IEEE Trans.Appl. Supercond., vol. 25, no. 3, pp. 1–5, Jun. 2015.

[2,] L. Xu and Y. Wang, “Dynamic modeling and control of DFIG-based wind turbinesunder unbalanced network conditions,” IEEE Trans. Power Syst., vol. 22, pp. 314–323, 2007.

[3] E. Echavarria, B. Hahn, G. J. W. van Bussel, and T. Tomiyama, “Reliability of Wind Turbine Technology Through Time,” Journal of Solar Energy Engineering, vol. 130. p. 031005, 2008.

[4] Varun Kumar * , Ajay Shekhar Pandey and Sunil Kumar Sinha, Stability Improvement of DFIG-Based Wind Farm Integrated Power System Using ANFIS Controlled STATCOM, Energies 2020, 13, 4707; doi:10.3390/en13184707.

[5] K. Malekian, U. Schmidt, A. Shirvani, and W. Schufft, “Investigation andmodeling of transient voltage stability problems in wind farms with DFIG andcrowbar system,” in 2014 6th International Conference on Information Technologyand Electrical Engineering (ICITEE), 2014, pp. 1–8

[6]Lokesh Vitonde, Surbhi Shrivastava, Alka Dharwal,Power Quality Improvement of Wind Energy by STATCOM,Irjet,Volume: 03 Issue: 07 | July-2016

[7] Arindam Chakraborty, Shravana K. Musunuri, Anurag K. Srivastava, and Anil K. Kondabathini, Integrating STATCOM and Battery Energy Storage System for Power System Transient Stability, Advances in Power Electronics Volume 2012, Article ID 676010, 12 pages doi:10.1155/2012/676010.

[8] Abdelsattar M, Arafa Hafez W, A. Elbaset A, et al. Voltage stability improvement of an Egyptian power grid-based wind energy system using STATCOM. Wind Energy. 2022; 25(6):1077-1120. doi:10.1002/we.2716.

[9] Varun Kumar1, Vipin Patel, A S Pandey, S K Sinha, Dilip Kumar,Transient Stability Enhancement of DFIG based Offshore Wind Farm Connected to a Power System Network using STATCOM,International Journal of Engineering &Technology, 7 (3.12) (2018) 1303 -1311.

[10] Qin, B., Zhang, R., Li, H, Ding, T, Liu, W. Disturbance attenuation control for LVRT capabilityenhancementofdoubly-fedwindgenerators. IET Gener, Transm, Distrib, 2021.

[11] Megha Vyas, Monika Vardia, Vinod Kumar Yadav, Shripati Vyas and Yashwant Joshi, Power Quality Improvement by using STATCOM for DFIG based Wind Energy Conversion System, Easy Chair Preprint March 3, 2021

[12] Thomas T, Asok P. Event analysis and real-time validation of doubly fed induction generator-based wind energy system with grid reactive power exchange under sub-synchronous and super-synchronous modes, Engineering Reports. 2020.

[13] Boubzizi, S., Abid, H., El Hajjaji, A.,. A comparative study of three types of controllers for DFIG in wind energy conversion systems Prot Control Mod Power Syst **3**, 21 (2018) https://doi.org/10.1186/s41601-018-0096-y

[14] Huang, Y., Chen, W., Deng, X., Tang, J., Zhu, G. and Zhang, H. (2019), Modelling of DFIG-based wind turbine for low-frequency oscillation analysis of power system with high penetration of distributed energy. The Journal of Engineering, 2019: 2625-2628. https://doi.org/10.1049/joe.2018.8548

[15] Khani, NG. Improving fault ride through capability of induction generator-based wind farm using static compensator during asymmetrical faults. International Trans Electrical Energy Syst. 2021; 31(11):e13103. doi:10.1002/2050-7038.13103

[16] Sunil Kumar J1 , Shalini J2 , Birtukan Teshome 3 , Milkias Berhanu Tuka4 , Fikadu Improvement of Active and Reactive Power at the Wind Based Renewable Energy Sources, International Journal of Scientific & Engineering Research, Volume 4, Issue 9, September-2013 ISSN 2229-5518.

[17] Kosuru, R.; Liu, S.; Shi, W. Deep Reinforcement Learning for Stability Enhancement of a Variable Wind Speed DFIG System, Actuators 2022, 11, 203.

[18] Ismail Moufid, Zineb En-nay, Soukaina Naciri, Hassan El Moussaoui, Tijani Lamhamdi, Hassane El Markhi, Impact of static synchronous compensator STATCOM installation in power quality improvement, IntJ Pow Elec & Dri Syst, Vol. 13, No. 4, December 2022, pp. 2296~2304.

[19] Yasoda Kailasa Gounder, Devarajan Nanjundappan , Veerakumar Boominathan1, Enhancement of transient stability of distribution system with SCIG and DFIG based wind farms using STATCOM, IET Renewable Power Generation, doi: 10.1049/iet-rpg.2016.0022

[20] Ayyarao, T.S.L.V. Modified vector-controlled DFIG wind energy system based on barrier function adaptive sliding mode control Prot Control Mod Power Syst **4**, 4 (2019). https://doi.org/10.1186/s41601-019-0119-3.

[21] Mr. Ketan G. Damor. Dr. Dipesh M. Patel, Mr. Vinesh Agrawal, Mr. Hirenkumar G. Patel, Improving Power System Transient Stability by using Facts Devices, IJERT ISSN: 2278-0181 www.ijert.org Vol. 3 Issue 7, July – 2014

[22] International Electrotechnical Commission (IEC) 61400 series standards for wind turbines: https://www.iec.ch/dyn/www/f?p=103:38:0::::FSP_ORG_ID,FSP_LANG_ID:1256,25

[23] Gabriela Glanzmann, FACTS Flexible Alternating Current Transmission Systems, EEH - Power Systems Laboratory ETH Z¨urich, Jan. 2005.

[24] Chong Han, Alex Q. Huang, Mesut E. Baran, Subhashish Bhattacharya, Wayne Litzenberger, Loren Anderson, Anders L. Johnson, and Abdel-Aty Edris, "STATCOM Impact Study on the Integration of a Large Wind Farm into a Weak Loop Power System," IEEE Trans. on Energy Conversion, vol. 23, no. 1, Mar. 2008.

[25] Okedu KE, Al Tobi M, and Al Araimi S (2021) Comparative Study of the Effects of Machine Parameters on DFIG and PMSG Variable Speed Wind Turbines during a Grid Fault Front. Energy Res. 9:681443. Doi: 10.3389/fenrg.2021.681443.

[26] J. Mohammadi, S. Vaez-Zadeh, S. Afsharnia, and E. Daryabeigi, "A Combined Vector and Direct Power Control for DFIG-Based Wind Turbines," IEEE Trans. Sustain. Energy, vol. 5, no. 3, pp. 767–775, Jul. 2014.

[27] Wikipedia contributors, "Direct-quadrature-zero transformation," Wikipedia, The Free Encyclopedia, https://en.wikipedia.org/w/index.php?title=Direct-quadrature zero_transformation&oldid=1128400363 (accessed April 29, 2023.

[28] J. Morren and S. W. H. De Haan, "Short-Circuit Current of Wind Turbines with Doubly Fed Induction Generator," IEEE Trans. Energy Convers, vol. 22, no. 1, pp. 174–180, 2007.

[29] A. Snyder, Michael, "Development of Simplified Models of Doubly-Fed Induction Generators (DFIG)," Goteborg, Sweden: Chalmers University of Technology, 2012.

[30] "Backstepping Control for Transient Stability Enhancement of Doubly Fed Induction Generator-Based Wind Turbine System," by A. G. Hamedani et al., IEEE Transactions on Sustainable Energy, vol. 7, no. 2, pp. 786-796, April 2016.

[31] L. G. c. E.-H. Narain G. Hingorani, consulting editor, Understanding FACTS: concepts and technology of flexible AC transmission systems New York: IEEE Press 2000.

[32] P. Therond, P. Cholley, D. Daniel, E. Joncquel, L. Lafon, and C. Poumarede, "FACTS research and development program at EDF," in Flexible AC Transmission Systems (FACTS) -

The Key to Increased Utilization of Power Systems, IEE Colloquium on (Digest No.1994/005), 1994, pp. 6/1-615.

[33] X.-P. Zhang, C. Rehtanz, and B. Pal, "FACTS-Devices and Applications," in Flexible AC Transmission Systems: Modelling and Control, ed: Springer, 2012, pp. 1-30.

[34] R. Mathur and R. Varma, "SVC Applications," in Thyristor-Based FACTS Controllers for Electrical Transmission Systems, ed: Wiley-IEEE Press, 2002, pp. 221-276.

[35] N. Hingorani and L. Gyugyi, "Static Series Compensators: GCSC, TSSC, TCSC and SSSC," in Understanding FACTS:Concepts and Technology of Flexible AC Transmission Systems, ed: Wiley-IEEE Press, 2000, pp. 209-265.

[36] N. Hingorani and L. Gyugyi, "Static Shunt Compensators: SVC and STATCOM," in Understanding FACTS:Concepts and Technology of Flexible AC Transmission Systems, ed: Wiley-IEEE Press, 2000, pp. 135-207.

[37] N. Hingorani and L. Gyugyi, "Combined Compensators: Unified Power Flow Controller (UPFC) and Interline Power Flow Controller (IPFC)," in Understanding FACTS:Concepts and Technology of Flexible AC Transmission Systems, WileyIEEE Press, 2000, pp. 297-352.

[38] N. G. Hingorani and L. Gyugyi, Understanding FACTS: Concepts and Technology of Flexible AC Transmission Systems: Wiley, 2000.

[39] Mohamed Metwally Mahmoud, 1 Hossam S. Salama, Mohit Bajaj, Mohamed M. Aly, Istvan Vokony, Syed Sabir Hussain Bukhari, Daniel Eutyche Mbadjoun Wapet, and Abdel-Moamen M. Abdel-Rahim, Integration of Wind Systems with SVC and STATCOM during Various Events to Achieve FRT Capability and Voltage Stability: Towards the Reliability of Modern Power Systems, International Journal of Energy Research Volume 2023, Article ID 8738460, 28 pages.

[40] Published by, www.ijert.org,ISSN: 2278-0181 Published by, www.ijert.org IC-QUEST - 2016 Conference Proceedings

[41] Varun Kumar * , Ajay Shekhar Pandey and Sunil Kumar Sinha,Stability Improvement of DFIG-Based Wind Farm Integrated Power System Using ANFIS Controlled STATCOM,Energies 2020, 13, 4707; doi:10.3390/en13184707.

[42] Mohamed Metwally Mahmoud,Hossam S. Salama, Mohit Bajaj, Mohamed M. Aly, Istvan Vokony, Syed Sabir Hussain Bukhari, Daniel Eutyche Mbadjoun Wapet, and Abdel-Moamen M. Abdel-Rahim, Integration of Wind Systems with SVC and STATCOM during Various Events to

Achieve FRT Capability and Voltage Stability: Towards the Reliability of Modern Power Systems, International Journal of Energy Research Volume 2023, Article ID 8738460.

[43] Subir Datta and Anjan Kumar Roy, ANFIS based 48-Pulse STATCOM Controller for Enhancement of Power System Stability, International Journal of Modeling and Optimization, Vol. 2, No. 4, August 2012.

[44] Juan Shi, Amin Noshadi, Akhtar Kalam, and Peng Shi, Fuzzy Logic Control of DSTATCOM for Improving Power Quality and Dynamic Performance, 978-1-4799-8725-2/15/$31.00 ©2015 IEEE

[45] Prabha Pandit1, Rohit Kumar2, Manju Gupta3, improvement of transient stability by using FLSTATCOM, ijtrs-v5-i12-005, Volume V Issue XII, ISSN No.: 2454- 2024, December 2020,

[46] Prerna Tundwal, R.R. Joshi, Fuzzy Logic Controller Based DSTATCOM For Power Quality Solution In Distributed Generated System, IJTRS-V6-I7-001, Volume VI, Issue VII, July 2021.

[47] Mahmood T. Alkhayyat1 , Mohammed Y. Suliman2, Adaptive Neuro-Fuzzy Controller Based STATCOM for Reactive Power Compensator in Distribution Grid, PRZEGLĄD ELEKTROTECHNICZNY, ISSN 0033-2097, R. 98 NR 4/2022.

APPENDIX I: Adama- II wind farm DFIG parameters

DFIG parameters		
Rated Power	1.5MW	1.0pu
Rated stator line-to-line voltage	690V(rms)	
Rated Stator Phase Voltage/Base voltage	398.4V(rms)	1.0pu
Rated Rotor Phase Voltage	79V(rms)	79/398.4=0.1983
Rated Stator current	1110A(rms)	$1110/I_B$=0.8844
Efficiency at rated power	>=95%	
Base current, I_B=1.5MW/sqrt3*690V	1255.11A(rms)	1.0pu
Rated Rotor current	1209.852A(rms)	0.964
Rated stator Frequency	50Hz	1.0pu
Rated Power factor	from cosφ =0.95 inductive to cosφ =0.95capacitive	
Rated stator speed, ωs	1500rpm	1.0pu
Rated Rotor speed	1800rpm	1.0pu
Nominal Rotor speed Range	1000-2000rpm	0.56-1.11pu
Wind Turbine rotor speed range	10.6-21.1rpm	
Rated speed of wind turbine Rotor	19rpm	
Rated slip, rated	ws-wr/ws=1500-1800/1500=-0.2	
Number of pole pairs	2	
Transformation Ratio, u	1/3	
Rotor/Stator connection	Delta/Star	
Rated mechanical torque	8.3KN-m	1.0
Stator winding resistance, R_s	0.006243 Ω	0.006243/0.3174=0.0197
Rotor winding resistance, R_r	0.011074 Ω	0.0349
Stator leakage inductance, Lls	0.198822mH	$Lls*\omega_s/Z_B$=0.000198822*2*л*50/0.3174=0.197
Rotor leakage inductance, Llr	0.198822mH	0.197
Magnetizing Inductance, Lm	3.976mH	3.9354
Base flux linkage, $\psi_B=V_B/\omega s$	1.2681Wb(rms)	1.0pu
Base Impedance, ZB=VB/IB=398.4/1255.1	0.3174Ω	1.0pu
Base inductance, LB=ψB/IB	1.0103	1.0pu
Turbine inertia, Jt	85.8	
Generator inertia, Jg(Kg-m2)	127	
Gear box ratio	94.7	
Base capacitance, CB=1/2лfZB	10028.7μF	=1.0pu
Air density, p	1.225Kg/m3	

B. **Converter Parameter**

Converter	**Rotor side (two modules are connected in parallel)**	
	IGBT voltage level	1700V
	Max. continuous operating Voltage	1100V
	Rated continuous DC Voltage	975V
	Grid side(single module)	
	IGBT voltage level	1700V
	Max. continuous operating DC voltage	1100V
	Rated continuous DC Voltage	975V
Cpmax	0.4865	
Lambda opt	6.2	
Stator wiring	Δ	
Rotor wiring	Y	
Δ-winding (stator side)	220V(L-L)	
Y-winding (stator converter)	220V(L-L)	
Machine Parameter		
Stator resistance		0.043pu
Rotor leakage Inductance		0.0613pu
Stator Leakage Inductance		0.0613pu
Mutual inductance		1.0pu
Angular moment of inertia(J)		1.0se

C, Turbine Data

Turbine Data		
Shaft stiffness	2.5pu/rad	
Turbine rotor speed range	9.5-2.1rpm	
Rated wind speed	12m/s	
Rotor diameter	75m	

D, Generator data

Rated power	2MW	
Rated voltage	690V	
Rated frequency	50Hz	
Stator resistance		0.048pu

Stator reactance		0.075pu
Mutual reactance		3.8pu
Rotor resistance		0.018pu
Rotor reactance		0.12pu
Generator rotor inertia	0.5s	
Number of pole pairs	2	
DC-bus	C=40μF,V_{dc}=1150V	
RI, filter	R_f=0.075Ω,L_f=0.75mH	

APPENDIX II, MATLAB code for placement of STATCOM

```
% Program for Newton-Raphson
Load Flow with STATCOM

Y = ybusppg();              %
Calling ybusppg.m..
busdata = busdata5();       %
Calling Busdata..
statdata = statdata5();     %
Statcom Data..
baseMVA = 100;              %
Base MVA..
bus = busdata(:,1);         % Bus
Number..
type = busdata(:,2);        % Type
of Bus 1-Slack, 2-PV, 3-PQ..
V = busdata(:,3);           %
Specified Voltage..
del = busdata(:,4);         %
Voltage Angle..
Pg = busdata(:,5);          % PGi..
Qg = busdata(:,6);          % QGi..
Pl = busdata(:,7);          % PLi..
Ql = busdata(:,8);          % QLi..
Qmin = busdata(:,9);        %
Minimum Reactive Power
Limit..
Qmax = busdata(:,10);       %
Maximum Reactive Power
Limit..
nbus = max(bus);            % To
get no. of buses..
P = Pg - Pl;                % Pi = PGi
- PLi..
Q = Qg - Ql;                % Qi =
QGi - QLi..
P = P/baseMVA;              %
Converting to p.u..
Q = Q/baseMVA;
Qmin = Qmin/baseMVA;
Qmax = Qmax/baseMVA;
Tol = 1;
Iter = 50;
Psp = P;
Qsp = Q;
G = real(Y);    % Conductance..
B = imag(Y);    % Susceptance..
Vsp = V;

% Details of STATCOM
statb = statdata(:,1); % Buses at
which statcoms are placed..
Vsh = statdata(:,2);
Thst = statdata(:,3);
Qsmx = statdata(:,4);
Qsmn = statdata(:,5);
gsh = 0.9901;
bsh = -9.901;
Vshmx = 1.1; Vshmn = 0.9;
Thstmx = pi; Thstmn = -pi;
np = length(statb); % Number of
STATCOMs..

pv = find(type == 2 | type == 1);
% Index of PV Buses..
pq = find(type == 3); % Index of
PQ Buses..

npv = length(pv); % Number of
PV buses..
npq = length(pq); % Number of
PQ buses..

while (Tol > 1e-5 && Iter <=
50)   % Iteration starting..

   P = zeros(nbus,1);
   Q = zeros(nbus,1);
% Calculate P and Q
for i = 1:nbus
for k = 1:nbus
        P(i) = P(i) + V(i)*
V(k)*(G(i,k)*cos(del(i)-del(k))
+ B(i,k)*sin(del(i)-del(k)));
        Q(i) = Q(i) + V(i)*
V(k)*(G(i,k)*sin(del(i)-del(k)) -
B(i,k)*cos(del(i)-del(k)));
end
      m = find(statb == i);
if ~isempty(m)
        P(i) = P(i) + V(i)^2*gsh
- V(i)*Vsh(m)*(gsh*cos(del(i)-
Thst(m)) + bsh*sin(del(i)-
Thst(m)));
        Q(i) = Q(i) - V(i)^2*bsh
+ V(i)*Vsh(m)*(bsh*cos(del(i)-
Thst(m)) - gsh*sin(del(i)-
Thst(m)));
end
end

% Checking Q-limit violations..
if Iter >= 2
for n = 1:nbus
if type(n) == 2
if Q(n) < Qmin(n)
            V(n) = V(n) + 0.01;
elseif Q(n) > Qmax(n)
            V(n) = V(n) - 0.01;
end
end
end
end

% Calculating PE,
   PE = zeros(np,1);
for i = 1:np
      m = statb(i);
      PE(i) = Vsh(i)^2*gsh -
V(m)*Vsh(i)*(gsh*cos(del(m)-
```

```
Thst(i)) - bsh*sin(del(m)-
Thst(i)));
end

% Calculate F, Control
Variables
   F = zeros(np,1);
for i = 1:np
      m = statb(i);
      F(i) = V(m) - Vsp(m);
end

% Calculate change from
specified value
   dPa = Psp-P;
   dQa = Qsp-Q;
   dQ = zeros(npq,1);
   k = 1;
for i = 1:nbus
if type(i) == 3
         dQ(k,1) = dQa(i);
         k = k+1;
end
end
   dP = dPa(2:nbus);
   dPE = -PE;
   dF = -F;
   M = [dP; dQ; dPE; dF];      %
Mismatch Vector

% Jacobian
% J11 - Derivative of Real
Power Injections with Angles..
   J11 = zeros(nbus-1,nbus-1);
for i = 1:(nbus-1)
      m = i+1;
      p = find(statb == m);
for k = 1:(nbus-1)
         q = k+1;
if q == m
for n = 1:nbus
            J11(i,k) = J11(i,k) +
V(m)* V(n)*(-
G(m,n)*sin(del(m)-del(n)) +
B(m,n)*cos(del(m)-del(n)));
end
         J11(i,k) = J11(i,k) -
V(m)^2*B(m,m);
if ~isempty(p)
            J11(i,k) = J11(i,k) +
V(m)*Vsh(p)*(gsh*sin(del(m)-
Thst(p)) - bsh*cos(del(m)-
Thst(p)));
end
else
            J11(i,k) = V(m)*
V(q)*(G(m,q)*sin(del(m)-
del(q)) - B(m,q)*cos(del(m)-
del(q)));
end
end
end

% J12 - Derivative of Real
Power Injections with V..
   J12 = zeros(nbus-1,npq);
for i = 1:(nbus-1)
      m = i+1;
      p = find(statb == m);
for k = 1:npq
         q = pq(k);
if q == m
for n = 1:nbus
            J12(i,k) = J12(i,k) +
V(n)*(G(m,n)*cos(del(m)-
del(n)) + B(m,n)*sin(del(m)-
del(n)));
end
         J12(i,k) = J12(i,k) +
V(m)*G(m,m);
if ~isempty(p)
            J12(i,k) = J12(i,k) +
2*V(m)*gsh -
Vsh(p)*(gsh*cos(del(m)-
Thst(p)) + bsh*sin(del(m)-
Thst(p)));
end
else
            J12(i,k) =
V(m)*(G(m,q)*cos(del(m)-
del(q)) + B(m,q)*sin(del(m)-
del(q)));
end
end
end


      J13 = zeros(nbus-1,np);
   J14 = zeros(nbus-1,np);
for i = 1:(nbus-1)
      m = i+1;
for k = 1:np
         p = statb(k);
if m == p
            J13(i,k) = -
V(m)*(gsh*cos(del(m)-Thst(k))
+ bsh*sin(del(m)-Thst(k)));
            J14(i,k) = -
V(m)*Vsh(k)*(gsh*sin(del(m)-
Thst(k)) - bsh*cos(del(m)-
Thst(k)));
end
end
end

% J21 - Derivative of Reactive
Power Injections with Angles..
   J21 = zeros(npq,nbus-1);
for i = 1:npq
      m = pq(i);
      p = find(statb == m);
for k = 1:(nbus-1)
         q = k+1;
if q == m
for n = 1:nbus
            J21(i,k) = J21(i,k) +
V(m)*
V(n)*(G(m,n)*cos(del(m)-
del(n)) + B(m,n)*sin(del(m)-
del(n)));
end
         J21(i,k) = J21(i,k) -
V(m)^2*G(m,m);
if ~isempty(p)
            J21(i,k) = J21(i,k) -
V(m)*Vsh(p)*(gsh*cos(del(m)-
Thst(p)) + bsh*sin(del(m)-
Thst(p)));
end
else
         J21(i,k) = -V(m)*
V(q)*(G(m,q)*cos(del(m)-
del(q)) + B(m,q)*sin(del(m)-
del(q)));
end
end
end


   J22 = zeros(npq,npq);
for i = 1:npq
      m = pq(i);
      p = find(statb == m);
for k = 1:npq
         q = pq(k);
if q == m
for n = 1:nbus
            J22(i,k) = J22(i,k) +
V(n)*(G(m,n)*sin(del(m)-
del(n)) - B(m,n)*cos(del(m)-
del(n)));
end
         J22(i,k) = J22(i,k) -
V(m)*B(m,m);
if ~isempty(p)
            J22(i,k) = J22(i,k) -
2*V(m)*bsh -
Vsh(p)*(gsh*sin(del(m)-
```

```
Thst(p)) - bsh*cos(del(m)-
Thst(p)));
end
else
            J22(i,k) =
V(m)*(G(m,q)*sin(del(m)-
del(q)) - B(m,q)*cos(del(m)-
del(q)));
end
end
end

Thsh..
   J23 = zeros(npq,np);
   J24 = zeros(npq,np);
for i = 1:npq
      q = pq(i);
      m = i+1;
for k = 1:np
         p = statb(k);
if q == p
            J23(i,k) = -
V(m)*(gsh*sin(del(m)-Thst(k))
- bsh*cos(del(m)-Thst(k)));
            J24(i,k) =
V(m)*Vsh(k)*(gsh*cos(del(m)-
Thst(k)) + bsh*sin(del(m)-
Thst(k)));
end
end
end

   J31 = zeros(np,nbus-1);
   J41 = zeros(np,nbus-1);
for i = 1:np
      m = statb(i);
for k = 1:(nbus-1)
if m == k+1
            J31(i,k) =
V(m)*Vsh(i)*(gsh*sin(del(m)-
Thst(i)) + bsh*cos(del(m)-
Thst(i)));
end
end
end

% J32 - Derivative of PE with
V..
% J42 - Derivative of F with V..
   J32 = zeros(np,npq);
   J42 = zeros(np,npq);
for i = 1:np
      m = statb(i);
for k = 1:npq
if m == pq(k)
            J32(i,k) = -
Vsh(i)*(gsh*cos(del(m)-Thst(i))
- bsh*sin(del(m)-Thst(i)));
end
if m == pq(k)
            J42(i,k) = 1;
end
end
end

Thsh..
   J33 = zeros(np,np);
   J34 = zeros(np,np);
   J43 = zeros(np,np);
   J44 = zeros(np,np);
for i = 1:np
      m = statb(i);
for k = 1:np
         p = statb(k);
if m == p
            J33(i,k) =
2*Vsh(k)*gsh -
V(m)*(gsh*cos(del(m)-Thst(k))
- bsh*sin(del(m)-Thst(k)));
            J34(i,k) = -
V(m)*Vsh(k)*(gsh*sin(del(m)-
Thst(k)) + bsh*cos(del(m)-
Thst(k)));
end
end
end

   J = [J11 J12 J13 J14;
      J21 J22 J23 J24;
      J31 J32 J33 J34;
      J41 J42 J43 J44]    %
Jacobian
   clear
J11J12J13J14J21J22J23J24J31J
32J33J34J41J42J43J44
   X = inv(J)*M;          %
Correction Vector
   dTh = X(1:nbus-1);
   dV = X(nbus:nbus+npq-1);
   dVsh =
X(nbus+npq:nbus+npq+np-1);
   dThst =
X(nbus+npq+np:nbus+npq+2*n
p-1);
   del(2:nbus) = dTh +
del(2:nbus);
   k = 1;
for i = 2:nbus
if type(i) == 3
         V(i) = dV(k) + V(i);
         k = k+1;
end
end
   Vsh = Vsh + dVsh;
   Thst = Thst + dThst;

% Calculate Qsh..
   Qsh = zeros(np,1);
for m = 1:np
      i = statb(m);
      Qsh(m) = -V(i)^2*bsh +
V(i)*Vsh(m)*(bsh*cos(del(i)-
Thst(m)) - gsh*sin(del(i)-
Thst(m)));
end
   Iter = Iter + 1;
   Tol = max(abs(M));
end

Iter = Iter - 1; % Number of
Iterations took..
V;
Del = 180/pi*del;
Thst = 180/pi*Thst;

disp('------------------------------');
disp('------------------------------
--------');
disp('| STATCOM | Vsh   | Thst
|  Qsh  |');
disp('|  Bus   |  pu   | Degree |
pu  |');
disp('------------------------------
--------');
for m = 1:np
   fprintf('  %4g',statb(m)),
fprintf('   %8.4f', Vsh(m)),
fprintf('    %8.4f',
Thst(m)),fprintf('  %8.4f',
Qsh(m)), fprintf('\n');
end
disp('------------------------------
--------');
E2 = [V Del]; % Bus Voltages
and angles..
disp('------------------------------');
disp('|  Bus  |    V    | Angle  |');
disp('|  No   |   pu    | Degree |');
disp('------------------------------');
for m = 1:nbus
   fprintf('%4g', m), fprintf('
%8.4f', V(m)), fprintf('    %8.4f',
Del(m)),fprintf('\n');
end
```

APPENDIX III; Transient stability analysis

```
%critical clearing angle and
CCT
X1 = 0.603;
E = 1.25;
V = 1.0;
Pm1 = E*V/X1;
% Electric power output before
fault
%Pe1 = Pm1*sin(del0)
% Pe1 = Pi; Pi = input
mechanical power
Pi = 1.0;
del0 = asin(Pi/Pm1)*180/pi %
angle before fault
% during fault condition, power
transfer = Pe2
X2 =0;
E = 1.25;
V = 1.0;
Pm2 = E*V/X2;
%Pe2 = Pm2*sin(del0)
% Post fault condition
X3 = 0.94;
E = 1.25;
V = 1.0;
Pm3 = E*V/X3;
% Power transfer after fault =
Pe3
% delm = maximum del angle
delm = 180-asin(Pi/Pm3)*180/pi
x = deg2rad(delm);  % convert
30 degrees to radians
% delcc = critical clearing angle
delcc=acos(((Pi*(delm-
del0)/57.3)+Pm3*(cos(x)))/(Pm
3))*57.3 %delc in radian
% CCA in degree
H=5; %inertia in MJ per KG
tcc=sqrt((2*H*(delcc-
del0)/(180*50*Pi)))% critical
clearing time in sec
%%%%%%%%%%%%%%
%%%%%%%%%%
del = [0,0.5,1.0,1.5,2.0,2.5,3];
Pi=[1.0,1.0,1.0,1.0,1.0,1.0,1.0,];
plot(del*180/pi,Pi,'r-'),hold
del = 0:0.1:pi;
Pe1 = Pm1*sin(del);
Pe2= Pm2*sin(del);
Pe3 = Pm3*sin(del);
x = [28.8423 28.8423 28.8423];
y= [0.0 1.0 1.0];
xx= [  46.7958   46.7958
46.7958];
yy = [0.0 1.8 1.8];
xxx=[131.2361 131.2361
131.2361];
yyy=[0.0 1.6 1.6];
plot(del*180/pi,Pe1,'k-
',del*180/pi,Pe2,'y-
',del*180/pi,Pe3,'g-',x,y,'b-
',xx,yy,'b-',xxx,yyy,'b-'),hold off
%legend('Pre- fault Power
Transfer', 'During fault Power
Transfer', 'Post
%fault power transfer','del0 Vs
Power','delc Vs Power')
title ('Transient stability
analysis')
xlabel('Rotor angle in degrees')
ylabel('Power in p.u.')
```